The activation states of LFA-1 (αLβ2) and related integrins

Cheng, Ming

2008

Cheng, M. (2008). The activation states of LFA-1 (αLβ2) and related integrins. Doctoral thesis, Nanyang Technological University, Singapore.

https://hdl.handle.net/10356/38777

https://doi.org/10.32657/10356/38777

The Activation States of LFA-1(αLβ2) and Related Integrins

Cheng Ming

School of Biological Sciences

A thesis submitted to the Nanyang Technological University
in fulfilment of the requirement for the degree of
Doctor of Philosophy

2008

The Activation States of LFA-1 (αLβ2) and Related Integrins

A Thesis for the Degree of Doctor of Philosophy

at Nanyang Technological University

Cheng Ming

Supervised by Professor Alex Law

School of Biological Sciences

Nanyang Technological University

Abstract

Leukocyte integrins (β2 integrins) are involved in many immune and inflammatory responses. The key function of leukocytes is impaired in the LAD-I patients due to the defects in β2 gene. Two missense LAD-1 mutations $N^{329}S$ and $R^{571}C$ were studied. $\alpha L\beta 2N^{329}S$ can mediate constitutive adhesion to both ICAM-1 and ICAM-3, $\alpha IIb\beta 3N^{339}S$ which is corresponding to $N^{329}S$ in β2 also can mediate adhesion to fibrinogen in the absence of activation reagents. Through mutagenesis analysis and conformation study, we demonstrate that this Asn is critical in shaping the I-like domain by stabilizing the conformation of the α7 helix and the β6-α7 loop in the I-like domain.

Although $\alpha L\beta 2R^{571}C$ is active in adhesion to ICAM-1, the $\beta 2R^{571}C$ cannot form heterodimer with αM or αX. We ruled out the domains in α subunit that is incompatible with the $R^{571}C$ mutation in the β2 subunit. We also showed that the positive charge in position 571 is important in heterodimer formation. Further experiments are required to pinpoint the residues that are responsible for the heterodimer formation for αMβ2 and αXβ2.

Combining the adhesion property of LFA-1 with conformation study, we defined two intermediate states between the resting state and fully active state. By introducing a disulfide bond between the PSI and IEGF2 domain, αLβ2cc is locked into a bent conformation. However, αLβ2cc can still be induced to express the epitope of MEM148 and mediate adhesion to ICAM-3. The results suggest that the leg extension and hybrid displacement can be independently regulated during integrin activation, and ligand binding and conformational change is not coupled in a cause and effect fashion.

Acknowledgements

I would like to express my deep appreciation and gratitude to my supervisor Prof. Alex Law for his direction and support. His serious attitude towards science and his insightful suggestions are essential to the completion of this project. I am grateful for his kindness and generosity.

I would also like to express thank to Dr. Tan Suet Mien for his advice and support. I could have not finished the work in Chapter 3 without his help.

I thank Dr. Liu Chuan Fa for synthesizing peptide for my work.

I would like to acknowledge and extend my heartfelt gratitude to my laboratory colleagues. We had a very good time during my four-year study. Without their help and advice, I cannot have finished my project smoothly. Many thanks to Manisha Cooray, Foo Shenyun, Shi Minglong, Tang Renhong, Susannah Elizabeth Walters, Elianna Bte Mohamed Amin, Florence Lim and Chan Hwee Sing. Also thanks to Li Yanfeng, Chua Geok Lin and Lim Kok Guan for their assistance in writing my thesis.

I would also like to thank all my friends in the School of Biological Sciences for their help and inspiration.

Finally, I would dedicate this thesis to my husband and my parents. They were very supportive during my study and gave me selfless care.

I am grateful for the financial support offered to me from Nanyang Technological University.

Contents

Abbreviations

bp	base paire(s)
BSA	bovine serum albumin
cDNA	complementary DNA
DMSO	dimethyl sulphoxide
DTT	dithiothreitol
E.coli	*Escherichia coli*
ECL	enhanced chemiluminescence
EDTA	ethylene-diamine-tetra acetic acid
EGTA	ethylene-glycol-bis(β-aminoethylether)-tetra acetic acid
EM	electron microscope
FACS	fluorescence activated cell sorter
FITC	Fluorescein isothiocyanate
HEPES	N-[2-hydroxyethy]piperazine-N'-[2-ethanesulfonic acid]
Ig	immunoglobulin
IP	immunoprecipitation
mAb	monoclonal antibody
NMR	nuclear magnetic resonance
PAGE	polyacylamide gel electrophoresis
PBS	phosphate buffered saline
PCR	polymerase chain reaction
SDS	sodium dodecyl sulphate
Tris	Tris(hydroxymethyl)-aminoethane
UV	ultravilolet
v/v	volume per volume
w/v	weight per volume

Chapter 1: Introduction

1.1 Overview

Cell adhesion molecules, which are both receptors and ligands for receptors, are typically transmembrane proteins. They are composed of three domains: an intracellular domain that interacts with the cytoskeleton, a transmembrane domain and an extracellular domain that interacts either with other cell adhesion molecules on another cell or the component of the extracellular matrix (ECM) (Joseph-Silverstein and Silverstein, 1998). Their functions include adhesion, recognition and communication between cells and between cells and components of the extracellular matrix.

Integrins are a family of cell adhesion molecules with key roles in cell-extracellular matrix and cell-cell interactions (Mould and Humphries, 2004). They are involved in many fundamental biological processes. First, they mediate stable adhesion of cells to their substrate by providing a physical link between the ECM and the cytoskeleton (Hynes, 1992). Second, integrins can act as signaling receptors that relay information from the substrate to the interior of the cell (outside-in signaling), which can, in turn, be interpreted as growth, differentiation, or survival signals (Giancotti and Ruoslanti, 1999; Miranti and Brugge, 2002). Third, integrins are vital for cell migration (Lauffenburger and Horwitz, 1996). Fourth, there is evidence that integrins are themselves involved in the assembly of the extracellular matrix substrate to which they bind (Schwarzbauer and Sechler, 1999).

Each integrin is a heterodimer with a α and a β subunit. These two subunits are type I transmembrane proteins and associated with each other by non-covalent forces. Integrins are present in all metazoans, including sponges and cnidarians (Bokel and Brown, 2002). Generally, the lower organism has a simple integrin system. In human, eighteen different integrin α subunits and eight different β subunits have been identified (Hynes, 2002). From these subunits, only 24 integrins have been identified (Fig. 1.1), which implies that not all possible combinations exist.

1.2 The β2 integrins

The β2 integrin consists of four integrins having the same β2 subunit but with different α subunits. They are αLβ2 (CD11a/CD18, Leukocyte Function-Associated Antigen-1 LFA-1), αMβ2 (CD11b/CD18, Mac-1, the Complement Receptor Type 3 or CR3), αXβ2 (CD11c/CD18, p150,95, the Complement Receptor Type 4 or CR4) and αDβ2 (CD11d/CD18). The β2 integrins form a close subset in the integrins superfamily, since none of the four α subunits interact with another β subunit, and the β2 subunit is not known to interact with α subunit other than the four listed.

The β2 gene is located at chromosome 21 (21g22.3) (Solomon et al., 1988) and the four α genes are located in a cluster at chromosome 16 (16p11.2) (Wong et al., 1996). Further refinement was obtained when the human genome was sequenced (Fig. 1.2).

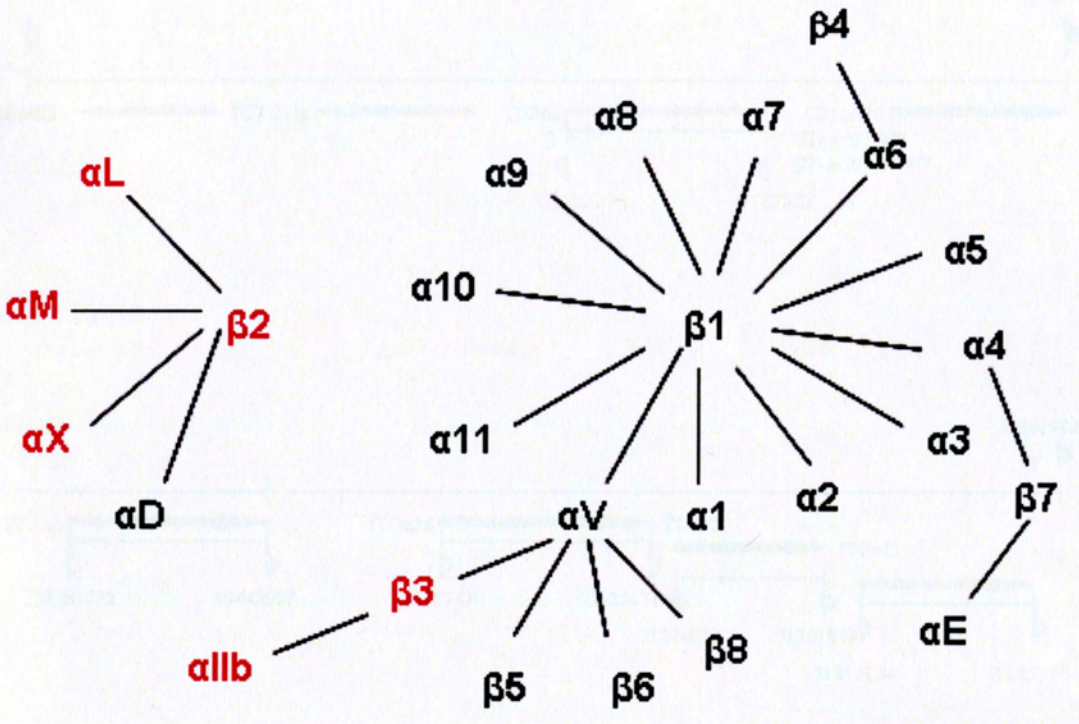

Fig. 1.1 The integrin family. 18 types of integrin α chains and 8 types of β chains can form 24 different integrins in human. The red color indicates the integrins involved in this thesis.

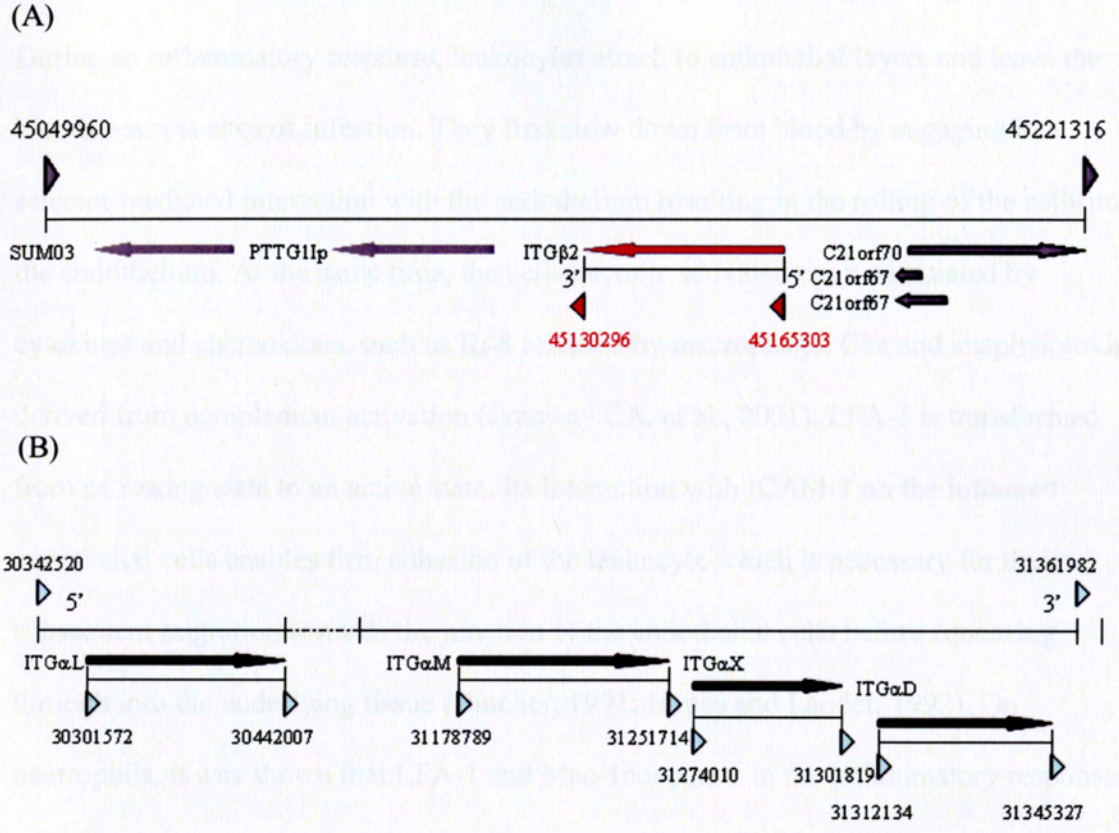

Fig. 1.2 The chromosome location of β2 gene and α genes. (A) The β2 gene (ITGβ2) is located at the chromosome 21q22.3 labeled with red color. The adjacent genes include SUM03, PTTG1IP, C21orf70, C21orf67. The numbers shown in this stretch indicate the distance from the centromere. (B) The α genes (ITGαL, ITGαM, ITGαX and ITGαD) of integrins are located at the chromosome 16p11.2. The genes (more than ten) between αL and αM are not shown. There are no other genes between αM and αX, αX and αD genes.

1.2.1 αLβ2 (LFA-1)

Lymphocyte function-associated antigen-1 (LFA-1) is expressed on all leukocytes. LFA-1 plays an important role in inflammation and leukocyte trafficking (Springer, 1994). During an inflammatory response, leukocytes attach to endothelial layers and leave the bloodstream at sites of infection. They first slow down from blood by engaging in a selectin-mediated interaction with the endothelium resulting in the rolling of the cells on the endothelium. At the same time, the cells become activated upon stimulated by cytokines and chemokines, such as IL-8 released by macrophage, C5a and anaphylotoxin derived from complement activation (Janeway CA. et al., 2001). LFA-1 is transformed from its resting state to an active state. Its interaction with ICAM-1 on the inflamed endothelial cells enables firm adhesion of the leukocyte which is necessary for their subsequent migration towards the junction of the endothelial cells before squeezing through into the underlying tissue (Butcher, 1991; Hynes and Lander, 1992). On neutrophils, it was shown that LFA-1 and Mac-1cooperate in the inflammatory responses of neutrophils (Henderson et al., 2001). LFA-1 contributes to neutrophil rolling by stabilizing the transient attachment or tethering phase of rolling while Mac-1 contributes to emigration from the vessel. LFA-1 is also involved in the migration of T cells into lymph nodes. However, this function is shared by the α4β1 integrin (Madri et al., 1996).

1.2.2 Mac-1

Mac-1 is primarily expressed on leukocyte of the myeloid monocytic lineage and natural killer lymphocytes (Larson and Springer, 1990). It is a remarkably versatile adhesion and recognition receptor, binding both endogenous ligands as well as an array of microbial

(Ehlers, 2000). Mac-1 can cooperate functionally with a variety of other surface receptors, including uPAR (the urokinase-type plasminogen activator receptor) (Tang et al., 2006), FcγRs (Fernandez-Calotti et al., 2003), Toll-like receptor 2 (TLR2) (Hajishengallis and Harokopakis, 2007) and CD14 (Ehlers, 2000). The interaction of Mac-1 and uPAR are required for fibrinolysis by myeloid cells (Simon et al., 1993) and it was reported that uPAR can promote Mac-1 binding to fibrinogen (Zhang et al., 2003). Mac-1 can recognize many pathogens directly and can mediate the phagocytosis of microbes.

The complement proteolysis product iC3b is one of the most important ligand of Mac-1, the efficiency of phagocytosis is enhanced significantly when Mac-1 binds to iC3b (Mayadas and Cullere, 2005). The functional study of Mac-1 has now been expanded to include a role in modulating the life span of neutrophils due to its involvement in adhesion-dependent neutrophil functions (Mayadas and Cullere, 2005).

1.2.3 p150,95

p150,95 is expressed mainly on myeloid cells and its tissue distribution overlaps with that of Mac-1. It also contributes to leukocyte adhesion to endothelium and phagocytosis (Stacker and Springer, 1991). The ligands of p150,95 include iC3b, fibrinogen, ICAM-1 and LPG (lipophosphoglycan) and denatured proteins. It was reported that the acidic residues that are exposed in denatured or proteolyzed fibrinogen function as a damage tag for recognition by the p150,95 (Vorup-Jensen et al., 2005).

1.2.4 αDβ2

αDβ2 is the latest discovered member of the β2 integrin subfamily (Van der Vieren et al., 1995). It is expressed on myelomonocytic cells, macrophage foam cells and splenic pulp macrophage (Noti, 2002). It can bind to ICAM-3 (Van der Vieren et al., 1995) and VCAM-1(Van der Vieren et al., 1999), but its function remains unknown.

1.3 The β3 integrins

The β3 integrins only have two members: αIIbβ3 (platelet glycoprotein IIb/IIIa complex, CD41/CD61) and αVβ3 (vitronectin receptor, CD51/CD61). The αIIb and β3 genes are both located at chromosome 17q21.23 (Fig 1.3), αV gene is located at chromosome 2q31-32. Through mediating cell-cell and cell-extracellular matrix interactions, β3 integrins are important for the maintenance of tissue integrity, the promotion of cellular migration, the regulation of gene expression, and cell survival, adhesion and differentiation (Switala-Jelen et al., 2004).

Fig 1.3 The αIIb (green) and β3 genes (red) of integrin αIIbβ3 are located at the chromosome 17q21.32. Some adjacent genes are shown in grey color.

αIIbβ3, a receptor for fibrinogen, vWF, fibronectin, and vitronectin, is absolutely required for platelet aggregation (Bennett, 2005). On resting platelets, αIIbβ3 is inactive, but when platelets are exposed to agonists such as thrombin, ADP and platelet-activating factor, αIIbβ3 undergoes changes to assume the extended, active conformation that binds fibrinogen. Ligands binding to αIIbβ3 crosslink platelets into a homeostatic plug or thrombus (Bennett, 2001). Because αIIbβ3 plays an indispensable role in homeostasis and thrombosis, it is among the most intensively studied integrins.

αVβ3 is expressed on the surface of endothelial cells, smooth muscle cells, monocytes, and platelets (Switala-Jelen et al., 2004). The αVβ3 receptors recognize a wide range of extracellular matrix ligands that are similar to those recognized by αIIbβ3. Although αVβ3 mediates platelet adhesion to osteopontin and vitronectin in vitro (Bennett et al., 1997; Paul et al., 2003), it is uncertain whether it plays a role in platelet function in vivo. Increased expression of αVβ3 is observed on the vasculature in tumors and on several invasive malignant cells, indicating a role in tumor angiogenesis and metastasis (Li et al., 2001; Mizejewski, 1999). αVβ3 is expressed on osteoclasts and plays an important role in bone resorption (Shimaoka and Springer, 2003).

1.4 Ligands for LFA-1 and αIIbβ3

The experiments described in this thesis involved LFA-1 mediated adhesion to ICAM-1 and ICAM-3 and αIIbβ3 mediated adhesion to fibrinogen, these three ligands are therefore described in more detail. Ligands for LFA-1 and αIIbβ3 are summarized in Table 1.1 and Table 1.2.

1.4.1 ICAM-1 and ICAM-3

Intercellular adhesion molecules (ICAMs) are cell surface glycoproteins (IgG superfamily) expressed on a wide variety of cell types, they play a critical role in the in immune and inflammatory responses. They are ligands for LFA-1 and Mac-1. They contain two or more of immunoglobulin-like domain, with a short cytoplasmic tail.

ICAM-1 (CD54) has five IgSF modules in its extracellular domains, the binding site for LFA-1 is located in the first IgSF module (Staunton et al., 1990; Vonderheide et al., 1994). ICAM-1 is expressed at low to moderate levels on vascular endothelial cells and on some lymphocytes and monocytes (Rothlein et al., 1986). However, its expression can be stimulated with inflammatory cytokines (Dustin et al., 1986), tumor necrosis factor (TNF) (Pober et al., 1986a), interferon (IFN)γ and Lipopolysaccharide (LPS) (Pober et al., 1986b). Its upregulation on endothelial cells during inflammation points to the importance of LFA-1 mediated adhesion role in leukocyte trafficking. As a ligand to β2 integrin, it also participates in signal transduction across cell membrane when the signal transmit from outside of the cell to inside (Hubbard and Rothlein, 2000).

ICAM-3 (CD50) has five Ig-like domains sharing low homology to ICAM-1 in the extracellular region. Unlike ICAM-1, ICAM-3 is absent on the endothelium and it restricted to resting lymphocytes, monocytes and neutrophils, representing the major LFA-1 ligand on these cells (de Fougerolles and Springer, 1992; Fawcett et al., 1992). It was thought that ICAM-3 is important in initiating immune responses for its constitutive expression on lymphocyte (de Fougerolles and Springer, 1992). However, this concept may need to be revised when it was found that mouse does not have ICAM-3 (Sugino, 2005). Nonetheless, it is a useful ligand in characterizing LFA-1 activation states (Tang et al., 2005).

ICAM-3 expression has been demonstrated on dendritic epidermal Langerhans cells, whereas it is absent on dendritic cells from other lymphoid organs. A function of ICAM-3 in initiation of Langerhans cell-leukocyte interactions taking place during immune reactions localized to skin has been postulated (Manara et al., 1996).

1.4.2 Fibrinogen

Fibrinogen molecule is a dimeric soluble plasma protein comprised of two sets of disulfide-bridged Aα-, Bβ-, and γ-chains. Each molecule contains two outer D domains connected to a central E domain by a coiled-coil segment (Weisel, 2005) (Fig. 1.4). Fibrin is formed after thrombin cleavage of fibrinopeptide A (FPA) from fibrinogen Aα-chains, thus initiating fibrin polymerization (Mosesson, 2005).

Table 1.1 Ligands of β2 integrins (Modified from Gahmberg et al., 1998)

	Ligands for β2 integrins
LFA-1 (αLβ2)	ICAM-1, ICAM-2, ICAM-3, ICAM-4 and ICAM-5
Mac-1 (αMβ2)	ICAM-1, ICAM-2, ICAM-3, iC3b, fibrinogen, factor-X, neutrophil inhibitory factor, kininogen and denatured proteins
p150,95 (αXβ2)	ICAM-1, fibrinogen, iC3b, LPS, LPG and denatured proteins.
αDβ2	ICAM-3 and VCAM-1.

Table 1.2 Natural ligands of β3 integrins (from Switala-Jelen et al., 2004)

	Natural ligands for β3 integrins
αIIbβ3	collagen, denatured collagen, decorsin, disintegrins, fibronectin, fibrinogen, plasminogen,prothrombin, thrombospondin, vitronectin, Von Willebrand factor, *Borrelia burgdoferi*
αVβ3	adenovirus penton base protein, bone sialoprotein, cytotactin, denatured collagen, disintegrins, fibronectin, fibrinogen, HIV Tat protein, laminin, matrix metalloproteinase-2, osteoponin, prothrombin, thrombospondin, Von Willebrand factor, vitronectin, *Candida albicans*

Fibrin(ogen) plays an important role in blood clotting, fibrinolysis, cellular and matrix interactions, inflammation, wound healing, angiogenesis, and neoplasia (Laurens et al., 2006). Through binding to fibrinogen, cross-linking of αIIbβ3 on platelets by fibrinogen is required for platelet aggregation, which is crucial in thrombus formation. The diagram of fibrinogen binding to αIIbβ3 is shown in Fig.1.5. Fibrinogen also binds to αMβ2 and αXβ2, and is involved in inflammation by facilitating leukocyte adhesion to fibrinogen-deposited tissue and implants. Besides fibrinogen, other natural ligands for β3 integrins are presented in Table 1.2.

All these ligands have an RGD or RGD-like motif that is exposed in the central part of their receptor-binding site. The sequences containing RGD and RGD-like motifs are key to β3 integrin interaction. Such sequences in integrin ligands are frequently flexible and often occur in loop regions (Kodandapani et al., 1995). The crucial recognition motif in αIIbβ3 is an RGD-like Lys-Gln-Ala-Gly-Asp-Val (KQAGDV) motif near the C-terminal end of the γ-subunit, although two RGD sites in the α-subunit may also be recognized (Shimaoka and Springer, 2003).

1.5 Integrin structures

Integrin is formed by two non-covalently associated subunits, α and β both are type I transmembrane glycoprotein. They have a large extracellular domain, a single transmembrane domain, and a short cytoplasmic tail. The electron microscopy shows that (Du et al., 1993; Weisel et al., 1992), the overall shape of the extracellular domain is a global headpiece with two long stalk anchoring the integrin to the membrane.

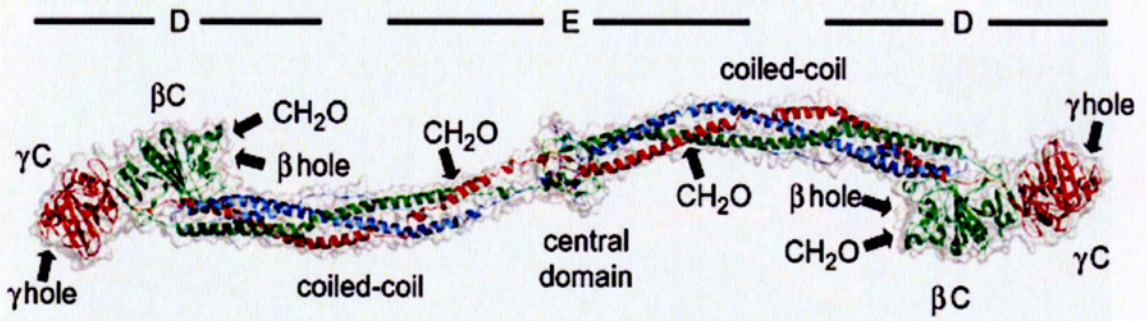

Fig. 1.4 X-ray crystallographic structure of fibrinogen. The Aα chains are blue, while the Bβ chains are green, and the γ chains are red. Most of the C-terminal portion of the chains is missing. The extent of fragments D and E, created by plasmin cleavage in the middle of the coiled coil, are indicated. The central domain is connected to the endregions via α-helical coiled-coil rodlike regions. The βC and γC nodules contain the holes that are complementary to the knobs in the central nodule, carbohydrate attachment sites are indicated by CH_2O. (from Weisel, 2005)

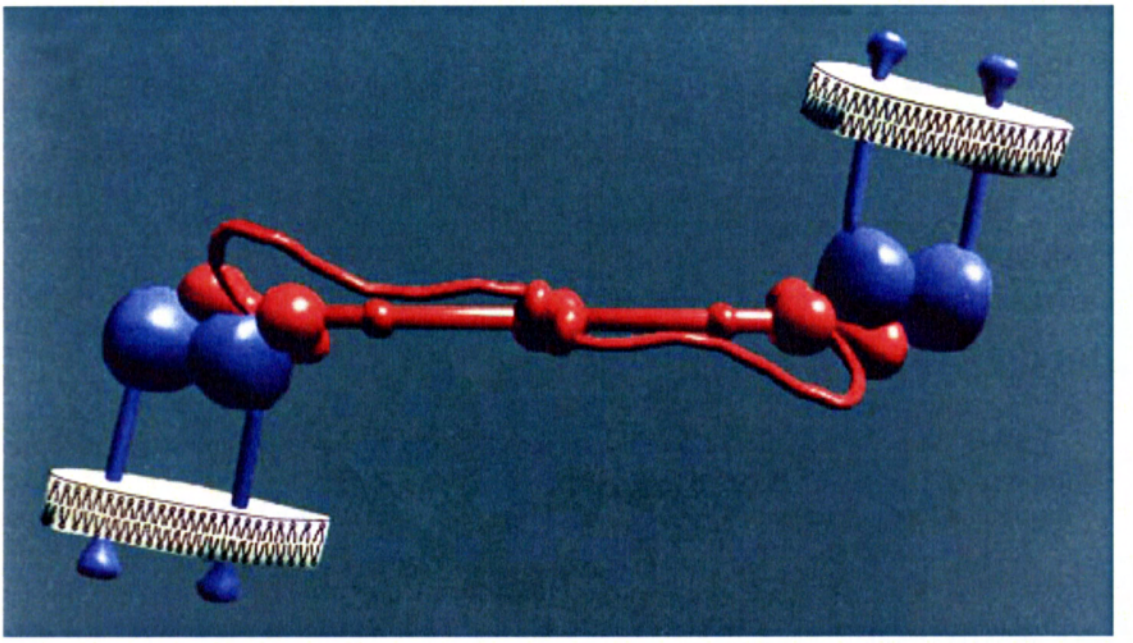

Fig. 1.5 Fibrinogen binding to the integrin αIIbβ3 in platelet aggregation. Diagram of fibrinogen-αIIbβ3 interactions, with fibrinogen in red and αIIbβ3 in blue. Two activated αIIbβ3 complexes, each with separated tails in the membrane of a different platelet, bind to the C-terminal chain at the ends of a fibrinogen molecule, such that the fibrinogen molecule forms a bridge between adjacent platelets. The shape and orientation of the proteins in the complex is based on structural studies. (from Weisel et al., 1992)

1.5.1 The α-subunit

The extracellular region of the integrin α-subunit is linearly organized to contain, from the N-terminus, β-propeller, thigh, genu, calf-1 and calf-2 domains (Takagi and Springer, 2002) (Fig. 1.6). Nine of eighteen α subunits also contain a inserted (I) domain in the β-propeller (see later).

1.5.1.1 β-propeller

Seven segments of about 60 amino acids in the N-terminal region have been predicted to fold into a seven-bladed β-propeller domain (Springer, 1997), which is analogous to the Gα/Gβ complex in G proteins. Each of the seven blades comprises four anti-parallel β-strands. Strands 1, 2, 3 and 4 are connected by successive hairpin turns, and strand 4 of one blade is connected to strand 1 of the next (Fig. 1.7). The inner strands (strand 1) line the channel at the center of the propeller, strands 2 and 3 of the same repeat radiate outwards, and strand 4 form the outer edge of the blade (Xiong et al., 2001).

Three solvent-exposed Ca^{2+} binding site are found in the loop connecting the strands 1 and 2 for blades 5-7 at the bottom of the propeller from the structure (Xiong et al., 2001). An additional site can be found in blade 4 of some integrin α subunits (Springer et al., 2000). The presence of calcium is likely to make the interface more rigid (Xiong et al., 2001). The β-propeller domain directly participates in ligand recognition in those integrins that lack a I-domain (Humphries, 2000).

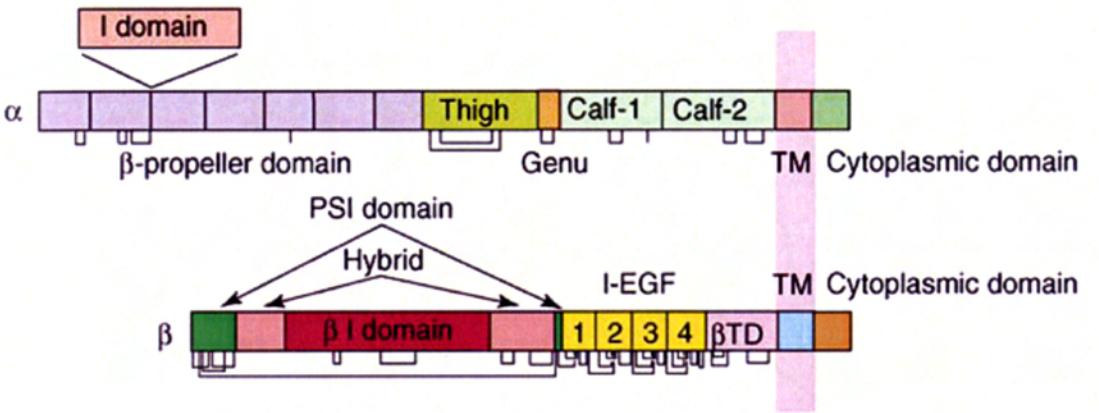

Fig. 1.6 Integrin domain organizations. Different domains are demonstrated. I-domain in the α subunit exits only in some integrins (from Luo et al., 2006).

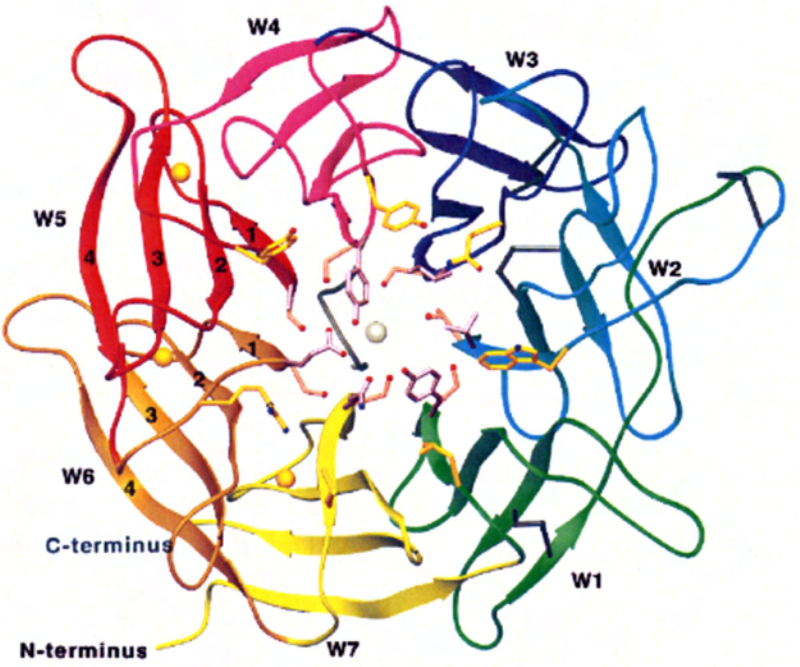

Fig. 1.7 α subunit β-propeller. Ribbon diagrams of the model for the integrin α4-subunit β-propeller domain. Views are from the top. Each blade of the β-propeller is shown in a different color and labelled W1-W7. The stands of each blade are labelled 1-4, from the center. A hypothetical polypeptide finger in the central cavity is gray. Cysteines in disulfides are black. Ca^{2+} ions and a hypothetical Mg^{2+} ion are gold and silver spheres, respectively. (from Springer, 1997).

1.5.1.2 I-domain

Nine of the eighteen human α-subunit (α1, α2, α10, α11, αE ,αL, αM, αX and αD) contain an additional I-domain, which is inserted between blades 2 and 3 of the β-propeller domain of the α subunit (Springer, 1997). The I-domain is composed of approximate 200 amino acids and is homologous to the von Willebrand factor A domain (Fig. 1.8). The I-domain adopts the dinucleotide-binding or Rossmann fold, with a central hydrophobic β-sheet surrounded by a number of α-helices (Emsley et al., 1997; Lee et al., 1995b; Legge et al., 2000; Mould et al., 2003c)

I-domain is the major ligand-binding domain in those integrins with an I-domain. It had been demonstrated that deletion of the I-domain in integrin αL abolished its binding to ligands (Leitinger and Hogg, 2000; Yalamanchili et al., 2000), and the isolated αL I-domain which is locked into high affinity is sufficient to bind ligands (Lu et al., 2001b).

Binding of the I-domain to ligand is divalent cation-dependent. A divalent cation coordination site designated the metal-ion-dependent adhesion site (MIDAS) binds negatively charged resides in the ligand, which is located on the upper surface of the I-domain. The cation in the MIDAS is ligated by five side chains located in the β1-α1, α2-α3, and β4-α4 loops. Three coordinating residues in the first loop reside in a characteristic sequence of I-domain, DXDXS. Mn^{2+} and Mg^{2+} have been shown to enhance ligand binding, whereas high concentration of Ca^{2+} results in the inactivity of integrin (Shimaoka et al., 2002b).

Two crystal structures of αM I-domain was obtained in the presence of different metal

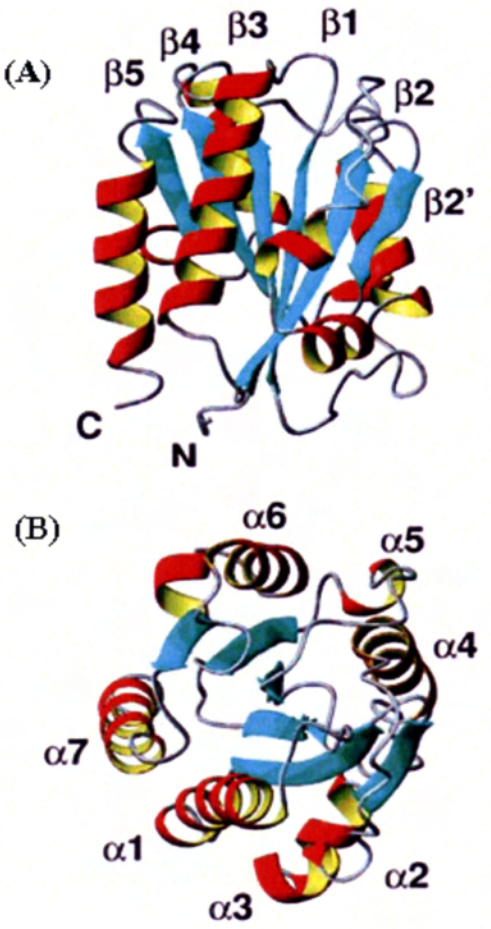

Fig. 1.8 Ribbon diagram of the mean NMR structure of the I-domain of αL subunit showing helices (red/yellow), β-sheets (blue) and loops (gray). The structure is rotated by 90° between views (A) and (B) in order to highlight the (A) β-sheet and the (B) α-helices. The location of the metal ion is not shown, but it would be in the top right of the molecule in A (from Legge et al., 2000).

ions (Lee et al., 1995a; Lee et al., 1995b). One is with Mg^{2+} representing the open form with a ligand-mimetic contact. The other one is with Mn^{2+} showing the closed form with no ligand binding. They differed in the structure of the surrounding loops and in the position of the C-terminal α-helix. In the open form (Fig. 1.9 A), two serines and one threonine make electrostatic bonds to Mg^{2+} via their side chains; two water molecules also interact with Mg^{2+} and two aspartic acids make indirect contacts via water molecules. In addition, the side chain of a glutamate residue from a neighboring I-domain completes the coordination sphere, which may be viewed as a liganded I-domain.

In the closed conformation (Fig. 1.9B), the bond to Thr^{209} is broken and replaced by a direct bond to Asp^{242}, thus reducing the electrophilicity of the metal. Three water molecules complete the coordination sphere. There is no equivalent of the exogenous glutamate, therefore the Mn^{2+} I-domain appears to be unliganded. The largest movement in the transition from the closed to the open structure is the C-terminal helix α6 which moves 10Å down the side of the domain (Lee et al., 1995a) (see later). The structural difference between the ligand bound and nonliganded of the I-domain in the α2 and αL subunit are remarkably similar to those of the αM I-domain (Emsley et al., 1997; Emsley et al., 2000; Huth et al., 2000; Legge et al., 2000).

1.5.1.3 Thigh, calf-1 and calf-2

C-terminal to the β-propeller are three large β sandwich domains: thigh, calf-1 and calf-2 (Xiong et al., 2001). The contact between the propeller and thigh domains has a surface

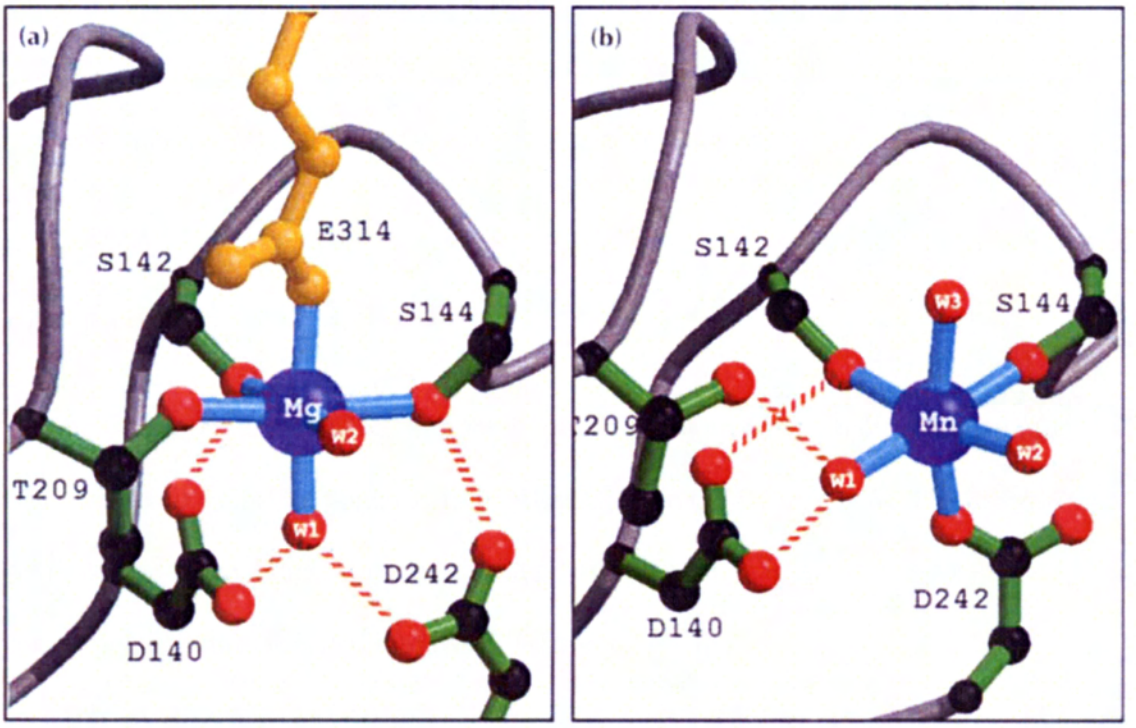

Fig. 1.9 Structural comparisons of the Mg^{2+} and Mn^{2+} I-domains. (a) The MIDAS motif in the Mg^{2+} form. (b) The MIDAS motif in the Mn^{2+} form. The color code is oxygen atoms (red), carbon (black), schematic backbone (grey) and the glutamate from a neighbouring molecule (gold).Water molecules are labelled wl-w3. Selected hydrogen bonds are shown as dashed red lines (form Lee et al., 1995a.)

area of ~700 $Å^2$, there maybe some interdomain movement in this area during activation, which could be regulated by the calcium ions in the propeller. Between the thigh and calf-1 is the "genu", which is capped by a divalent cation. It has been shown that the genu/calf-1 interface is important in maintaining integrin activation, and the extension of the integrin legs may occur by a structural rearrangement at the thigh/genu interface (Xie et al., 2004). The interface between calf-1 and calf -2 domains (~500 $Å^2$) is largely hydrophobic, suggesting that these two domains form a rigid structural entity (Xiong et al., 2001).

1.5.2 The β subunit

The β-subunit ectodomain consists of eight domains: PSI domain, the hybrid domain, the I-like domain, four EGF-like domains and a β-tail domain (βTD) (Fig. 1.6). The integrin β-subunit contains two domain insertions: the β I-like domain is inserted in the hybrid domain, which is in turn inserted into the PSI domain.

1.5.2.1 PSI domain

The N-terminal cysteine-rich region of β-subunit share sequence homology with membrane protein including plexins and semaphorins, it is therefore known as the PSI (for plexin-semaphorin-integrin) domain (Bork et al., 1999). The integrin PSI forms a two-stranded antiparallel β-sheet flanked by two short helices, and a highly conserved side chain of Trp^{25} form a small hydrophobic core of this domain. The integrin PSI contains four cysteine pairs connected in a 1-4, 2-8, 3-6, 5-7 pattern with the eighth

cysteine being located, in the primary structure C-terminal to the hybrid domain (Xiong et al., 2004).

1.5.2.2 Hybrid domain

The hybrid domain is a β-sandwich domain that is folded from amino acid sequence segments on either side of the I-like domain. From the structural data, the hybrid domain is inserted into the last loop of PSI domain (Xiong et al., 2004).

In α5β1, Mould et al (Mould et al., 2003c) have provided biochemical evidence that activation of the head region involves a swing of the hybrid domain away from the β subunit which is coupled to the downward shift of the C-terminal α helix of the I-like domain. Several antibodies that mapped to this domain can only stain the integrin when it was activated, which also suggest that the hybrid domain may be displaced outward during integrin activation (Mould et al., 2003c; Tang et al., 2005). The displacement of the hybrid domain had also been shown to be important in propagation of the activation signal in αLβ2 (Tan et al., 2001a; Tang et al., 2005; Tng et al., 2004), and part of this work will be discussed in this thesis.

1.5.2.3 I-like domain

I-like domain of β subunit, which is inserted in the hybrid domain, is the ligand binding domain in integrins that lack I-domain in α subunit. It assumes the nucleotide-binding (or Rossmann) fold found in Gβ and integrin α I-domains and it contains a putative metal-binding DXSXS sequence motif similar to that of the MIDAS in the α subunit I-domain (Lee et al., 1995b; Ponting et al., 2000). In addition to the basic structure of the I-domain,

it contains two extra loops. One is named SDL (specificity determining loop) (Takagi et al., 2002a) which is crucial for integrin dimer formation and ligand binding; the other forms the main interface with the β-propeller domain of the α subunit (Arnaout et al., 2005).

I-like domain consists of a central six-stranded β sheet surrounded by eight helices. The MIDAS motif occupies a crevice at the top of the central β strand, as in the α I-domains (Lee et al., 1995b). The overall geometry of the metal-ligand coordination is similar to that of α I-domain. Mutation of MIDAS in β2 I-like domain abolishes ligand binding by αLβ2 (Bajt et al., 1995). Unlike the I-domain, the I-like domain has two additional metal ion coordination sites. Adjacent to MIDAS lies a metal ion-binding site (ADMIDAS) and it was previously predicted to be an inhibitory high Ca^{2+} binding site and an active Mn^{2+} binding site (Nishida et al., 2006). Mutation of ADMIDAS in αLβ2 (Nishida et al., 2006) and α4β7 activated ligand binding (Chen et al., 2003). A ligand-induced-metal-binding-site (LIMBS) is located in the I-like domain, which is only 6Å away from the MIDAS. All the residues coordinating LIMBS are conserved in I-like domains (Xiong et al., 2002). LIMBS were assigned as the Ca^{2+} binding site (Xiao et al., 2004), LIMBS mutations have been reported to abolish ligand binding to α4β7 (Chen et al., 2003) and also abolish ligand binding to αLβ2 (Kamata et al., 2002). Collective data from α4β7 (Chen et al., 2003), α5β1 (Mould et al., 2003a) and αLβ2 (Nishida et al., 2006), suggest that the LIMBS and ADMIDAS are the site for positive and negative regulations by Ca^{2+}, respectively.

1.5.2.4 IEGF domain

Following the hybrid domain are four tandem cysteine-rich repeats (IEGF domains), similar to the epidermal growth factor (EGF) modules. The boundaries of these modules were defined (Tan et al., 2001b) and the paring of cysteines in these repeats have been characterized in the C1-C5, C2-C4, C3-C6, C7-C8 pattern (Takagi et al., 2001a). The EGF domains found in the integrins as well as those in TIED (ten β-integrin EGF-like repeat domains) are distinct from the EGF domains found in the laminin whose eight cysteines are arranged in the C1-C3, C2-C4, C5-C6, C7-C8 pattern. Unlike the integrin-EGF domains 2, 3, and 4, each of which has 8 cysteine residues, the IEGF1 has only a total of 6 cysteines engaged in three disulfide bonds with the C2-C4 disulfide pair missing (Shi et al., 2005).

Three β2 activating antibodies KIM185, MEM48 and KIM127 are located in the different domain of the four EGF domains. The KIM127 epitope localizes within cysteine-rich repeat 2, MEM48 bind to epitopes in cysteine-rich repeat 3, and mAb KIM185 maps near the end of cysteine-rich repeat 4 (Lu et al., 2001a).

Two crystal structures of the IEGF domains of β2 have been solved in our laboratory (Shi et al., 2007; Shi et al., 2005). Their significance will be discussed in Section 1.8 in association with conformational change of the integrins during activation.

1.5.2.5 βTD

β2 tail domain (βTD) consists of a four-strand β sheet that contain antiparallel and parallel strands and face an NH2-terminal α helix (Xiong et al., 2001). In the structure,

only two weak hydrophobic contacts are found between βTD and EGF4, indicating the interface between them is flexible (Xiong et al., 2001). In the β3 integrins, βTD is not essential for heterodimer formation, but it can restrain β3 integrin in a resting, low ligand-affinity state (Butta et al., 2003).

It has been reported that the variation of contact region between the βTD and the β I-like domain can regulate integrin αMβ2 binding to iC3b, which suggests βTD plays a role in integrin activation (Gupta et al., 2007). However, another study demonstrated that the mutation or deletion the β3 tail domain loops had no effect on the ligand binding of integrin αVβ3 and αIIbβ3 (Zhu et al., 2007a).

1.5.2.6 Transmembrane (TM) domain

The transmembrane segment is about 25-29 amino acid long, it is likely tilted or coiled inside the membrane (Armulik et al., 1999). Modulation of the interhelical TM interface has been suggested to involve in signaling in both directions across the membrane, however, there is no consensus on the precise nature of the TM interface movement and its effect on activation (Arnaout et al., 2005).

1.5.2.7 Cytoplasmic domain

The cytoplasmic domain of integrin α and β subunit are comparatively short, generally with only 20-40 and 45-60 residues in length, respectively. Integrin β4 is an exception, which is specialized to connect to the keratin cytoskeleton and contains fibronectin type-III domains (Hynes, 2002). The cytoplasmic domains of integrins play a pivotal role in

the bi-directional signaling processes, through interaction with the cytoskeleton proteins, signaling molecules and other cellular proteins.

Deletion of the membrane proximal seven residues of the β3 subunit cytoplasmic causes constitutive ligand binding of αIIbβ3, indicating that this membrane proximal region of the β3 subunit is critical to maintain αIIbβ3 in a low affinity state (Hughes et al., 1995). Complete truncation of the β2 cytoplasmic domain also resulted in constitutive activation of αLβ2 and αMβ2, demonstrating the importance of this membrane proximal region in the regulation of integrin adhesive function (Lu et al., 2001d).

Integrin β cytoplasmic tails make direct association with many signaling and structural proteins, which include actin-binding proteins, enzymes, adapter proteins, transcriptional co-activator and additional proteins of unknown function (Liu et al., 2000). The first cytoplasmic protein that was shown to bind to integrin β is the actin-binding protein talin (Horwitz et al., 1986). Their interaction is important for a variety of integrin function (Liu et al., 2000)

Unlike the β subunit, different α subunit cytoplasmic domains share little sequence similarity. However, all integrin α subunits cytoplasmic tails contain a conserved "GFFKR" sequence at the membrane proximal region. The α subunit cytoplasmic domain is important in the regulation of integrin-mediated biological responses. For example, R-ras can enhance α4β1 mediated cell migration. Migration is enhanced by R-ras when the α4 cytoplasmic tail is replaced by that of α2, but decreased when replaced with that of α5 subunit (Keely et al., 1999).

"GFFKR" is important for retaining integrin in its resting state, deletion of this sequence in α subunit cytoplasmic domain results in an active αIIbβ3 (Lu and Springer, 1997). Similarly, removal of this sequence from integrin αL subunit can promote αLβ2 clustering and make it constitutively active (van Kooyk et al., 1999).

Interaction between the α and β tails is important in regulating integrin function. Mutagenesis studies suggest that R^{995} from the αIIb subunit cytoplasmic tail and D^{723} from the β3 tail forms a salt bridge, which stabilizes the association of the membrane proximal regions and maintain αIIbβ3 in a low affinity state (Hughes et al., 1996).

Some cellular proteins that can directly associate with a cytoplasmic domain have been identified, for instance, F-actin binds to the α2 cytoplasmic domain (Kieffer et al., 1995), calreticulin can directly interact with the GFFKR motif (Rojiani et al., 1991); paxillin, an intracellular adaptor protein, binds directly and tightly to the α4 tail (Liu et al., 1999).

1.6 Integrin related diseases

1.6.1 Leukocyte Adhesion Deficiency type I

More than 25 years ago, a group of patients were diagnosed with delayed separation of the umbilical cord, neutrophilia, neutrophil defects and recurrent bacterial and fungal infections and impaired wound healing (Crowley et al., 1980). Subsequently, these patients were found to have defective β2 integrins. Molecular analysis showed that the defect is due to mutations in the β2 integrin gene. The disease is now known as leukocyte adhesion deficiency (LAD)-I.

The degree of severity of the symptoms of LAD-I is correlated with the level of CD11/CD18 expression and residual adhesion activities on the patient's leukocytes. Patients with less than 1% normal levels of CD11/CD18 are susceptible to frequent and life threatening systemic infection (severe form). Patients with higher level of CD11/CD18 expression up to 10% of normal may survive up to adulthood with proper medical care (Anderson et al., 1985).

The molecular basis of LAD-I can be broadly categorized into two main groups. One group of mutations leads to grossly abnormal gene products. These mutations include nucleotide deletion and abnormal splicing defects. Grossly abnormal gene products can also arise from nonsense mutations in which a stop codon replaces an amino acid codon, leading to premature termination of translation.

The second group of mutation involves missense mutation, which results in a protein in which one amino acid is substituted for another. Biochemically, CD18 with these mutations translate into either a non-expressed CD18 protein, or the expression of a non-functional CD18 protein (Hogg et al., 1999). There are also mutations, which result in a differential ability to associate with the three CD11 subunits to form the LFA-1, Mac-1 and p150, 95 heterodimers (Shaw et al., 2001), and/or with abnormal adhesion properties.

To date, there are 18 different missense mutations described at the molecular level. All the missense LAD-1 mutations found are listed in the Table 1.3. Most mutations do not support CD11/CD18 expression or at a very low level. Two mutations $S^{116}P$ (Hogg et al.,

1999) (MIDAS) or $D^{219}H$ (Mathew et al., 2000) (LIMBS) were capable of supporting the expression of LFA-1, Mac-1 and p150,95, but none of CD11/CD18 with these two mutations possess any adhesion activities. Most LAD-I mutations located in the I-like domain of the β2 subunit results in impaired integrin heterodimer formation or defective function. Surprisingly, LFA-1 with mutation $N^{329}S$ can constitutively adhere to ICAM-1 and ICAM-3. Another two mutations $R^{571}C$ and $C^{568}R$ which are located in the IEGF-4 also can promote LFA-1 to constitutively adhere to ICAM-1, though their expression are lower than the wild type (Shaw et al., 2001). The mechanism of these three mutations activate β2 integrin will be studied in this thesis work.

1.6.2 Leukocyte Adhesion Deficiency type II

Patients with LAD-II have a defect in the fucosylation of various cell surface glycoproteins, some of which function as ligands for selectins. As a result, the initial "rolling" of leukocytes over the endothelial vessel wall in areas of inflammation is disturbed. Thus, the leukocytes do not slow down, leading to decreased leukocyte adhesion to the vessel wall and decreased transendothelial migration into the tissues. The molecular defect in LAD-II has been identified as a deficiency in a GDP-fucose transport protein in the Golgi system (Luhn et al., 2001).

1.6.3 Galnzmann's thrombasthenia's

Glanzmann thrombasthenia (GT) is an autosomal recessive bleeding disorder characterized by deficient or dysfunctional glycoprotein (GP) IIb/IIIa (αIIbβ3) complex. The hallmark of the disease is impaired platelet aggregation stemming from

Table 1.3 Missense LAD-1 mutations

Nucleotide changes	Amino acid change	References
-64T → A	-21 Met → Lys	Sligh et al., 1992
316 G → A	106 Asp → ASn	Matsuura et al. 1992
326 A → C	109 Tyr → Ser	Uzel et al., 2007
346T → C	116 Ser → Pro	Hogg et al.1999
380 T → C	127 Leu → Pro	Wright et al. 1995
439 G → A	147 Gly → Arg	Wardlaw et al.1990
467C → T	156 Pro → Leu	Back et al. 1992
521 A → C	174 Lys → Thr	Arnaout et al., 1990
625 G → c	209 Asp → His	Mathew et al.2000
688 T → C	230 Trp → Arg	Roos et al. 2002
787 C → T	248 Ala → Val	Shaw et al. 2001
751 G → A	251 Gly → Arg	Hogg et al., 1999
784 G → A	262 Gly → Ser	Wright et al., 1995
955 G → C	319 Ala → Pro	Shaw et al. 2001
986 A → G	329 Asn → Ser	Nelson et al., 1992
1690 C → T	564 Arg → Trp	Nelson et al., 1992
1702 T → C	568 Cys → Arg	Shaw et al.,2001
1711 C → T	571 Arg → Cys	Wright et al., 1995

defective fibrinogen binding to GPIIb/IIIa. Affected patients exhibit a prolonged bleeding time, absent of clot retraction and failure of platelets to aggregate in response to ADP, collagen, thrombin and epinephrine, but ristocetin-induced aggregation remains intact (Seligsohn, 2002).

Patients with severe (less than 5% of normal) GPIIb/IIIa deficiency are termed type I, patients with moderate (10–20% of normal) GPIIb/IIIa deficiency are termed as type II, and the patients with half normal to normal GPIIb/IIIa levels were termed variants (George et al., 1990). Some Glanzmann's thrombasthenia patients have been reported with normal or near normal levels of GPIIb/IIIa but with their platelets fail to bind fibrinogen and the ability to aggregate (Ginsberg et al., 1986). Currently, more than 100 mutations in either GPIIb gene or GPIIIa gene have been reported (Seligsohn, 2002).

1.7 Inside-out and Outside-in signaling

1.7.1 Inside-out signaling

Circulating peripheral blood lymphocytes (PBLs) generally express a resting form of LFA-1 that does not bind ligands. Intracellular signals can be generated after lymphocyte activation, for instance through the T-cell receptor TCR/CD3 complex or by phorbol 12-myristate 13-acetate (PMA) or encountering chemokines, which cause the transient activation of LFA-1 to bind ligands (Dustin and Springer, 1989; van Kooyk et al., 1989). In the unstimulated platelet, αIIbβ3 is in a resting state. After activated by thrombin or ADP, it undergoes conformational changes in the extracellular domain that result in

increased affinity for adhesive ligands (Shattil and Newman, 2004). All these process are referred to as "inside-out" signaling.

"Inside-out" activation signals are propagated from the integrin cytoplasmic tail across the plasma membrane to allosterically induce ligand binding of the ectodomian of integrin. For an inside-out activation signal to be propagated, it must pass through the TM and cytoplasmic tail, so the cytoplasmic tail and the transmembrane domain have been regarded as the key integrators of inside-out signaling. Deleting or mutating in the cytoplasmic and transmembrane domain invariably leads to constitutive active integrins (Hughes et al., 1996; Hughes et al., 1995; O'Toole et al., 1991; Peterson et al., 1998). It is proposed that membrane-proximal helices of the α and β subunits were found to a clasp in a weak "handshake" which, when disrupted, would lead to integrin activation (Vinogradova et al., 2002).

1.7.2 Outside-in signaling

Extracellular ligand binding to integrin, initially reversible, becomes progressively irreversible, and promotes clustering of integrin on the cells, and further conformational changes that are transmitted to the cytoplasmic tails. This results in the recruitment and/or activation of enzymes (e.g. FAK/C-Src complex, Ras and Rho GTPase), adaptors (e.g. Cas/Crk, Paxillin), and effectors to form integrin-based signaling complexes, leading to downstream signaling events (Shattil and Newman, 2004). This process is called outside-in signaling.

It has been demonstrated that binding of soluble, monovalent ICAM-1 to K562 cells can cause spatial separation of αL and β2 cytoplasmic tail but no detectable αLβ2 micro clustering (Kim et al., 2003). However, the binding of multivalent ligand fibrinogen caused detectable αIIbβ3 clustering (Buensuceso et al., 2003). Micro clustering of α5β1 has also been demonstrated in fibronectin-adherent cells (Wiseman et al., 2004). Because of multivalent nature of the physiological ligands of integrin, it is possible that both integrin clustering and intramolecular modulation contribute to the overall outside-in signal transduction.

Several protein kinases and phosphatases have been demonstrated to attach directly to integrin, which provide a logical mechanism for initiation of outside-in signaling. For example, Src family protein kinases (SFKs) involve in numerous aspects of adhesion signaling, which is required for integrin mediated cellular response (Klinghoffer et al., 1999). Integrin clustering can promote the activation of SFK by initiating the autophosphorylation of SFKs tethered to the cytoplasmic tails (Shattil, 2005).

1.8 Integrin conformational regulation

Numerous functional and structural data had confirmed that integrins undergo conformational changes when it becomes activated or binds to ligand.

1.8.1 From bent to extension

An extended integrin extracellular domain with a globular head connected to two legs of extended from had been demonstrated in several EM studies (Du et al., 1993; Nermut et al., 1988; Takagi et al., 2001b). However, the major advance in understanding the

conformation and function of integrin come from the X-ray structure αVβ3 (Xiong et al., 2001). The crystal of αVβ3 extracellular domain showed a compact, V-shaped structure. The αV subunit is bent at the "genu" located between the thigh and calf-1 domain. The IEGF domain of the β3 subunit was poorly resolved in this structure, but the bent must occur somewhere within the integrin (Xiong et al., 2001). This bent αVβ3 is also observed by negative stain electron microscopy in later studies (Takagi et al., 2002b). Subsequently, the crystal structures of a complex consisting of the part of the extracellular domain of αIIbβ3 revealed an open, presumably high-affinity conformation (Xiao et al., 2004), which matched the EM images of the ligand binding extended αVβ3 (Takagi et al., 2002b).

The I-EGF1 and I-EGF2 domains are not resolved in the αVβ3 structure because of poor electron density (Xiong et al., 2001) and are absent in the αIIbβ3 head piece structure (Xiao et al., 2004). In our laboratory, the structure of PHE1 fragment comprising the PSI/Hybrid domain/I-EGF 1 of the β2 subunit was determined (Shi et al., 2005). The structure reveals an elongated molecule with a rigid architecture stabilized by nine disulfide bonds (Fig. 1.10A). Superposition with the integrin β3 receptor in its bent conformation suggests that the bend in the β2 subunit is present at the linkage between its I-EGF1 and I-EGF2 modules and emphasize the importance of this region in integrin conformational change.

Based on the PHE1 structure, we have further determined the structures of two fragments of integrin β2 subunit (Shi et al., 2007). The first fragment (PHE2), consisting of the PSI,

hybrid, I-EGF1 and I-EGF2 domains, showed an L-shaped conformation with the bend located between the I-EGF1 and I-EGF2 domains (Fig. 1.10B). By introducing disulfide bond in the integrin β2 subunit, we found that the bent conformation adopted by LFA-1 integrins mirrors the PHE2 structure (see Chapter 5). The second fragment PHE3, which includes, in addition to PHE2, the I-EGF3 domain, showed an extended conformation (Fig. 1.10C). The extended structure of PHE3 reflects the extended conformer of LFA-1 because of its reactivity with the extension repoter mAb KIM127. The major reorientation of I-EGF2 with respect to the other domains in the two structures is accompanied by a change of torsion angle of the disulfide bond between Cys^{461}-Cys^{492} by 180° and the conversion of a short α-helix (residues Ser^{468}-Cys^{475}) into a flexible coil. The work on PHE1, PHE2 and PHE3 suggests that the conformational changes within the I-EGF2 domain may be a key to the transition between the bent (resting) and the extended (active) state of the β2 integrins.

Taken together, a bent integrin with close association of the α and β subunits, after activation, leads to moving apart of the juxtamembrane domains and separation of the α and β subunit stalks, results in dramatic rearrangement of the quaternary structure to an extended conformation. This transition from bent to extended conformation has been described as analogous to a "switchblade-like" movement (Fig. 1.11) (Beglova et al., 2002).

In an alternative integrin activation model, "deadbolt" model, inside-out signals are postulated to transmit conformational changes through the transmembrane helices into the immediately proximal β TD. It was proposed that α helix in the β TD interacts with

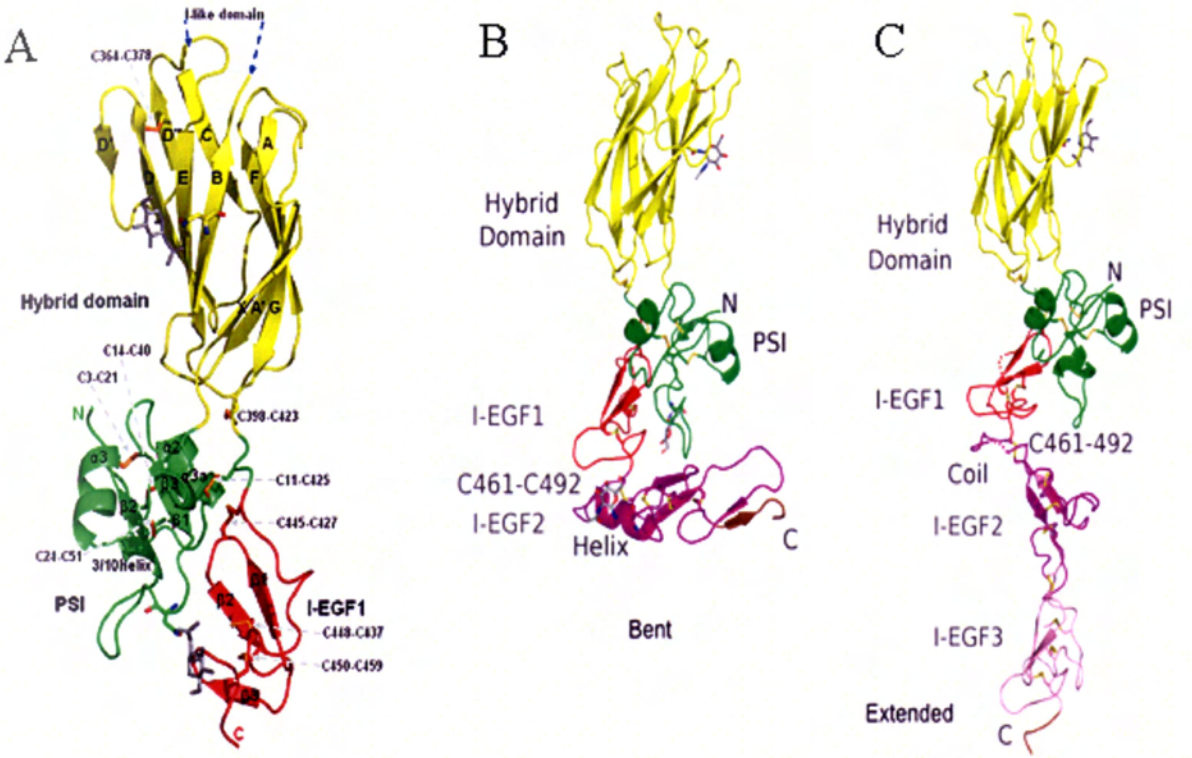

Fig. 1.10 Structures of PHE1, PHE2 and PHE3. (A) Overall view of the PHE1 molecule with its secondary structure elements labeled. The nine disulfide bridges and the two N-linked N-acetylglucosamine residues resolved in the structure are represented as sticks and labeled. The positions of the I-like domain insertion in the native integrin structure between β-strands βB and βC of the hybrid domain is indicated. **(B)** The structure of the PHE2 fragment. I-EGF2 is roughly perpendicular to the PSI hybrid tandem shown as a vertical arm here. **(C)** The structure of the PHE3 fragment, which features an extended conformation. The Cys^{461}-Cys^{492} disulfide bridge in IEGF2 is labeled, as well as the segment of the I-EGF2 domain that undergoes an order (α-helix in PHE2) to disorder (coil in PHE3) transition (from Shi et al., 2005, 2007).

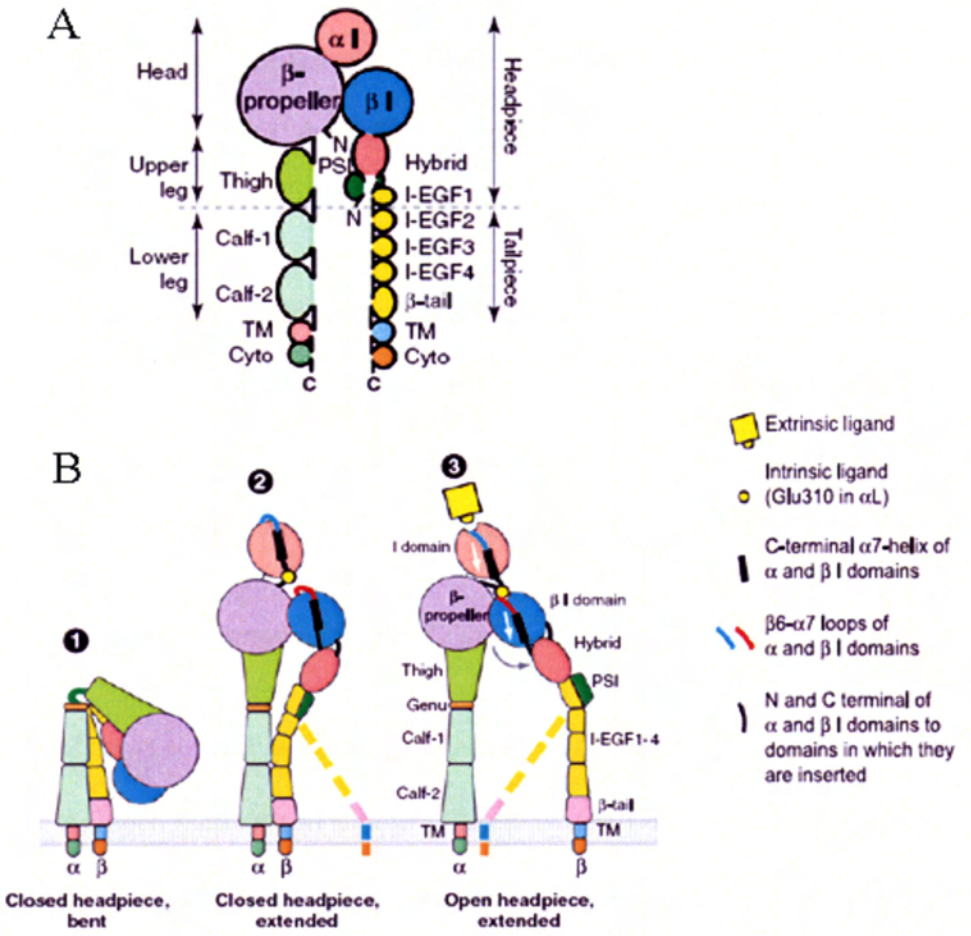

Fig. 1.11 "Switchblade-like" movement of integrin. (A) Schematic of the course of the α an β subunit polypeptidechains throug domains from the N to C termini. (I Rearrangement of domains during activation of integrins that contain α I domain. The β subunit lower leg are flexible and are therefore showr in what may be the predominant (*solid representation*) and less predominant (*dashed lines*) orientations. (from Luo et al., 2007) (C) Ribbon diagrams of the alternative conformations of the extracellular segment of αVβ3 integrin. (from Takagi et al., 2002b)

the β I-like domain α7 helix and "locks" the integrin in an inactive state. Inside-out activation through the cytoplasmic tail leads to some movement of the α helix in TD helix to unlock the adjacent βTD "deadbolt". Upon activation, the "deadbolt" slides away from β I-like domain, rendering it ligand binding competent (Arnaout et al., 2005).

Additional studies are required to thoroughly test and refine existing models of integrin activation and, in particular, to fully understand coordinated transitions among the integrin extracellular, transmembrane, and cytoplasmic domains, molecular movements that will likely affect outside-in as well as inside-out signaling.

1.8.2 Conformation change of I-domain and I-like domain

I-domain of the α subunit is the major ligand-binding domain in I-domain containing integrins. An open (active) and a closed (inactive) αM I-domain were crystallized and their structures were determined. When compared to the closed conformation, there is a 10Å movement of the C-terminal helix down the body of the I-domain in the open conformation, accompanied by a large rearrangement and downward movement of the loop connecting this helix to the preceding β-strands (Lee et al., 1995a; Lee et al., 1995b). It has been confirmed that the similar structure modulation of the β6-α7 loops take place in α2 (Emsley et al., 1997; Emsley et al., 2000).

Crystal structures of the closed, intermediate and open conformation of αL I-domain showed that downward movement of the β6-α7 loop with a disulfide bond could convey the conformational change from other domain to the I-domain (Shimaoka et al., 2003). An isolated αL I-domain when locked in the open conformation with a disulfide bond is

constitutively active (Lu et al., 2001b). The structural differences of β6-α7 loop in the open and close conformation of I-domain of α subunit is shown in Fig. 1.12.

The β I-like domain binds ligand directly in I-less integrins and it regulates binding ability of the integrin with an I-domain. Integrins with mutation in the I-domain can affect the ligand binding capacity of integrins (Bajt et al., 1995; Hogg et al., 1999). It was demonstrated that a conserved Glu^{310} in the I-domain of the α subunit, functions as an intrinsic ligand for the β I-like domain. It is thought that MIDAS of the β I-like domain binds to this Glu and exerts a pull on the α7 helix that activates the α I-domain (Yang et al., 2004b).

Similarly, I-like domain may be regulated by pulling down of the α7 loop. Disulfide bonds were introduced into the I-like domain of β3 integrin, to constrain its β6-α7 loop and α7 helix. Depending on the location of the disulfide bond, β3 integrin can be locked into high or low affinity (Luo et al., 2004). The deletion of the final turn in the C-terminal α-helix in β I-like domain also confer constitutive activation of the αLβ2 and α4β7 integrin (Yang et al., 2004a). This is in agreement with comparative analysis of the structures of the compact αVβ3 and the open headpiece αIIbβ3. From the compact unliganded αVβ3, the β1-α1 has to move inwards whereas the β6–α7 loop and the α7 helix move downward and assume the position in the liganded αIIbβ3 structure (Fig. 1.13A). Changes in metal ion coordination are closely related to loop movements in the β I-like domain. The LIMBS and MIDAS were not occupied in the unliganded-closed

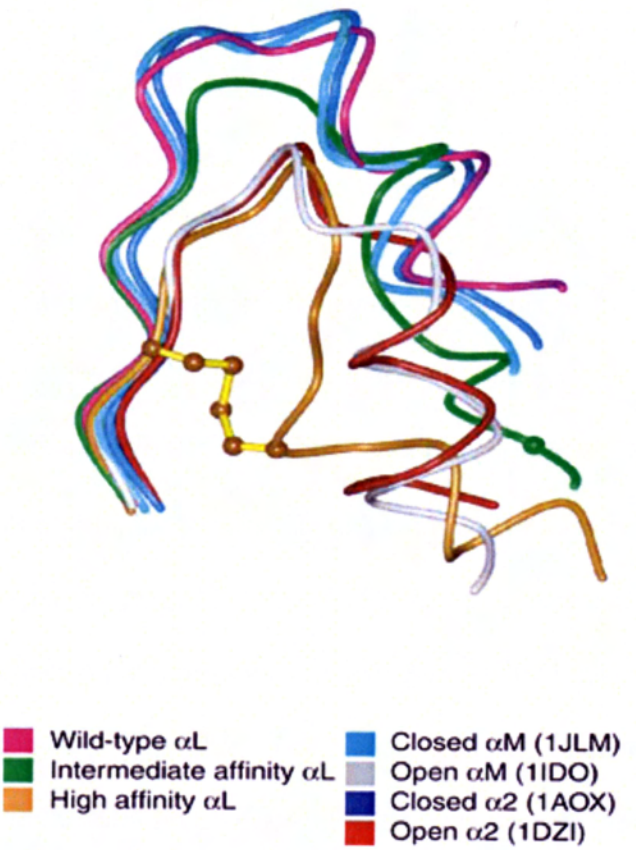

Fig. 1.12 The structure of β6-α7 loop of the I-domain. The C-terminal fragments encompassing the β6-α7 loop for the three unligated αL conformations and open and closed α2 and αM I-domain structures (color keys on bottom left and middle). The side chain bonds of Cys^{287} and Cys^{294} in the designed disulfide bridge in the high-affinity mutant are shown in yellow; the C atom of Cys^{299} in the designed disulfide of the intermediate mutant is shown as a green sphere. (from Shimaoka et al., 2003b.)

structure. Coordination of the Met^{335} backbone carbonyl in the β6–α7 loop to the ADMIDAS in the unliganded-closed conformation is broken in liganded-open αIIbβ3 (Fig. 1.13B).

1.8.3 The hybrid domain displacement

The most revealing information in αIIβ3 crystal structure is the piston-like displacement of the α7-helix resulting in a 62° reorientation between I-like and hybrid domain of the β3 integrin subunit when compared to the αVβ3 crystal structure (Fig. 1.14) (Xiao et al., 2004). It was proposed that this orientation plays a critical role in the global conformational change that regulates affinity. This hypothesis was supported by experimental data from other systems. Recombinant truncated α5β1 with a mutation $L^{358}A$ in the α7 helix of β I-like domain has high constitutive ligand binding activity. Two conformation-sensitive mAb 15/7 and HUTS-4, which were mapped to a region of the hybrid domain close to the lower face of I-like domain, are highly expressed on the this mutant α5β1 (Mould et al., 2003b). Therefore, it was suggested that the hybrid domain is involved in the transduction of conformational changes through β I-like domain, which is linked to a swing out of the hybrid domain. A glycan wedge at the interface of the I-like domain and the hybrid domain was introduced to open the angle between these two domains in αIIbβ3, αVβ3 and α5β1 integrins. They all show constitutively high affinity (Luo et al., 2003). The displacement of the hybrid domain had also been shown to be important in propagation of the activation signal in αLβ2 in our laboratory, because the mAb 7E4 located in the hybrid domain can block the signal

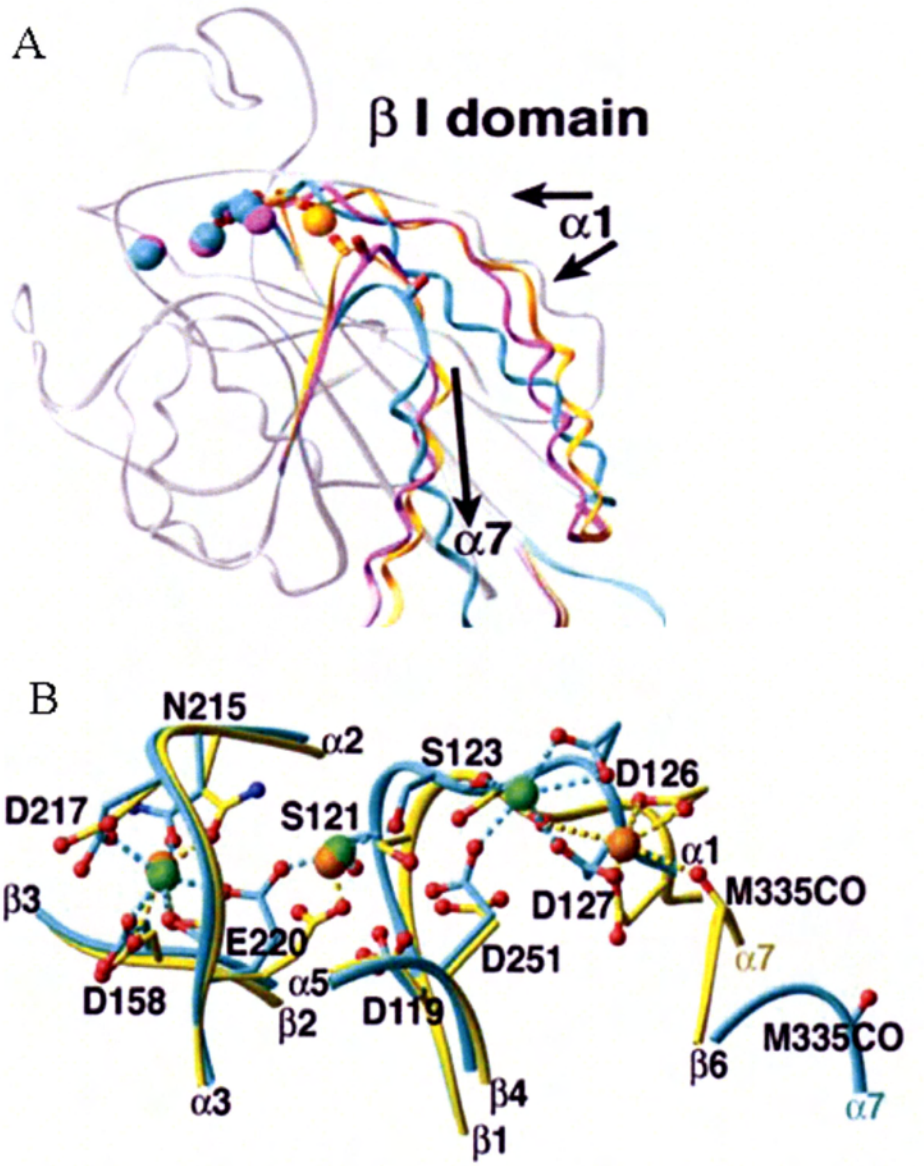

Fig. 1.13 β I-like domain structural change. **(A)** Overview of motions in the β3 I-like domains. Non-moving parts of the backbone are shown as a grey worm. Moving segments shown as Ca-traces are from unliganded-closed αVβ3 (gold), liganded-closed αVβ3 (magenta) and liganded-open αIIbβ3 (cyan). The direction of movement is shown with arrows. **(B)** β3 I-like domain metal coordination sites in liganded-open αIIbβ3 (cyan) and unliganded-closed αVβ3 (yellow). LIMBS, MIDAS and ADMIDAS positions are shown left to right in similar orientation as in A. The LIMBS and MIDAS were not occupied in the unliganded-closed structure. (form Xiao et al., 2004.)

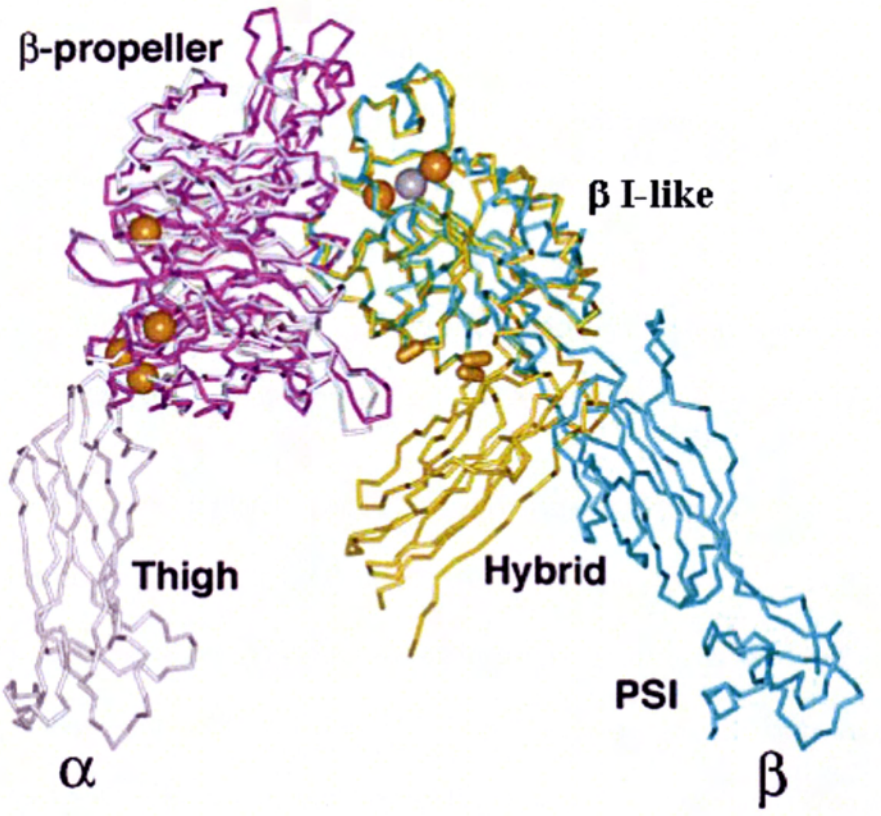

Fig. 1.14 Hybrid domain displacement. Liganded-open αIIbβ3 and unliganded-closed αVβ3 headpieces are superimposed using the β I-like domain β-sheet. The α and β subunits are colored magenta and cyan in αIIbβ3 and grey and yellow in αVβ3. Calcium and magnesium ions in αIIbβ3 only are gold and silver spheres, respectively. (from Xiao et al., 2004)

transduction from the membrane proximal side of the hybrid domain to the ligand-binding site (Tng et al., 2004). Thus, these studies all support the significance of the change in the interface between I-like domain and the hybrid domain in integrin activation.

1.9 Activation states

Previously, the requirement of different affinity states of αLβ2 to different ICAMs has been observed (Buckley et al., 1997). From electron microscopy images and crystal structures of integrin αIIbβ3, αVβ3 and α5β1, it shows that integrin may undergo at least three activation states depicted by different quaternary conformations (Takagi et al., 2002b; Takagi et al., 2003; Xiao et al., 2004; Xiong et al., 2001; Xiong et al., 2002).

It had been shown on platelets and Chinese Hamster ovary cells that three different conformation exist for α2β1: (a) a nonactivated, resting state with no collagen nor IAC-1 (activation reporter mAb) binding; (b) an intermediate state, induced by outside manipulation, with collagen but no IAC-1 binding; and (c) a fully activated state, induced after inside-out stimulation, with both collagen and IAC-1 binding. These different conformations are related to different function: α2β1 induced after outside manipulation, resulted in significantly more cell spreading on coated collagen compared with nonactivated or inside-out stimulated cells (Van de Walle et al., 2005).

Meanwhile, LFA-1 can transit between a bent conformation and two extended conformations (with or without hybrid displacement) from the negative stain electron microscopy observation (Nishida et al., 2006). Our laboratory also showed that LFA-1

binding to ICAM-3 need a higher affinity state than binding to ICAM-1(Tang et al., 2005). Further study on activation states will be discussed in this thesis.

1.10 Study in this thesis

Activation of LFA-1 was studied by ICAM-1 and ICAM-3 adhesion, the conformation of the LFA-1 in these states was characterized by the expression of the KIM127 epitope (reporting for leg extension) and the MEM148 epitope (reporter for hybrid displacement or hinge open). This is described in the beginning of the Chapter 5. During these studies, two LFA-1 variants were constructed and they were invaluable in contributing to our understanding of the structure-function relationship of LFA-1, The first one is the mutation found in a LAD patient $N^{329}S$ (Chapter 3), which revealed, in atomic details, how the I-like domain of the β2 integrin may be constrained in their resting state. The other was created by protein engineering: a disulfide bond was introduced between the PSI and IEGF2 domain which gave a LFA-1 that is locked into the bent conformation (Chapter 5), leading to a new understanding that ligand binding, leg extension and hybrid domain displacement may be independent of each other. Other studies are discussed in Chapter 4, which include the characterization of the $R^{571}C$ mutation found in another LAD patient and the study of the different requirement for αLβ2 and αMβ2 heterodimer formation. The studies in the Chapter 4 are incompletely but it will provide a platform for further experiment.

Chapter 2: Materials and Methods

2.1 Materials

2.1.1 General reagents

Most general chemicals and solvents were of analytical grade, and were obtained from Sigma Aldrich Chemical Company Ltd., BDH Chemicals Ltd., Becton-Dickenson Ltd., GIBCO-BRL Ltd., Pierce Ltd., unless otherwise stated. All restriction endonucleases, ligase and other enzymes were obtained from New England Biolabs, Promega Ltd., Fermentus Ltd, Roche Diagnostics unless otherwise stated and were used according to the manufacturers' instructions. DNA marker was bought from Fermentas Ltd, Protein marker are from New England Biolabs. Protease inhibitors Complete-mini protease tablet was from Roche. DNA polymerase pfu was bought from Promega Ltd. DNA loading dye was purchased from Fermentas Ltd. Biotin was bought from Pierces Ltd.

2.1.2 Commercial kits

QIAprep Spin Miniprep Kit, QIAquick PCR purification kit, Plasmid Maxi Kit, Gel extraction kit all are purchased from QIAGEN Ltd; ECL Detection Kit was bought from GE Amersham. Site directed mutation kit was purchased from Strategen.

2.1.3 Cells

MOLT-4 cells (human T lymphoblast), 293T cells (human embryonic kidney cell with SV40 large T antigen) were purchased from ATCC. COS-7 cells (African green monkey kidney cells) were purchased from ATCC.

2.1.4 Vectors and cDNA

pcDNA3.0 was bought from Invitrogen. CD11a (integrin αL), CD11b (integrin αM), CD11c (integrin αX) and CD18 (integrin β2) are provided by Prof Law SK (School of Biological Scciences (SBS), Nanyang Technological University (NTU)). ICAM-1-(D1-D5)-Fc and ICAM-3-(D1-D5)-Fc are kindly provided by Dr. Simmons (IMM, Oxford). pEGFP-N1 was offered by Dr. Liu Ding Xiang (SBS, NTU).

The αIIb and β3 pcDNA3.0 expression plasmids were kindly provided by P.J. Newman (blood center of Wisconsin and Medical College Wisconsin).

2.1.5 Antibodies

Monoclonal antibodies	Epitope	Function	Sources
MHM24	I-domain of the αL subunit	anti-αL blocking mAb	From Prof. McMichael (John Radcliff Hospital, Oxford, UK)
LPM19c	I-domain of the αM subunit	anti-αM blocking mAb	From Prof. Law SK (SBS, NTU)
KB43	I domain of the αX subunit	anti-αX blocking mAb	From K. Pulford (LRF Diagnostic Unit, Oxford, UK)
1B4	I-like domain of the β2 subunit	anti αLβ2 heterodimer blocking mAb	From Prof. Law SK(SBS, NTU)
MEM48	IEGF-2/3 of the β2 subunit	anti-β2 activating antibody	From Prof. Horejsi (Prague, Czech Republic); From Zymed laboratories
MEM148 MEM148-FITC	Hybrid domain of the β2 subunit	anti-β2, bind to active integrin LAF-1	From Serotec
KIM127	IEGF-2/3 of the β2 subunit	anti-β2 activating mAb	From Dr. Robinson (UCB, CellTech, UK)
KIM185	IEGF-4,β TD of the β2 subunit	anti-β2 activating mAb	From Dr. Robinson (UCB, CellTech, UK)
KIM202	Hybrid domian of the β2 subunit	anti-β2 mAb	From Dr. Robinson (UCB, CellTech, UK)
MHM23	I-like domain of the β2 subunit	anti αLβ2 heterodimer blocking mAb	From Prof. McMichael (John Radcliffe Hospital, Oxford, UK)
10E5	β-propeller of αIIb subunit	anti-αIIbβ3 blocking mAb	From Dr.B.S.Coller (The Rockefeller University, NY)
7E3	I-like domain of the β3 subunit	anti-β3 blocking mAb	From Dr.B.S.Coller (The Rockefeller University, NY)

Anti-GFP mAb developed in rabbit was bought from Molecular Probes, Purified IgGs of MHM24, LPM19c, KB43, KIM127, KIM185, 1B4 were prepared from hybridoma supernatants using Hi-Trap protein G columns (Amersham Pharmacia Biotech)

2.1.6 Ligands for cell binding analysis

ICAM-1-(D1-D5)-Fc and ICAM-3-(D1-D5)-Fc	Prepared by Miss Elianna Bte Mohamed Amin and Adeline Sen-Yun Foo (SBS, NTU)
Fibrinogen	Bought from Sigma

2.1.7 Media

All media were sterilized by autoclaving unless otherwise stated.

LA broth	LB medium containing 60 μg/mL ampicillin
LA plate	LB agar plate containing 60 μg/mL ampicillin
293 and 293T cell culture media	DMEM (JRH) containing 10% (v/v) heat-inactivated FBS, 100 IU/mL penicillin, 100 μg/mL streptomycin
LB medium	1% (w/v) Bacto-tryptone (BD), 0.5% (w/v) yeast extract (BD), 1% (w/v) NaCl
LB agar	LB medium plus 1.5% (w/v) Bacto-agar (BD)
MOLT-4 cell culture media	RPMI1640 (JRH) containing 10% (v/v) heat-inactivated FBS, 100 IU/mL penicillin, 100 μg/mL streptomycin
COS-7 cell culture media	RPMI1640 (JRH) containing 10% (v/v) heat-inactivated FBS, 100 IU/mL penicillin, 100 μg/mL streptomycin

2.1.8 Solutions

blocking buffer (western)	PBS containing 1% (w/v) non-fat milk, 0.1% (v/v) Tween20
blotting buffer (western)	12.5 mM Tris pH 8.0, 96 mM glycine, 10% (v/v) ethanol
cell freezing media	10% DMSO in heat-inactivated FBS
immunoprecipitation buffer	50 mM Tris pH 7.5, 150 mM NaCl, 1% (v/v) NP-40, 0.5 mM PMSF, 2.5 mM iodoacetamide
10x SDS-PAGE running buffer	0.25 M Tris, 1.9 M glycine, 1% (w/v) SDS
4x resolution gel buffer	0.25 Tris, 0.4% (w/v) SDS, pH 8.8
4x stacking gel buffer	0.5M Tris, 0.4% (w/v) SDS, pH 6.8
sodium bicarbonate buffer	1.36 g sodium carbonate, 7.35 g sodium bicarbonate, pH 9.2
20mg/mL ampicillin	20 mg/mL in ddH_2O, pH 8.4, filtered (0.22μm) and stored at -20C°

2.2 Methods

2.2.1 *General Methods for DNA Manipulation*

2.2.1.1 Miniprep and maxiprep plasmid DNA

The bacteria clone were cultured in 3-5 mL LB with antibiotic in shaking incubator at 37°C overnight and the plasmid was purified according to the manual provided by the plasmid purification kit. For maxiprep plasmid, the bacteria clone was cultured in 3-5 mL LB in 15 mL tube for 8-12 hr first, transferred to a flask containing 100 mL LB with antibiotics overnight. The following step was performed according to the manual.

2.2.1.2 Quantitation of DNA

The concentration of DNA was determined by its absorbance at wavelength 260nm based on the calculation; 50 μg/mL double-stranded DNA gives an OD_{260} of 1. The OD_{280} was also read and the ratio of OD_{260}/OD_{280} was calculated to estimate the purity of the DNA solutions. An OD_{260}/OD_{280} ratio between 1.6 and 2.0 was considered satisfactory.

2.2.1.3 Restriction endonuclease digestion

Restriction endonuclease digestions were usually carried out in a 20-80 μl reaction volume: 2-5 U of enzyme used for up to 500 ng DNA together with BSA and appropriate buffer for 1-3 hr at 37°C. Digests with more than one enzyme were carried out simultaneously in a suitable buffer. When the buffer requirements were incompatible, restriction digestions were performed sequentially with individual buffer for each enzyme.

2.2.1.4 DNA electrophoresis

A 40 mL 1% (w/v) agarose gel (Agarose was melted in 1×TAE) was regularly used for analysis of 0.1-8 kb DNA fragments. Ethidium bromide was added to a final concentration of 1 μg/mL followed by casting in a mini-gel apparatus. Electrophoresis was carried out in horizontal apparatus with the gel submerged in 1x TAE. DNA samples were loaded with loading dye. DNA fragments were visualized by fluorescence over a UV light (302 nm, UV transilluminator TM-20, UVP), under which DNA/EB complexes fluoresce and the image was recorded with a Mitsubishi video copy processor.

2.2.1.5 Purification of DNA fragments from agarose gel

When a particular fragment of DNA in a mixture of fragments was required, e.g. in ligations or as a PCR template, it was routinely separated from other fragments by agarose gel electrophoresis. Gel slice containing the DNA fragments to be purified was cut from the gel using a razor blade, carefully avoiding their exposure to the UV light. DNA was extracted using a QIAquik Gel Extraction Kit.

2.2.1.6 DNA ligation

DNA vectors with complementary ends to be used for ligation were prepared by restriction enzyme digestion and where necessary treated with alkaline phosphatase and purified using agarose gel electrophoresis. Vector DNA (~ 10 ng) and insert DNA (20-40 ng) were ligated by incubation at RT for 2-3 h, using 1U of T4 DNA ligase with ligase buffer provided together with the enzyme in a 20 μl reaction volume. A reaction with uncut vector, a reaction without insert DNA and a reaction without both insert DNA and T4 DNA ligase were included in the experiments as controls.

2.2.1.7 Preparation of *E.coli* competent cells

The *E.coli* strain DH5α was used to prepare competent cells in advance which were stored at -70°C. A fresh plate of cells was prepared by streaking out cells from frozen stocks and growing overnight at 37°C. On the second day, an individual colony was picked and grown in 10 mL LB broth culture overnight. On the third day, 5 mL of overnight culture was transferred into each of two flasks containing 500 mL LB broth. Incubate at 37°C with aeration until the culture reaches OD_{550} of 0.5. This should take approximately 2 h. The cells were transferred to centrifuge bottles and spin at 4°C for 8 min at 8000 rpm. Pellets were gently resuspended in 250 mL ice cold 0.1 M $CaCl_2$ and combined into a single bottle. Cells were resuspended again in 250 mL ice cold 0.1 M $CaCl_2$ and centrifuged at 8000 rpm for 8 min at 4°C. Finally the pellet was resuspended in 43 mL ice cold 0.1 M $CaCl_2$ in ddH_2O with 7 mL sterile glycerol. Competent cells were distributed into convenient aliquots (0.2 mL) in cold microcentrifuge tubes. Cells were store at -70°C. A portion of the cells was saved to assay for viability, purity and competence.

2.2.1.8 Transformation of plasmid DNA

50-100 μl of competent cells are necessary for one reaction. Competent cells were defrosted on ice. DNA was added to cells: plasmid DNA 1-2 μg, ligation product 10 μl. The mixture was incubated on ice for 30 min followed by a heat shock in a 42°C water bath for 2 min and in ice for another 2 min. 500ul LB broth was added to the tube. The tube was incubated at 37°C with constant shaking 150-200 rpm for 30 min to 1h. 50-500 μl of the mixture was streaked out onto plates containing the appropriate antibiotics.

2.2.1.9 Purification of plasmid DNA

For small-scale purification of plasmid DNA, 5 mL LB with appropriate antibiotics was inoculated with a single colony that contains recombinant plasmid from an agar plate and incubated at 37°C with constant shaking overnight. A QIAprep Spin Miniprep Kit (QIAGEN) was used to extract DNA according to the manufacturers' instructions. For large-scale purification of plasmid DNA, a Plasmid Maxi Kit (QIAGEN) was used according to the manufacturers' instructions. This kit routinely yielded between 200-750 μg DNA from 100 mL of overnight bacterial cultures.

2.2.1.10 Standard PCR protocol

PCR was routinely performed in a 50 μl reaction volume containing less than 1 μg template DNA, 1 μM of each oligonucleotide primer, 200 μM of each dNTP, and 1 U DNA polymerase. *Taq* polymerase (Fermentas) was used for PCR colony screening. Pfu DNA polymerase (Fermentas), which possesses a 3'-5' proofreading activity resulting in a twelve-fold increase in fidelity of DNA synthesis over *Taq* DNA polymerase, was used for high fidelity DNA synthesis. Each polymerase has its own reaction buffer, normally supplied by the manufacturer. The reaction mixtures were subjected to a varying number of cycles of amplification using the DNA Thermal Cycler (MJ research).

2.2.1.11 Selection of colonies

After transformation of competent cells, colonies of interest were identified using either PCR screening or restriction digestion, depending on the availability of suitable PCR primers for screening and the degree of background indicated by the control plates. Each colony to be tested was used to inoculate 15 μl LB. 1 μl of this inoculated

LB broth was added to a 25 µl PCR reaction containing 0.5 U *Taq* polymerase. A negative control and, where possible, a positive control were included in the experiment. Colonies containing the recombinant plasmid of interest were identified by the size of their PCR products using agarose gel electrophoresis. Positives from PCR screening were confirmed using restriction digestion.

2.2.1.12 Site-directed mutagenesis

Point mutations were made using Quick Change Site-Directed Mutagenesis (SDM) Kit (Stratagene), and following the manufacturer's protocols. Overlay primers with the desired mutations were used in the long PCR cycle. The restriction enzyme Dpn I was used to digest the original template. The Dpn I treated PCR product was transformed in competent *E.coli* and plated onto LB agar plates with appropriate antibiotics. All constructs were verified by sequencing (Research Biolabs).

2.2.2 *General methods for cell culture*

All cell lines were maintained in 5% CO_2 at 37°C in a humidified tissue culture incubator using Nunc tissue culture flasks or dishes.

2.2.2.1 Cell storage in liquid nitrogen

Cells were sedimented at 400 g for 5 min, resuspended in cell freezing media at a concentration of $5x10^6$ cells/mL and dispensed into Cryo Vials (Greiner). Cells were frozen in a NALGEN™ Cryo 1°C Freezing Container (Nalgen) for 24 h at -70°C to achieve a 1°C/min cooling rate. Thereby the vials were transferred into liquid nitrogen for long-term storage.

2.2.2.2 Cell recovery from liquid nitrogen

Cells were removed from the liquid nitrogen storage and quickly brought to 37°C in a water bath. Cells were washed in 10 mL warmed media to remove DMSO. Each cell pellet was resuspended in complete media and cultured in 75 cm^2 flask.

2.2.2.3 Culture of 293T cells and COS-7 cells

293T cells were maintained in DMEM with 10% (v/v) heat-inactivated FBS, 100 IU/mL penicillin and 100 μg/mL streptomycin in a 5% CO_2 and humidified tissue culture incubator at 37°C. Cells were passaged when they were subconfluent. Cells were washed twice in PBS, incubated in 0.25% (w/v) trypsin (GIBCO) for 5 min at RT, followed by tapping of each flask to dislodge the adherent cells. Trypsin was inactivated by adding full media and cells were directly seeded into fresh culture media in new flasks at desired cell density. COS-7 cells were cultured in the same methods, except PRMI 1640 was used.

2.2.2.4 Culture of MOLT-4 cells

MOLT-4 were grown in cell culture flasks in RPMI1640 with 10% (v/v) heat-inactivated FBS, 100 IU/mL penicillin and 100 μg/mL streptomycin. Cells were passaged by diluting cells with fresh media.

2.2.3 Transfection of cells

2.2.3.1 Transfection of 293T cells by the calcium phosphate method

Cells were seed in 10 cm dishes the night before to give 40-50% confluence at the day of transfection. Next day, 10 mL of fresh media containing 25 μM chloroquine was added to replace the old media one hour prior to the transfection. 10 μg DNA was

added to ddH_2O (1095 μl total) in a 15 mL sterile tube, followed by adding in 155 μl 2M $CaCl_2$, 1250 μl of 2xHBS (8.0g NaCl, 0.37g KCl, 201mg $Na_2HPO_4 \cdot 7H_2O$, 1.0 g glucose, 5.0 g HEPES/500mL pH 7.05 and filter sterile, store at 4°C) was added to that tube drop by drop with gentle mixing. Finally, this mixture was added directly to the cells drop by drop. This step should be done within 1-2 min after adding 2xHBS. The cells were then incubated for 7-11 h. After incubation, 10 mL of fresh media was added to replace the old media which contain chloroquine. Cells, or culture supernatant, can be harvested 48-72 h after transfection

2.2.3.2 Transfection of COS-7 cells

COS-7 cells were seed in 75 cm medium flasks the day before transfection to give a 50-80% confluence. On day of transfection, trasfection mixture was prepared as follows: 5ug plamid DNA, 0.1 mL 10mM chloroquine in PBS (filter with 0.2 μm filter) and 0.04 mL EDTA DEXTRAN were added into 10 mL RPMI (no FBS, no PS) in tube. Cells was washed once with RPMI (no FBS, no PS) before adding the transfection mixture. Then the cells with transfection mixture were incubated 4-5 hr at 37C°. After that, the contents of the cell culture flask was jettisoned and washed 1 time with PBS, then 10 mL DMSO in PBS was added to the flask, after exactly 3 min washing twice with PBS, and full medium (with FBS and PS) was add to the flask. Next day, wash the flask with 2 times PBS, trypsinized the cells with 1mL trypsin and add new full medium, and transfer to a new flask to culture for another day before collecting them.

2.2.3.3 Harvesting transfected cells (adherent)

24-48 h after transfection, the cells in each plate were washed in PBS and detached in

5 mL 0.5 mM EDTA in PBS by incubation at RT for 10 min with gentle rocking. Cells were collected and mixed with 10 mL full media and transferred to centrifuge tubes. Cells were spun down (400 g, 5 min, 4°C) for subsequent analysis.

2.2.3.4 FACS analysis

Cells were incubated with 10 μg/mL primary mAb in RPMI1640 for 1 h at 4°C. The cells were then washed twice and incubated with FITC-conjugated sheep anti-mouse $F(ab')_2$ secondary antibody (1:400 dilution; Sigma) for 30 min at 4°C. Stained cells were washed once in RPMI1640 and fixed in 1% (v/v) formaldehyde in PBS. Cells were analyzed on a FACS Calibur flow cytometer (Becton Dickinson). Data were analyzed using CellQuest pro software (Becton Dickinson). Expression index was calculated by (% cells gated positive) x (geomean fluorescence intensity). For the analysis of MEM148 epitope expression, MOLT-4 cells were incubated with MEM148-FITC with or without activation reagents: Mg/EGTA (5 mM $MgCl_2$ and 1.5 mM EGTA), mAbs MEM48, KIM127 (each at 10 µg/mL), KIM185 (2.5 µg/mL) at 37°C for 30 min. Stained cells were washed once and fixed in 1% (v/v) formaldehyde in PBS. Data were collected on a FACScan flow cytometer (BD Biosciences) and analyzed using the CellQuest software (BD Biosciences).

2.2.3.5 Surface biotinylation of 293T cells

Biotin was diluted in PBS with a concentration 2 mg/mL, 0.5 mM $MgCl_2$ and 0.15 mM $CaCl_2$ in PBS to make up Solution A. Then 2mg/mL Biotin solution was 10 times diluted in Solution A. Aspirate away medium in dishes, the cells was washed once with PBS. 4-5 mL Diluted Biotin Solution was gently added into the dishes, and incubated in RT for 0.5 hr. Then, the cells was washed once with Solution A and

quenched by washing once with quench buffer (10mM Tris-HCl pH 8.0 and 0.1% BSA in PBS). After that, cells can be collected and for later Immonoprecipitation Assay.

2.2.3.6 Preparation of rabbit anti-mouse IgG coupled onto protein A sephrose beads

Protein A sepharose (PAS-RaM) (Manara et al.) (Sigma) (1g) was swelled by rotating in an excess of PBS overnight at 4°C. The swelled PAS beads, which occupied a bed volume of 4 mL, was sedimented by centrifugation (3000 g, 5 min, 4°C), washed twice, and finally resuspended to a 25 % (v/v) suspension in PBS. Rabbit anti-mouse IgG (RaM, Sigma) (4 mg) was added and the mixture was rotated for 1 h at 4°C. The PAS-RaM bead were washed once in PBS, once in IP buffer, and resuspended to a 25 % (v/v) suspension in IP buffer. The PAS-RaM suspension was stored at 4°C.

2.2.3.7 Immunoprecipitation of biotinylated cell lysates

Cells were colleted to tubes with PBS and spin down followed by washing once with PBS. Cells were lysed in ice for 20 min with lysis buffer with protein inhibitor cocktail. Spin down cells in 13000 RPM 10 min to assure the cell debris was precipitated, The cell lysate in the supernatant was collected in the eppendorf tube. 0.5 mL of biotinylated cell lysates were precleared by adding 3 µg of irrelevant mAb as appropriate, and incubated at 4°C for 45 min with rotation. 40 µl PAS-RaM suspension was added and the mixture was rotated at 4°C for 30 min. The PAS-RaM was sedimented by centrifugation (10000 g, 2 min, 4 °C) and the supernatant was transferred to a fresh tube. 3 µg of appropriate mAb was added to the precleared cell lysate and incubated at 4°C for 45 min with rotation. Subsequently, 70 µl PAS-RaM suspension was added and the mixture was incubated at 4°C for 1 h with rotation.

For MEM148 and KIM127 immnoprecipitation, cells were incubated in Mg/EGTA with mAbs (MHM23, MEM148, or KIM127) in RPMI media containing 5% (v/v) heat-inactivated fetal bovine serum and 10 mM HEPES (pH 7.4) for 30 min at 37 °C. Cells were washed twice with PBS and lysed in lysis buffer with protease inhibitors (Roche) followed by immunoprecipitation with PAS-RaM.

The PAS-RaM was sedimented by centrifugation (10000 g, 4°C, 2 min) and the supernatant was discarded. The PAS-RaM was washed in 500 µl IP-buffer for three times. Thereafter, 100 µl protein solubilisation buffer containing 40 mM DTT was added to the PAS-RaM which was then vortexed, heated at 100°C for 5 min. The immunoprecipitated proteins were resolved by directly running on SDS-PAGE gels, or were stored at -20°C until used.

2.2.3.8 Sodium dodecyl sulphate polyacrylamide gel electrophoresis (SDS-PAGE)

SDS-PAGE was performed as described by Laemmli (1970) with slight modifications. Protein sample (15 µl for minigel system) was mixed with an equal volume of sample loading buffer (2x) under non-reducing conditions or in the presence of 40 mM DTT under reducing conditions. Electrophoresis was carried out at 200V in a Mini Electrophoresis Set (Biorad) in SDS-PAGE eletrophoresis buffer.

2.2.3.9 Western blotting

Proteins separated by SDS-PAGE were transferred onto a PVDF membrane (Immobilon-P, Millipore) by western blotting. The PVDF membrane was prepared according to the manufacturer's instructions: the membrane was equilibrated by washing in ethanol for 10 sec, then water for 10 min until miscible, and then in

blotting buffer (12 mM Tris-HCl, 95 mM glycine, 10 % (v/v) ethanol) for 5-10 min. The SDS-PAGE gel was equilibrated by washing in blotting buffer once. One western blot sponges, the PVDF membrane, the SDS-PAGE gel and finally the second sponge, was assembled and placed in a semi-dry western blot apparatus (Biorad), bubbles between each layer were removed carefully. Western blotting was performed at 25 V for 30 min. After protein transfer, the PVDF membrane was transferred to blocking buffer and was rotated at RT for an hour or overnight at 4°C.

2.2.3.10 ECL detection biotinylated proteins blotted onto immobilon-P membrane

Biotinylated proteins which had been transfered onto PVDF membranes by Western blotting were labeled with a streptavidin-HRP (Horse radish peroxidase) conjugate (Amersham) and were then detected by enhanced chemiluminescence (ECL). The membrane was removed from blocking buffer and were washed three times in PBS-T (PBS, 0.1% (v/v) Tween-20 (Sigma)) at RT for 10 min. The membrane was then incubated with the streptavidin-HRP conjugate (1:1000 dilution in PBS-T) at RT for 60 min with gentle agitation, and was washed again for three times in PBS-T at RT for 10 min. Thereafter, the membrane was developed using an ECL Plus Detection Kit (Amersham) according to the manufacturer's recommendations. The membrane was then exposed to Kodak X-Omat film and developed using a Kodak X-OMAT ME-1 processor.

2.2.3.11 Coating microtitre plates with ICAMs or fibrinogen for cell adhesion assay

Goat anti-human IgG (Fc specific) (Sigma) was diluted to 5 µg/mL in sodium bicarbonate buffer , pH 9.2, and 50 µl was added to each well of a microtitre plate (Polysorb, Nunc Immuno-Plate). The microtitre plates were left at 4 °C overnight. On

the next day, the solution was discarded and the wells were washed twice with 150 µl PBS per well. A solution of 0.5 % (w/v) BSA in PBS was added to each well (150 µl per well) and the plates were incubated at 37°C for 30 min. The plates were washed with PBS once (150 µl per well) before the addition of 50 µl per well of ICAM-1/Fc or ICAM-3/Fc (1 µl /mL in PBS containing 0.1 % BSA). After 2-3 h incubation at RT, the plates were washed twice in RPMI/HEPES/FBS (RPMI1640 supplemented with 10 mM HEPES, pH 7.4 and 5% (v/v) heat inactivated FBS before use.

For fibrinogen adhesion assay, fibrinogen at 1 µg/mL in sodium bicarbonate buffer was added into each mocrotiter. The microtitre plates are incubated in 37° for 3-4 h. The solution was discarded and the wells were washed twice with 150 µl PBS per well. A solution of 1.0 % (w/v) BSA in PBS was added to each well (150 µl per well) and the plates were incubated at 37°C for 30 min. The plates were washed twice in RPMI/HEPES/FBS before use.

2.2.3.12 Cell adhesion assays

Plates were prepared as described in 2.3.3.11. Cells were then incubated with BCECF dye (2',7'-bis-(2-carboxyethyl)-5(and -6) carboxy fluorescein, acetoxymethyl ester) (Molecular Probes), at the concentration of 1 µg/mL for 20 min at 37°C. Labeled cells were transferred to wells ($2x10^4$ cells/well) alone or with stimulation/inhibition reagents and incubated for 30 min at 37°C. Nonadherent cells were removed by washing. Cell fluorescence, which indicated the number of cells adhering to ligand-coated wells was measured using FL600 fluorescence plate reader (Bio-Tek).

2.3 Plasmid construction details

2.3.1 Wild type plamids

The β2 cDNA in J8.1E (Douglass et al., 1998) was used as a template for construction of the β2 in mammalian expression vector pcDNA3.0 (Invitrogen) (Fig. 2.1). KpnI and SpeI were used to digest β2 cDNA from J8.1E and the fragment was ligated into pcDNA3.0 vector which was digested with KpnI and XbaI (SpeI and XbaI digested DNA fragments have compatible ends). αL, αM and αX cDNA plasmids were in pcDNA 3.0 vector with the restriction cutting sites KpnI and XbaI.

2.3.2 β2 variant construction

2.3.2.1 β2 with GFP tag

β2 cDNA was amplified from the original β2 cDNA plasmid with the primers carrying XhoI or KpnI enzyme site respectively. The PCR product was digested with XhoI and KpnI and the fragment was ligated to the pCDNA3.0 vector which was digested with the same enzymes to obtain the new β2 CDNA. GFP fragment was amplified from pEGFP-N1 plasmid with the primers bearing XhoI and XbaI site respectively and digested with XhoI/XbaI. The new β2 CDNA was digested with XhoI and XbaI as a vector, then was ligated with the GFP fragment digested with the same enzymes to get β2/GFP plasmid. All the β2 variants in Chapter 4 used were constructed by SDM based on the β2/GFP plasmid. The primers for SDM are not listed.

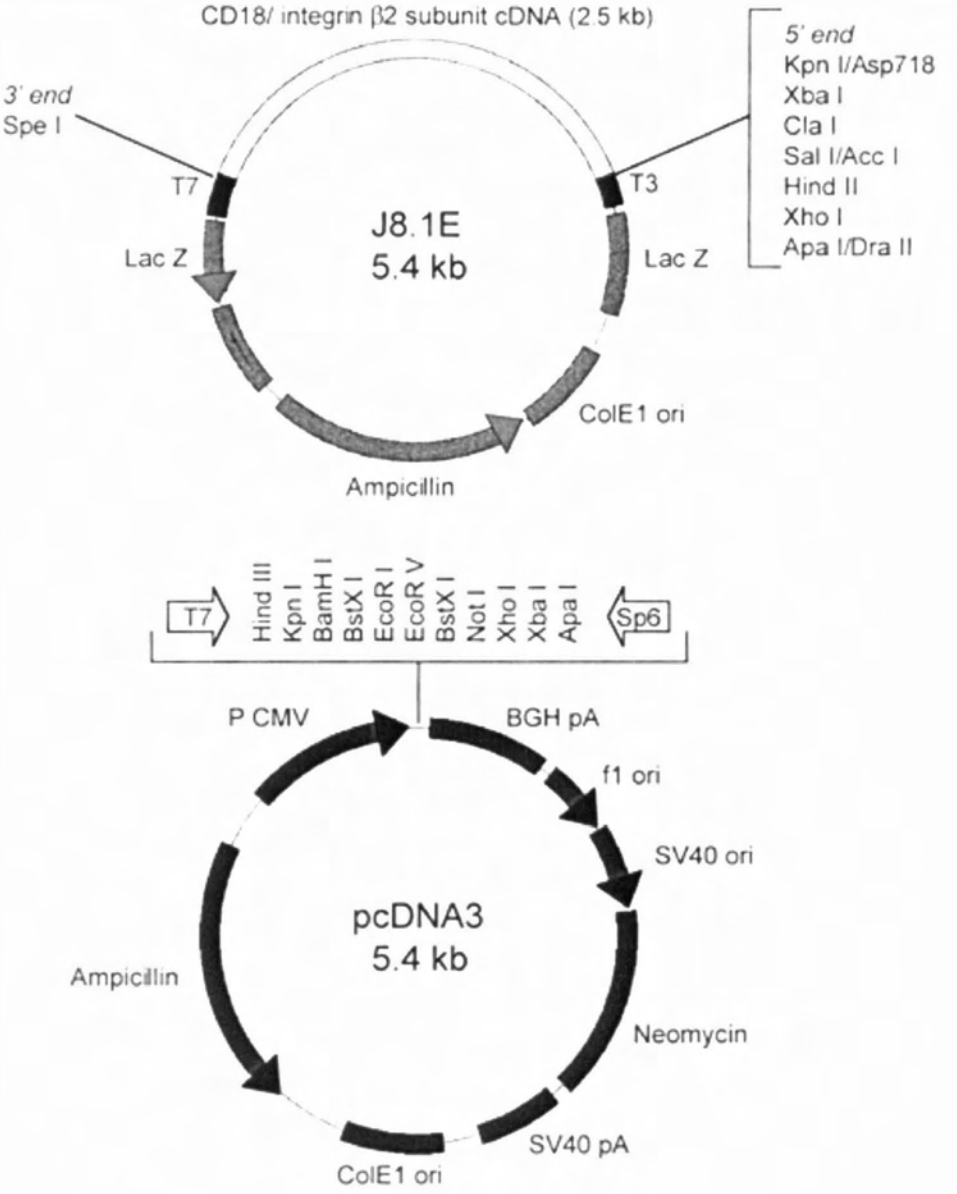

Fig 2.1 Schemetic illustration of plasmid J 8.1E and pcDNA3.0.
The β2 cDNA in J8.1E (Dougless et al., 1998) was used as a template for the construct of the β2 in mammalian expression vector pcDNA3.0. KpnI/SpeI was used to digest β2 cDNA from J8.1E and the fragment was ligated into pcDNA3.0 vector which was digested with KpnI and XbaI (SpeI and XbaI digested DNA fragment have compatible ends). αL plasmid was in pcDNA3.0 vector with the restriction cutting sites KpnI and XbaI.

2.3.2.2 β2 variants used in chapter 3 and chapter 5

The β2 constructs bearing $N^{329}S$ (Nelson et al., 1992) or $R^{571}C$ (Shaw et al., 2001) mutations was generated using SDM kit with the relevant primer pairs. β2C23* is a β2 truncation mutant in which the codon of Cys^{461} (the 23rd of the 56 conserved cysteines in the extracellular domain of the β2 subunit) was converted to a stop codon (Tan et al., 2000). β2NV1 is a human β2/β1 chimera in which the I-EGF and βTD domains of β2 were replaced with the corresponding region of β1 (Douglass et al., 1998). β2cc in which a disulfide bond was introduced by converting Gly^{33} in the PSI domain and Gly^{486} in I-EGF2 to cysteines was described in Shi et al., work (Shi et al., 2007). αLcc with an engineered disulfide bond by converting Lys^{287} and Lys^{294} into cysteines was constructed according to Lu C *et al.* (Lu et al., 2001c). Integrins with more than one mutation were generated by sequential SDM, these include $\beta2N^{329}S/D^{209}H$, $\beta2N^{329}S/S^{116}P$, $\alpha Lcc/D^{209}H$, $\alpha Lcc/S^{116}P$, $\beta3N^{339}S/D^{217}H$ and $\beta3N^{339}S/S^{123}P$. All constructs were verified by sequencing (Research Biolabs sequencing service, Singapore).

2.3.3 αL subunit chimeras

The $\alpha L(I_M)$ were constructed by swap the the I-domain of αL with that αM subunit; and $\alpha M(I_L)$ were constructed by swap the I-domian of αM with that of αL.
They were constructed by three steps PCR: Fragment 1, 2 and 3 were separately amplified, they then were joined together by PCR. The long PCR fragment was digested with HindIII and XbaI followed by ligated into the vector (αL or αM plasmid) digested with the same enzymes.

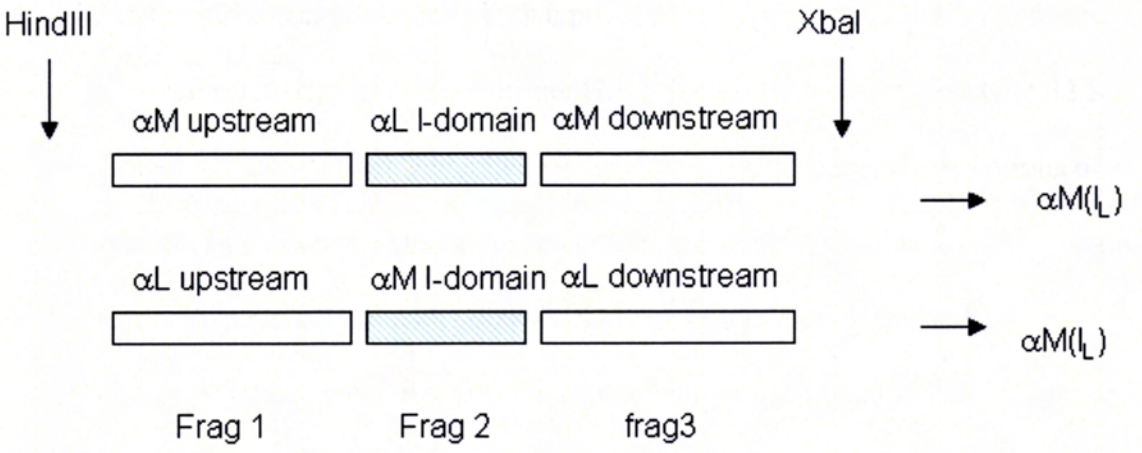

αLM consists of the head-thigh (include β-propeller, I-domain and thigh) of the αL subunit and the calf-tail (include calf-1, calf-2 and cytoplasmic tail) of the αM subunit. Conversely, αML consists of the head-thigh of αM subunit and the calf-tail of αL subunit. To get αLM and αML chimeras, NheI restriction enzyme site was introduced in the linkage site between thigh and calf-1domain in the αL and αM plasmids respectively by SDM. For αML, the fragment digested from original αM plasmid was ligated to αL plasmid which was digested with HindIII/NheI. For αLM, the fragment digested from original αL plasmid was ligated to αM plasmid which was digested with HindIII/NheI. Subsequently, the NheI site was changed back to original sequence using SDM. All the constructs were confirmed by sequencing. The primers used are not listed here.

2.4 Structural Images and Modeling

LSQKAB (Collaborative Computational Project, CCP4) was used for molecular least-squares superposition of the three I-like domain conformers. Fig. 3.1B and Fig. 3.7 in

chapter 3 were created using PyMOL. The solvent accessible surface area of β3 Asn^{339} of the three conformers was calculated using AREAIMOL (Collaborative Computational Project Number 4) with a probe of 1.7 Å radius: 46.1 $Å^2$ (conformer I); 16.5$Å^2$ (conformer II); 68.8$Å^2$ (conformer III). Structural models of wild-type β2 I-like domain or variants were generated using Modeler 9.1. Energy computations of wild-type β2 I-like domain model or variants having Asn^{329} substituted with Gln, Ala, Ser, Thr, or Asp were done with GROMOS96 implementation of Swiss-PdbViewer. The models generated were examined for potential hydrogen bond(s) formation between Gln^{329}, Ala^{329}, Ser^{329}, Thr^{329}, or Asp^{329} of the α7 helix with Ser^{324} and Glu^{322} of the β6 strand. In the wild-type β2 I-like domain, Asn^{329} δ^1O and δ^2NH2 hydrogen-bond with Ser^{324} and main chain carbonyl of Glu^{322}, respectively. In variant $N^{329}Q$, $Gln^{329}\varepsilon^1O$ hydrogen-bonds with Ser^{324}. The variants $N^{329}A$, $N^{329}S$, and $N^{329}T$ lack a hydrogen bond between Asn329 and Ser^{324} or Glu^{322}. In variant $N^{329}D$, Asp^{329} hydrogen-bonds with Ser^{324} but not with Glu^{322}.

Note: Amino acid numbering of the integrins is based on Barclay et al., 1997 in this thesis (Barclay, 1997). Amino acid numbering started from Glutamine in β2 subunit that is the first one after the signal peptide is cleaved. Amino acid numbering starts from methionine in some of our publications (Shaw et al., 2001; Tng et al., 2004), we had made corrections in this thesis for the purpose of consistency.

Chapter 3 $N^{329}S$ mutation Promotes Constitutively Active Integrins αLβ2 and αIIbβ3

Integrins are bidirectional signal transducers despite having no known intrinsic enzymatic properties (Hynes, 2002). Integrins with an I-domain in the α subunit binds ligands via the metal ion-dependent adhesion site (MIDAS) in the I-domain. Integrins that lack the I-domain (henceforth referred to as I-less integrins) are found to bind ligand via the β propeller of the α subunit and the I-like domain of the β subunit (Arnaout et al., 2005; Luo et al., 2007). The I-like domain in the integrin β subunits is structurally similar to that of the I-domain. However, it contains a specificity determining loop, which was reported to contribute to the specificity of ligand binding and the αβ subunits association of the integrin heterodimer (Takagi et al., 2002a). The MIDAS of the I-like domain is flanked by the adjacent MIDAS (ADMIDAS) and the ligand-induced metal binding site (LIMBS), which serve as negative and positive regulators of ligand binding respectively (Chen et al., 2003; Chen et al., 2004; Mould et al., 2003a). The conserved coordinating residues that are involved in the three cation-binding sites of the I-like domain are highlighted in Fig. 3.1.

The $N^{329}S$ mutation was due to $A^{964}\rightarrow G$ nucleotide transition in one of the alleles of the β2 genes in a LAD patient (Nelson et al., 1992). The other allele of this patient carries a point mutation in intron 6 which leads to a splicing defect resulting in the insertion of four amino acid residues at the exon 6/7 junction. The β2 subunit with the four additional residues was shown incapable of supporting the expression of the β2 integrins (Wright et al., 1995). Incidentally, another substitution was found in this allele, $R^{564}W$, which was shown not to contribute to the LAD phenotype (Nelson et al.,

1992). The patient's mother was heterozygous with an abnormal allele that carrying splicing defect, but the patient's farther was found to carry two normal alleles. Therefore, the $N^{329}S$ mutation in the patient was not inherited from his parents and must arise from a mutational event. The β2 subunit with the $N^{329}S$ mutation has found to support moderate integrin αMβ2 expression when transfected into COS cells. However, functional studies were not carried out in 1992.

In previous studies, we have demonstrated that transfectants expressing the LFA-1 variant $\alpha L\beta 2N^{329}S$ can constitutively adhered to ICAM-1 (Tng et al., 2004). The $N^{329}S$ mutation is located in the I-like domain, and it may affect the overall conformation of the αLβ2 integrin. From the work described in this chapter, it shows that the LFA-1 variant $\alpha L\beta 2N^{329}S$ can also mediate the adhesion to ICAM-3 without any activating agent, and is therefore in a high affinity state. When the same mutation was introduced into β3 integrin, the I-less integrin αIIbβ3 is also active.

Two other mutations $S^{116}P$ and $D^{209}H$ were identified from LAD-1 patients. β2 integrin with either mutation was able to support αLβ2, αMβ2 and αXβ2 surface expression, but these integrins cannot mediate adhesion to all the ligands tested (Hogg et al., 1999; Mathew et al., 2000). Ser^{116} and Asp^{209} are located in the I-like domain of the β2 subunit. Ser^{116} is one of the coordinating residues both for the MIDAS and the ADMIDAS, whereas Asp^{209} is one of the coordinating residues for LIMBS (Fig. 3.1). Combinatorial analyses of $N^{329}S$ with $S^{116}P$ or $D^{209}H$ showed that the activating effect of $N^{329}S$ requires functional MIDAS and LIMBS of the I-like domain to allow propagation of the activating signal to the I-domain of the αL subunit.

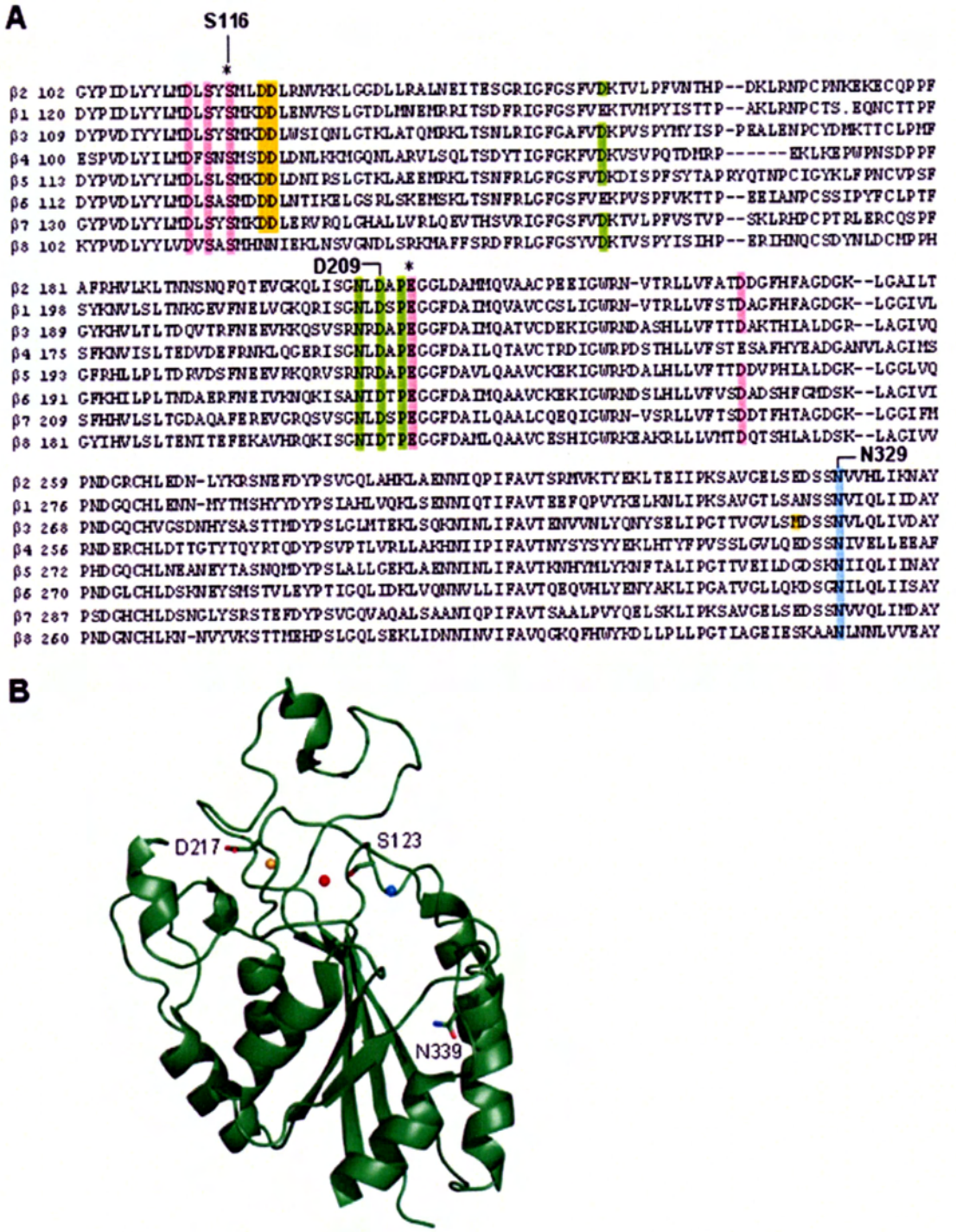

Fig 3.1 (A) Alignment of the human integrin I-like domains. MIDAS, LIMBS, and ADMIDAS coordinating residues that are conserved are highlighted in pink, green, and orange respectively. The β2 Asn^{329} and the corresponding Asn in all other β subunits are highlighted in cyan. The Ser^{116}, Asp^{209}, and Asn^{329} of the β2 subunit are indicated. MIDAS residues that can contribute to ADMIDAS coordination (Xiao et al., 2004) are indicated with asterisks. **(B)** The β3 I-like domain structural data (Xiong et al., 2002) were used to show the positions of Asp^{217}, Ser^{123}, and Asn^{339} with their side chains depicted. The metal ions of the MIDAS, LIMBS, and ADMIDAS are colored pink, gold, and blue respectively.

3.1 $N^{329}S$ generates a high affinity αLβ2 that adheres to ICAM-1 and ICAM-3 substrates constitutively

We have previously shown that αLβ2$N^{329}S$ can mediate adhesion to ICAM-1 constitutively (Tng et al., 2004). Since then, we and others have demonstrated that there are at least three activation states (Nishida et al., 2006; Tang et al., 2005). An intermediate state affinity LFA-1 can mediate the adhesion to ICAM-1, but a high affinity is required to mediate adhesion to ICAM-3 (Tang et al., 2005). Thus, αLβ2$N^{329}S$ is at least an intermediate state conformer, but the adhesion to ICAM-1 cannot distinguish between an intermediate and a high affinity conformer. In the experiment shown in Fig. 3.2, αLβ2$N^{329}S$ transfectant can mediate adhesion to ICAM-3 in the absence of activating agents Mg/EGTA and the integrin β2-specific activating mAb KIM185 (Fig. 3.2). Thus, the mutation $N^{329}S$ generates a high affinity αLβ2 with respect to ICAMs adhesions.

3.2 The requirement of Cβ instead of Cγ amide functional group at position 329 of the β2 I-like domain

The Asn at position 329 of the β2 is conserved in all integrin β subunits. Since the native structure of the β2 I-like domain has not been determined, and the fact that the corresponding residue in the β3 is Asn^{339}, we made use of the resolved structure of the β3 I-like domain of αVβ3 in complex with a RGD ligand (Xiong et al., 2002) to visualize the position of this conserved Asn, and the three metal-binding sites. The β3 Asn^{339} lies before the last helix of the I-like domain (Fig. 3.1B). Further, the position of LIMBS (gold), MIDAS (pink), and ADMIDAS (blue) cations, and the location of Asp^{217} (coordinating residue for LIMBS) and Ser^{123} (coordinating residue for MIDAS) are illustrated.

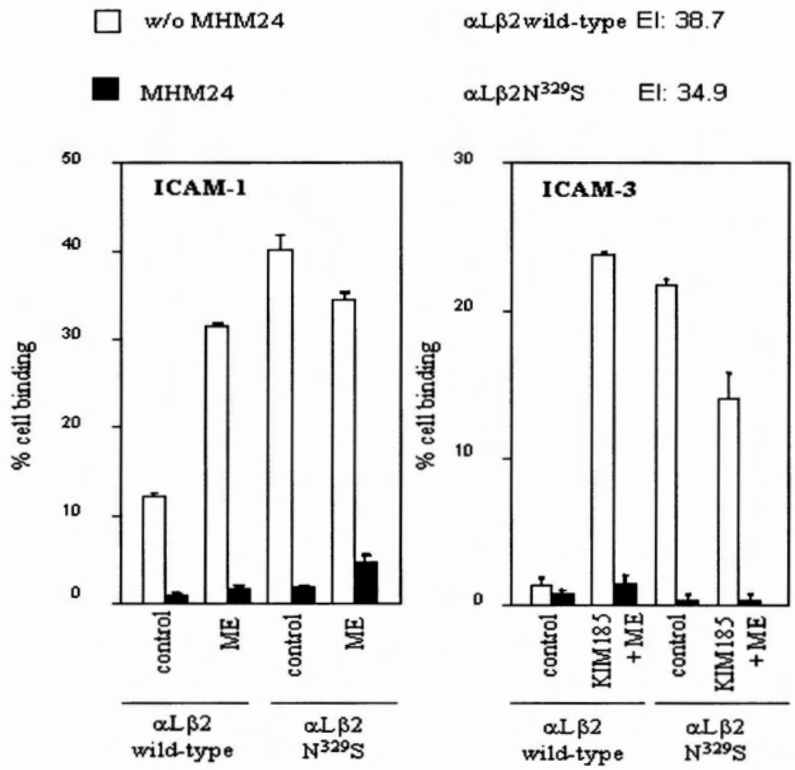

Fig. 3.2 Adhesion of αLβ2N^{329}S transfectants to ICAM-1 and ICAM-3. Mg/EGTA (ME) and KIM185 (10 μg/mL) were used to activate αLβ2. Adhesion specificity was demonstrated using the αLβ2-specific function-blocking mAb MHM24. The cell surface expressions of wild-type αLβ2 and αLβ2N^{329}S were assessed by flow cytometry analyses using mAb MHM23 (β2-specific heterodimer-recognizing mAb). The expression level was represented by the Expression Index (EI) that was calculated by % cells gated positive x geo-mean fluorescence intensity.

In the liganded I-domain in α2 and αM, a significant downward displacement of its C-terminal helix was observed (Emsley et al., 2000; Lee et al., 1995a). Consistent with this observation, open conformation αL and αM I-domains, which have high affinity ligand binding properties, were generated by introducing cysteine that stabilized the last helix of the I-domains (Shimaoka et al., 2001; Shimaoka et al., 2002a). Similar to the I-domain, the last helix of the β3 I-like domain was displaced in a ligand-mimetic-bound αIIbβ3 (Xiao et al., 2004). How β2N^{329}S confers αLβ2 constitutive propensity to adhere to ICAM-1 is unclear (Tng et al., 2004). The substitution of an amide to a hydroxyl side chain (Asn-Ser) hints at the possibility of functional group contribution towards the marked difference in the activity of αLβ2 with β2 Asn^{329} or Ser^{329}. Therefore, four other variants, αLβ2N^{329}T, αLβ2N^{329}Q, αLβ2N^{329}A, and αLβ2N^{329}D, were generated and tested for their capacities to adhere to the ICAMs (Fig. 3.3). All four transfectants showed constitutively adhesion both to ICAM-1 and ICAM-3 in the absence of Mg/EGTA (Fig. 3.3). The expression levels of αLβ2N^{329}T, αLβ2N^{329}Q, αLβ2N^{329}A, and αLβ2N^{329}D were shown to be similar by flow cytometry. It is apparent that the introduction of a hydroxyl group as a result of N^{329}S mutation does not have a primary role in generating a constitutively active αLβ2 because the substitutions N^{329}Q, N^{329}A, and N^{329}D in β2 promoted comparable ICAM-adhesion activity. The altered binding property of αLβ2 N^{329}S is likely to be attributed mainly to the loss of the side chain amide group at position 329 of the β2. However, the β2 mutation N^{329}Q, which has a side chain amide and also confer constitutive activity, suggests that a Cβ instead of Cγ amide group at position 329 of the β2 I-like domain is required to maintain the functional integrity of αLβ2.

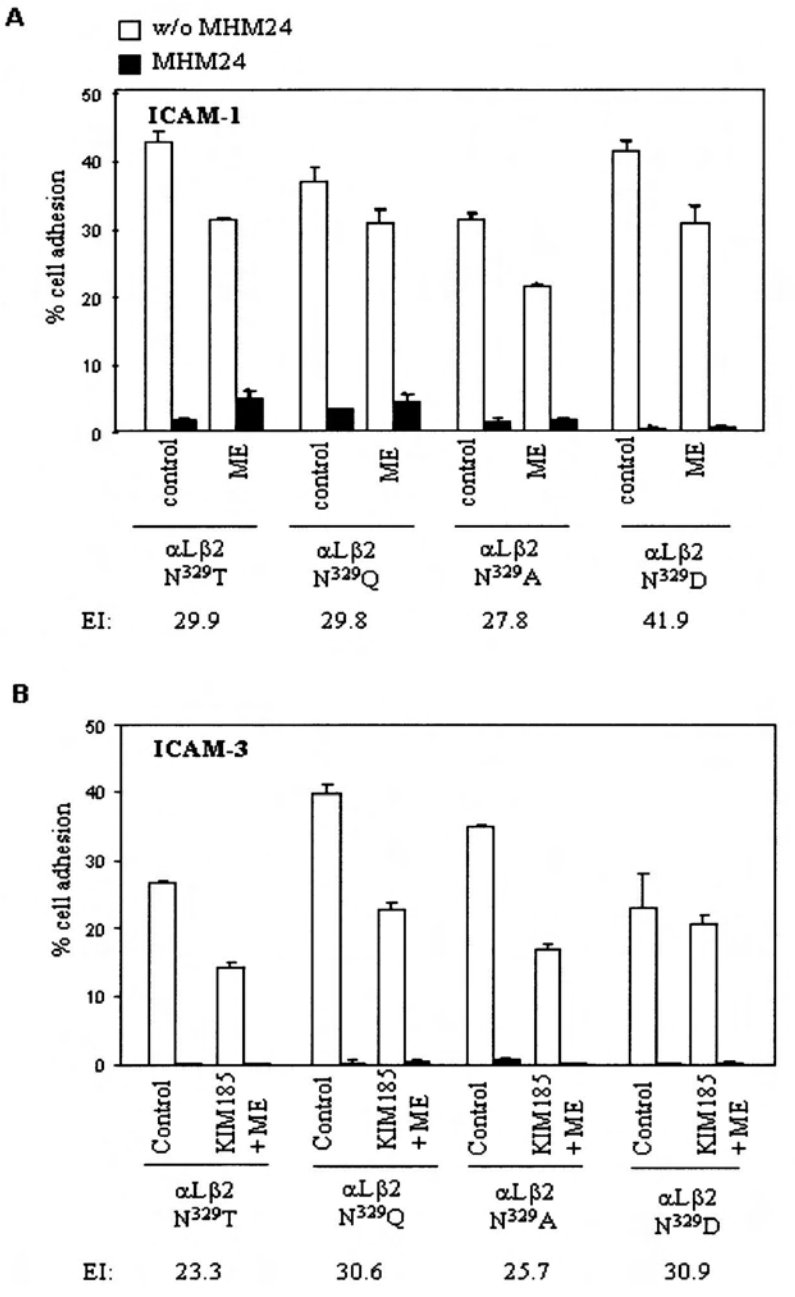

Fig. 3.3 Adhesion of αLβ2N329 variants to ICAM-1 and ICAM-3. (A) αLβ2N^{329}T, αLβ2N^{329}Q, αLβ2N^{329}A, and αLβ2N^{329}D transfectants adhered to ICAM-1 constitutively even without Mg/EGTA (ME). **(B)** Constitutive adhesion of these transfectants to ICAM-3 was also detected. MHM23 was used for flow cytometry analyses and surface expression represented as EI.

3.3 The LIMBS and MIDAS of the I-like domain are required for the activating effect of $N^{329}S$ in I-domain-containing αLβ2

In I-domain containing integrins, the I-like domain allosterically regulates the ligand-binding activity of the I-domain (Yang et al., 2004b). It is reasonable to suggest that structural changes at the locality of β2$N^{329}S$ are propagated to the ligand-binding face of the I-like domain. This may trigger I-like domain binding of the invariant Glu in the last C-terminal helix of the αL I-domain, hence activating I-domain ligand-binding. Therefore, disrupting the ligand-binding sites of the I-like domain should abrogate the activating signal of $N^{329}S$. Indeed, transfectants bearing αLβ2 having composite mutations $N^{329}S$ and $S^{116}P$ or $D^{209}H$ failed to adhere to ICAM-1 even in the presence of activating agents (Fig. 3.4). The adhesion specificity mediated by αLβ2 was demonstrated in all cases by the complete abrogation of adhesion in the presence of mAb MHM24. Ser^{116} is the third coordinating residue found in the MIDAS motif DxSxS of the I-like domain, and the function disrupting effect of $S^{116}P$, identified in LAD-1 patient, has been reported (Hogg et al., 1999). Asp^{209} is a LIMBS coordinating residue. The LAD-1 $D^{209}H$ mutation abolished β2 integrins ligand-binding capacity (Mathew et al., 2000), which corroborates well with the role of LIMBS in stabilizing MIDAS mediated firm adhesion (Chen et al., 2003). Collectively, these data suggest that the activating effect of $N^{329}S$ is propagated through the ligand-binding site(s) of the β2 I-like domain, which subsequently activates the αL I-domain.

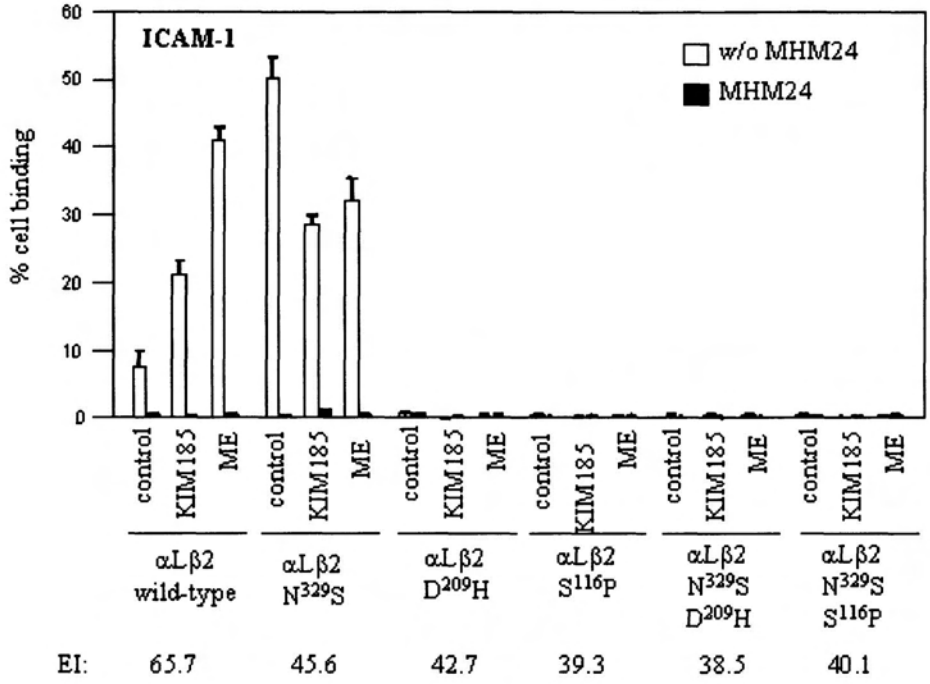

Fig. 3.4 Effect of $N^{329}S$ in combination with $S^{116}P$ or $D^{209}H$ on αLβ2-mediated adhesion to ICAM-1. The mutations $S^{116}P$ and $D^{209}H$ abrogated the activating effect of ME or KIM185 on wild-type αLβ2 ICAM-1 adhesion. Similarly, these mutations abolished constitutive adhesion of αLβ2$N^{329}S$ transfectants to ICAM-1. MHM23 was used for flow cytometry analyses and surface expression represented as EI.

3.4 Introduction of $N^{339}S$ in β3, which corresponds to $N^{329}S$ in β2, generates a constitutively active I-less integrin αIIbβ3

To further demonstrate that the activating signal of Asn mutation is propagated to the ligand-binding site(s) of the I-like domain, we extended the investigation to the I-less integrin αIIbβ3 because the β3 I-like domain participates directly in extrinsic ligand-binding (Xiao et al., 2004; Xiong et al., 2002). The corresponding Asn^{339} in β3 (Fig. 3.1B) was substituted with Ser to generate $\beta3N^{339}S$. Ser^{116} and Asp^{209} of the integrin β2 are also conserved in all integrin β subunits. The corresponding residues in integrin β3 are Ser^{123} and Asp^{217}. Thus, the MIDAS variant $\beta3S^{123}P$ and the LIMBS variant $\beta3D^{217}H$ were constructed. In addition, the composite variants $\beta3N^{339}S/S^{123}P$ and $\beta3N^{339}S/D^{217}H$ were generated (Fig. 3.5). Expression levels of αIIbβ3 and its variants on transfectants were shown to be similar by flow cytometry using the β3-specific mAb 7E3. Wild-type αIIbβ3 transfectants adhered avidly to its ligand fibrinogen only in the presence of activating Mn^{2+}. By contrast, $\alpha IIb\beta3N^{339}S$ showed constitutive adhesion to fibrinogen. The specificity of αIIbβ3-mediated adhesion was demonstrated using αIIb-specific function blocking mAb 10E5. Substitutions $S^{123}P$ and $D^{217}H$ in β3 abolished αIIbβ3-mediated adhesion to fibrinogen, both in the wild type and $N^{329}S$ variant. Therefore, we conjectured that the mutations $N^{329}S$ in αLβ2 and $N^{339}S$ in αIIbβ3 affect the respective I-like domain in a similar manner.

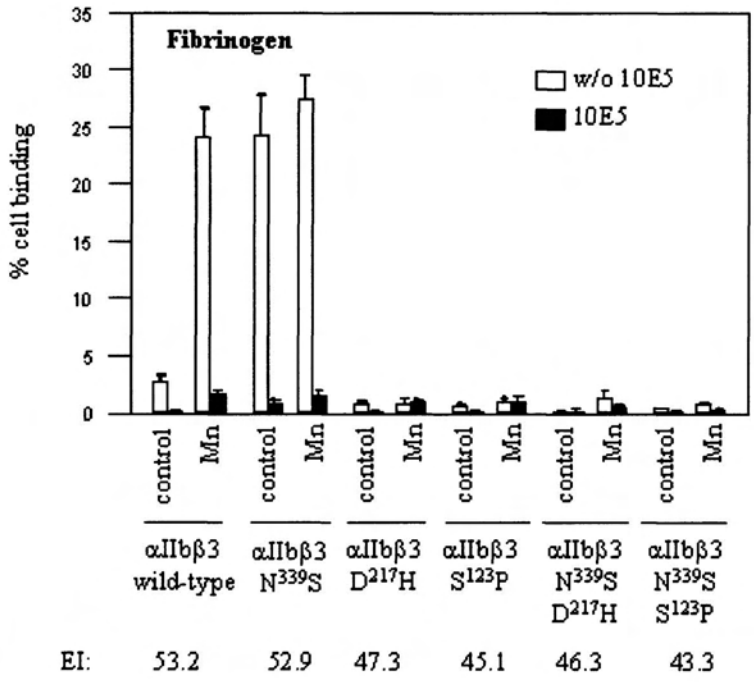

Fig. 3.5 Effect of $N^{339}S$ with $S^{123}P$ or $D^{217}H$ on I-less integrin αIIbβ3-mediated adhesion to fibrinogen. Adhesion specificity was demonstrated using the αIIbβ3-specific function-blocking mAb 10E5. 1 mM $MnCl_2$ (Mn^{2+}) was used as the activating agent. The cell surface expressions of wild-type αIIbβ3 and variants were assessed by flow cytometry using mAb 7E3 (β3-specific mAb) and represented as EI.

3.5 A functional β2 I-like domain is required for αLβ2 I-domain-mediated ligand-binding even if the latter is made constitutively active

The MIDAS ($S^{116}P$) and LIMBS ($D^{209}H$) mutations nullified the activating effect of $\beta2N^{329}S$ in αLβ2. We noted that $S^{116}P$ and $D^{209}H$ also abrogated αLβ2 function in the presence of activating agents such as KIM185 or Mg/EGTA (Fig.3. 4). The disrupting effect of $S^{116}P$ and $D^{209}H$ on KIM185-activated αLβ2 function may be explained by having a dysfunctional I-like domain that is unable to engage and propagate the activating signal of KIM185 that is initiated at the C terminal stalk region of αLβ2 to its I-domain. On the other hand, Mg/EGTA may act on different sites on αLβ2, considering that there are eight other possible cation-binding sites other than the I-domain MIDAS (Arnaout et al., 2005). Thus, it is unclear whether I-like domain disrupting mutations can negate the ligand-binding property of a pre-existing activated I-domain. We therefore use the constitutively active αLβ2 that has its I-domain locked in an open conformation with an engineered cysteine (Shimaoka et al., 2001), the αLccβ2 transfectant adhere to ICAM-1 constitutively (Tng et al., 2004), but does not adhere to ICAM-3 unless activated by either Mg/EGTA or KIM185 (Fig. 3.6A). Thus, αLccβ2 is in an intermediate affinity state. Next, we tested the effect of β2 substitutions $N^{329}S$, $S^{116}P$ or $D^{209}H$ on αLccβ2 ICAM-1 binding (Fig. 3.6B). The level of adhesion to ICAM-1 was comparable between the αLccβ2 and $\alpha Lcc\beta2N^{329}S$ transfectants. By contrast, transfectants expressing $\alpha Lcc\beta2S^{116}P$ and $\alpha Lcc\beta2D^{209}H$ failed to adhere to ICAM-1. These data suggest that a functional I-like domain is required for αLβ2 ligand-binding even when the I-domain is activated independently.

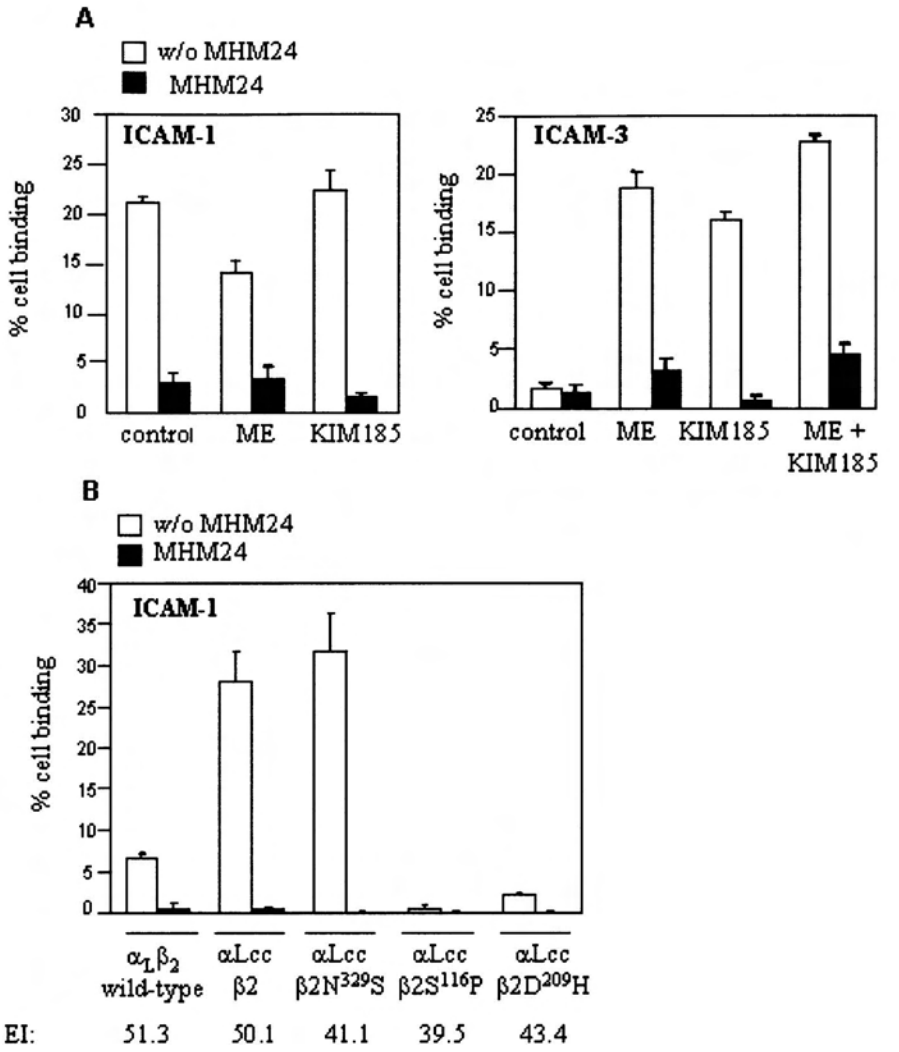

Fig. 3.6 The effect of I-like domain disrupting mutations $S^{116}P$ and $D^{209}H$ on αLccβ2 variant. (A) Binding of transfectants expressing αLccβ2 to ICAM-1 and ICAM-3. **(B)** Binding of αLccβ2 with I-like domain mutations to ICAM-1. MHM23 was used for flow cytometry analyses and surface expression represented as EI.

3.6 The extended conformation of αLβ2N^{329}S

The conversion from a severely bent to a highly extended conformation was shown to be an important event during integrin affinity state transition (Nishida et al., 2006; Xiao et al., 2004). We examined the conformation of αLβ2N^{329}S using two β2 integrin specific reporter mAbs. The mAb KIM127 recognizes an epitope that is buried in the β2 I-EGF2 in a bent αLβ2 conformer. This epitope is, however, exposed when αLβ2 adopts an extended conformation (Beglova et al., 2002; Lu et al., 2001a). The mAb MEM148 recognizes a masked-epitope in the β2 hybrid domain, and it serves to report hybrid domain displacement (Tang et al., 2005). In 293T transfectants, both KIM127 and MEM148 can give a positive signal in flow cytometry because they can stain free β2, which can at times be seen on the cell surface. We therefore chose the method of surface labeling and immunoprecipitation, which would allow us to examine heterodimer reactivity with the β2-specific reporter mAbs by detecting the level of αL coprecipitated with β2. Cell surface αLβ2 and αLβ2N^{329}S on transfectants were labeled with biotin and immunoprecipitated with MHM23, KIM127, or MEM148 with or without Mg/EGTA. In this study, αLccβ2 was also included. Wild-type αLβ2 was precipitated by MHM23 (β2 integrin heterodimer-specific mAb and it serves as a control in this experiment) (Fig. 3.7). However, wild-type αLβ2 was only precipitated by KIM127 or MEM148 in the presence of activating Mg/EGTA. A similar profile was detected for αLccβ2. In contrast, αLβ2N^{329}S was precipitated by KIM127 and MEM148 even in the absence of Mg/EGTA. These data suggest that αLβ2N^{329}S adopts an extended conformation and a displacement of the hybrid domain. This conformation was proposed to depict a high affinity integrin (Xiao et al., 2004), and it is in agreement with our binding data. The lack of αLccβ2 precipitated by KIM127 in the absence of exogenous activation was also consistent with previous

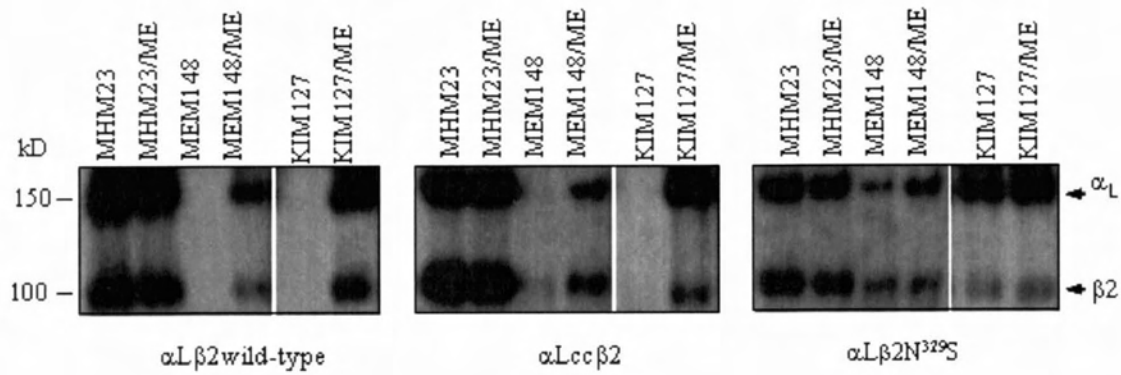

Fig. 3.7 The $N^{329}S$ mutation transforms αLβ2 into an extended conformation. Cell surface labeled wild-type αLβ2, αLccβ2, and αLβ2$N^{329}S$ were subjected to reporter mAbs MEM148 or KIM127 binding at 37°C with or without ME followed by precipitation using protein A-Sepharose beads (Experimental Procedures). Immunoprecipitated integrins were resolved on a 7.5% SDS-PAGE gel under reducing conditions, and detected by ECL. MHM23 was included as control mAb.

observation that αLccβ2 was stained weakly with KIM127 by flow cytometry (Lu et al., 2001c).

3.7 Discussion

Naturally occurring mutations identified in LAD-1 patients provide useful insights into the possible functions of residues and domains of the β2 integrins (Hogg and Bates, 2000). Two such mutations $S^{116}P$ and $D^{209}H$ exemplify the importance of the MIDAS and LIMBS respectively of the β2 I-like domain in αLβ2 ligand-binding function (Hogg et al., 1999; Mathew et al., 2000). Many LAD-1 mutations disrupt β2 integrin biosynthesis, heterodimer formation or generate dysfunctional cell surface expressed β2 integrins (Anderson and Springer, 1987; Hogg and Bates, 2000). Previously, we reported three LAD-1 mutations $C^{568}R$,$R^{571}C$ and $N^{329}S$ in the β2 that generated αLβ2 variants with ligand-binding activity (Shaw et al., 2001; Tng et al., 2004). This study further characterized the $N^{329}S$ mutation. The Asn^{329} is conserved in all human integrin β subunits (Fig. 3.1A) as well as the β subunits of lower metazoans including coral and sponge (Brower et al., 1997). Our data suggests that a Cβ instead of Cγ amide group at position 329 of the β2 I-like domain is required to maintain αLβ2 functional integrity. Because of the availability of structural information of β3 I-like domain, we first reviewed Asn^{339} in β3 that corresponds to the Asn^{329} in β2. The β3 Asn^{339} is located before the α7 helix (last helix) of its I-like domain (Fig.3.8A). The orientations of the β6 strand and the α7 helix in the β3 I-like domain are different in the structures of a bent αVβ3 (red) (conformer I) (Xiong et al., 2004), a bent liganded-αVβ3 (green) (conformer II) (Xiong et al., 2002), and the fibrinogen mimetic-bound αIIbβ3 with open headpiece (blue) (conformer III)(Xiao et al., 2004).

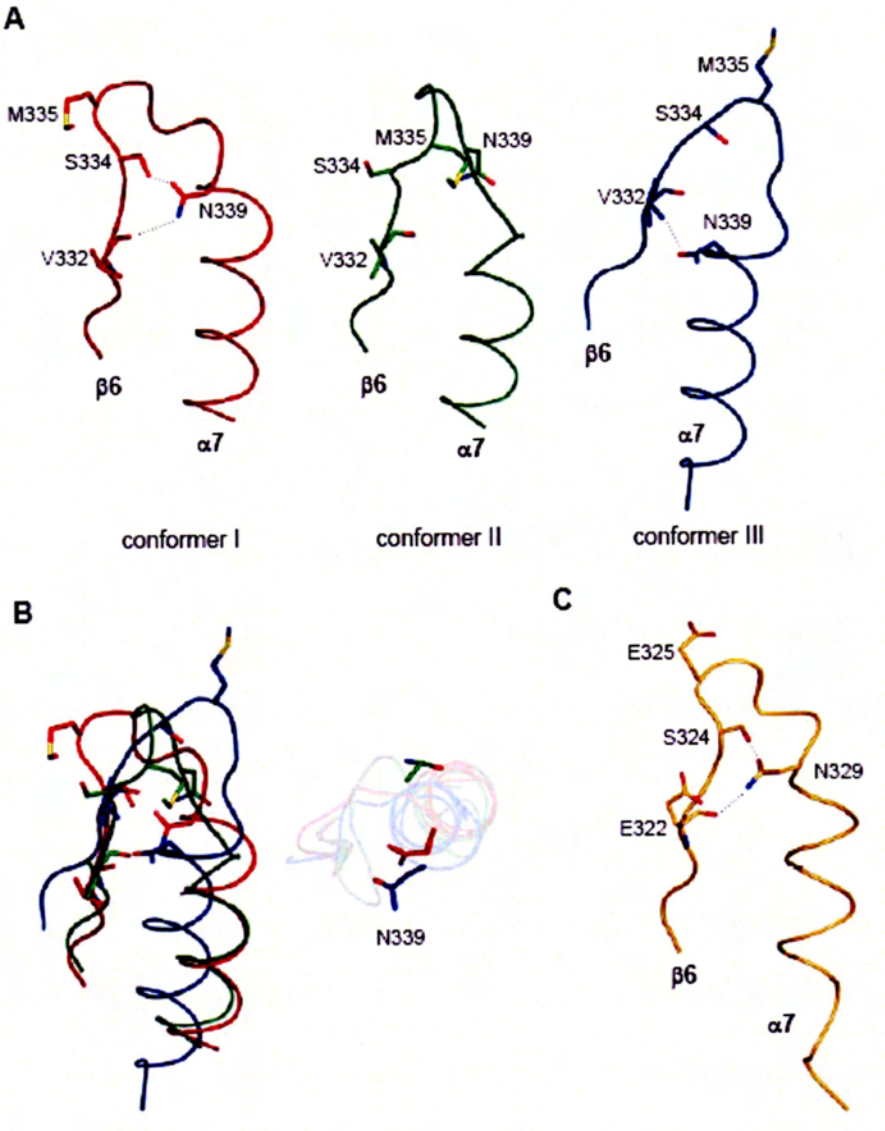

Fig. 3.8 Illustrations of the β6-α7 loop of the β3 and β2 I-like domains. (A) Three structures of β6-α7 loop of β3 I-like domain. Conformer I (Katayama et al.) [PDB:1U8C] (Xiong et al., 2004) a new refined model of αVβ3 [PDB:1JV2] (Xiong et al., 2001); conformer II (Nermut et al.) [PDB:1L5G] (Xiong et al., 2002); conformer III (blue) [PDB:1TYE] (Xiao et al., 2004). Met^{335}, a non-conserved ADMIDAS coordinating residue, in β3 I-like domain is shown. (B) Superposition of the β6-α7 loops from the three structures. The orientation of the Asn^{339} in these structures (top view) is shown. (C) Model of the β6-α7 loop of β2 I-like domain based on the structural coordinates of Xiong et al. (Xiong et al., 2004) using the software program Modeler. Figures were created using the software program Pymol (W.L. DeLano, http://www.pymol.org).

The bent αVβ3 may represent a resting integrin conformer whereas the fibrinogen mimetic bound αIIbβ3 with hybrid domain displaced may represent a high affinity conformer (Arnaout et al., 2005). The structure of the bent liganded-αVβ3 may require careful interpretation because the Arg-Gly-Asp (RGD) ligand was soaked into the performed αVβ3 crystals and may therefore account for the absence of α7 helix displacement (Xiong et al., 2002). Thus, the re-positioning of the Asn^{339} herein was examined mainly between conformer I and conformer III. In conformer I, Asn^{339} of the β3 I-like domain projects its amide side chain in an orientation that can allow hydrogen-bonds to be established with main chain carbonyl oxygen of Val^{332} in the β6 strand, and the side chain hydroxyl group of Ser^{334} that resides in the loop connecting the β6 strand and the α7 helix. Interestingly, these are different in conformer III. Hydrogen-bond can form between δ^1O of Asn^{339} with the main chain amide of Val^{332} but not between Asn^{339} and Ser^{334}. This observed difference between the two conformers is attributed to the downward movement of the α7 helix, and the outward rotation of the Asn^{339} in conformer III with respect to conformer I (Fig. 3.8B). The solvent accessible surface area (SASA) of Asn^{339} of conformer I is about 50 $Å^2$, whereas that of conformer III is about 70$Å^2$, which corroborates well with its outward re-orientation in conformer III having a displaced α7 helix. It is therefore possible that the formation of polar contacts between Asn^{339} and Val^{332} and Ser^{334} is required in part to maintain the I-like domain of β3 subunit in a resting conformation. Disruption of these contacts as a result of a mutation such as $N^{339}S$ may destabilize these interactions, hence generating an activated αIIbβ3.

In β2, similar polar contacts may be formed as depicted in a homology model of β2 I-like domain generated based on the bent αVβ3 structural coordinates (Fig. 3.8C). The

Ser^{324} side chain may hydrogen-bond with Asn^{329} δ^1O in the β2 I-like domain model. The residue at position 322 of β2 and 332 of β3 is different. This is, however, irrelevant because it is the backbone carbonyl of this residue that may hydrogen-bond with the conserved Asn. β2 I-like domain models with the Asn^{329} substituted by Gln, Ala, Ser, Thr, or Asp (materials amd methods) showed potential disruptions in hydrogen-bond formation between these residues at position 329 with Ser^{324} and main chain Glu^{322}, which may account for the activating effect of these mutations on αLβ2. Taken together, these suggest that the polar contacts between Asn^{329} with Ser^{324} and Glu^{322} may serve to stabilize the β2 I-like domain in a fashion similar to that in β3 conformer I. It is noted that although β2Ser^{324} (β3Ser^{334}) can potentially hydrogen-bond with the conserved β2Asn^{329} (β3Asn^{339}), this should be extrapolated with caution to other integrins because β2Ser^{324} is conserved in β3, β1, and β7 but not in other β subunits (Fig. 3.1A). In addition, the contribution of the conserved Asn towards the function of other β subunits awaits further studies.

Integrin affinity states are governed by its varied conformations under different conditions (Arnaout et al., 2005; Luo and Springer, 2006). In a global setting, the bent integrin conformer depicts a resting low affinity state and the extended integrin conformers are assigned as the active receptors (Takagi et al., 2002b). The extended integrin conformers are further divided into two major populations based on structural differences in their headpieces (Xiao et al., 2004). Extended integrin conformers with or without hybrid domains displaced are assigned high or intermediate affinity states respectively. In this study, the mutation $N^{329}S$ induced an extended αLβ2 conformation because in the absence of activating agent, αLβ2$N^{329}S$ was immunoprecipitated by the reporter mAb KIM127 (Beglova et al., 2002; Salas et al.,

2004). Under the same conditions, αLβ2N^{329}S was precipitated by mAb MEM148, which reports hybrid domain displacement (Tang et al., 2005). These data suggest a high affinity αLβ2 generated by the β2N^{329}S mutation. Indeed, our functional data showing αLβ2N^{329}S binding constitutively and effectively to ICAM-3 supported the assignment of a high affinity receptor. It is unclear at present how N^{329}S triggers such a dramatic global conformational change in αLβ2. Not only does N^{329}S incur activation of the I-like domain, as demonstrated in αIIbβ3N^{329}S, it also induces unbending of the entire integrin. However, this need not be unexpected because it was reported that one-turn deletion in the α7 helix of the β2 I-like domain promoted αLβ2 binding to ICAM-1, and exposed the epitopes of extension reporter mAb KIM127, and the activated I-like domain reporter mAb 24 (Yang et al., 2004a).

Our data also point to a dominant role of the I-like domain over the display of a functional I-domain. It is well demonstrated that the I-like domain regulates the I-domain allosterically (Yang et al., 2004b) but the overbearing effect of a dysfunctional I-like domain on an engineered I-domain that was made constitutively active (αLccβ2) warrants attention. It is apparent that αLccβ2 conforms to an intermediate affinity receptor because it bound ICAM-1 constitutively but required an additional activating condition for ICAM-3 binding in this study. Further, mAbs KIM127 and MEM148 failed to precipitate αLccβ2 without Mg/EGTA activation. Thus, these observations suggest that αLccβ2 is unlikely to be in an extended open conformation. The lack of reactivity of αLccβ2 to mAbs KIM127 and 24 was also reported previously (Lu et al., 2001c). Collectively, these observations suggest that αLccβ2 is not adopting a fully extended conformation. Abrogation of αLccβ2 constitutive ICAM-1-adheison activity by the β2 I-like domain mutations S^{116}P or

$D^{209}H$ suggest that these mutations possibly revert αLccβ2 into a conformation such that steric factors disfavor disulfide-locked I-domain binding to ligand.

In summary, we have further characterized the LAD-1 mutation $N^{329}S$. This mutation generates a high affinity αLβ2 with an extended conformation. $N^{329}S$ activates the β2 I-like domain. The corresponding mutation in $\beta3N^{339}S$ had similar activating effect on αIIbβ3. The conservation of this Asn in all integrin β subunits through evolution suggest a primary role of this residue in the shaping of the I-like domain. Based on available structures of the β I-like domains, and structural predictions, this Asn may serve to stabilize the conformation of the α7 helix and its interaction with the preceding β6 strand. However, definitive revelation of its role in the shaping of the I-like domain will require structural studies of integrins with these mutation(s).

Chapter 4: Characterization of LAD mutation $R^{571}C$

Previous study in Prof Alex Law's laboratory had shown that the β2 subunit with the $R^{571}C$ mutation can support αLβ2 expression on COS-7 transfectants. These transfectants can adhere to ICAM-1 coated surface but would require an additional activation agent, such as Mg/EGTA to adhere to ICAM-3 (see Chapter 5). Surprisingly, this mutant $\beta2R^{571}C$ does not support the expression of Mac-1 and p150,95 (Shaw et al., 2001). Since αM and αX share much similarity in sequence, we focused on comparing $\alpha L\beta2R^{571}C$ and $\alpha M\beta2R^{571}C$ in this study.

4.1 β2 with $R^{571}C$ cannot form dimers with αM

Previously, it was shown that $\alpha M\beta2R^{571}C$ can not be expressed on the cell surface (Shaw et al., 2001). It was not known if the heterodimer cannot be formed or it is formed but failed to be transported on the cell surface. αM subunit with either (wt) β2 or $\beta2R^{571}C$ was transfected into 293T cells. The transfected cells were biotinylated and then lysed, followed by immunoprecipitation with KIM202 and MHM23 (Fig. 4.1 A). αMβ2 can be precipitated by KIM202 (anti-β2) and MHM23 (heterodimer specific). Very faint bands were seen with the sample from the $\alpha M\beta2R^{571}C$ transfectants, confirming that the $\beta2R^{571}C$ can only support minimal heterodimer expression with αM. In addition, it also showed that $\beta2R^{571}C$ is not expressed on the cell surface as a monomer, because no $\beta2R^{571}C$ band was precipitated with KIM202. The control experiment with αLβ2 shows that both αLβ2 and $\alpha L\beta2R^{571}C$ were expressed on the cell surface.

In order to detect whether there is $\beta 2R^{571}C$ or $\alpha M\beta 2R^{571}C$ inside the cell, β2 subunit with a C-terminal GFP tag were used. The lysate of the $\alpha L\beta 2R^{571}C$ and $\alpha M\beta 2R^{571}C$ transfectants were subjected to immunoprecipitation with KIM202 and MHM23. After SDS-PAGE, the β2 subunits were detected by Western blot with an anti-GFP antibody. $\alpha L\beta 2R^{571}C$ can be precipitated by KIM202 and MHM23, however, $\beta 2R^{571}C$ was precipitated by KIM202 from the $\alpha M\beta 2R^{571}C$ transfectants, but not precipitated by MHM23 (Fig.4.1 B). It suggests that the β2 subunit is synthesized but cannot combine with αM. Thus, $\beta 2R^{571}C$ is synthesized in the $\alpha M\beta 2R^{571}C$ transfectants, but it is restricted intracellularly and cannot form a heterodimer with αM.

4.2 αL/αM chimeras

In order to find out why the β2 subunit with the $R^{571}C$ mutation can associate with αL to form functional LFA-1, but not with αM to form Mac-1, two α subunit chimeras were generated (Fig.4.2). In one, the αL I-domain is replaced with that of the αM I-domain, $\alpha L(I_M)$. In the other, the αM I-domian is replaced with that of αL I-domain, $\alpha M(I_L)$. These two α subunit chimeras are co-transfected into the 293T cell with β2 or $\beta 2R^{571}C$. Heterodimer expression was assessed by flow cytometry, with the anti-α mAb LPM19c or MHM24 and the heterodimer-specific mAb MHM23. MHM24 is an anti-αL subunit mAb and its epitope is located in the I-domain, and was used to test for the chimeric $\alpha M(I_L)$ expression. LPM19c is an anti-αM subunit mAb and binds to the I-domain of the αM, and was used to detect the chimeric $\alpha L(I_M)$ expression (Violette et al., 1995). From the expression profile, $\alpha L(I_M)\beta 2$ can be detected by both LPM19c and MHM23; $\alpha M(I_L)$ can be detected by both MHM24 and

A

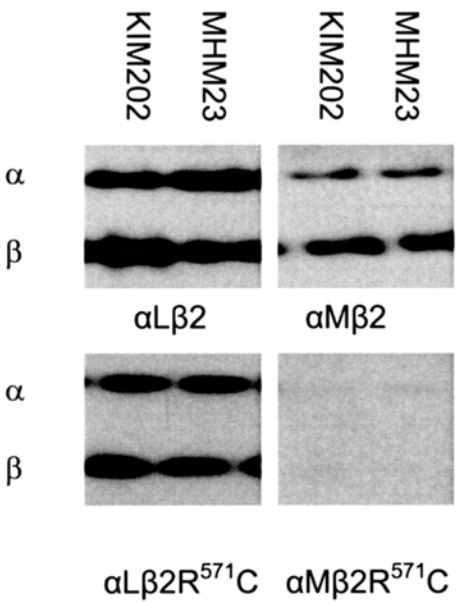

B

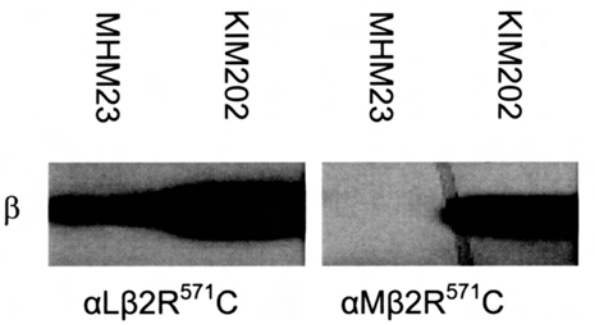

Fig. 4.1 β2 with $R^{571}C$ cannot from dimer with αM, only single $\beta 2R^{571}C$ are synthesized inside the cell. A: very faint $\beta 2R^{571}C$ and heterodimer $\alpha M\beta 2R^{571}C$ band on the cell surface. After biotinylation, cell lysate are immunoprecipitated with anti-β2 antibody KIM202 or anti-heterodimer antibody MHM23. **B**: Single $\beta 2R^{571}C$ are synthesized inside the cell which can be detected by mAb KIM202.

MHM23. It suggests that these two α subunit chimeras can associated with β2 subunit and were expressed on the cell surface. On the other hand, MHM23 can only detect the $\alpha L(I_M)\beta 2R^{571}C$ expression, but not the $\alpha M(I_L)\beta 2R^{571}C$, suggest that the I-domain of αL subunit cannot rescue the expression of $\alpha M\beta 2R^{571}C$. These results are consistent with the previous report that the I-domain is not essential for the folding, heterodimer formation, and surface expression of Mac-1 and LFA-1(Yalamanchili et al., 2000). It should be noted that the $\alpha M(I_L)\beta 2R^{571}C$ transfectants are MHM24 positive. It is known the αM subunit can be expressed on COS-7 and 293T transfectants without the β2 subunit (Berman et al., 1993; Goodman et al., 1998). It is demonstrated here that this monomer expression is not affected by the I-domain.

Another two chimeras were generated, they are αLM and αML (Fig. 4.2): αLM consists of the head-thigh (include β-propeller, I-domain and thigh) of the αL subunit and the calf-tail (include calf-1, calf-2 and cytoplasmic tail) of the αM subunit. Conversely, αML consists of the head-thigh of αM subunit and the calf-tail of αL subunit. Both chimeras can combine with wild type β2 to form heterodimer which is demonstrated by MHH23 and MHM24 or LPM19c expression (Fig. 4.3). Heterodimer formation can also be detected by MHM23 in $\alpha LM\beta 2R^{571}C$ transfectants, but not in $\alpha ML\beta 2R^{571}C$ transfectants. Again, αML chimera subunit alone can be stained by LPM19c.

Thus, the determinant factor on the non-expression of $\alpha M\beta 2R^{571}C$ lies in the head-thigh region of αM. Furthermore, since we have demonstrated that the I-domain does

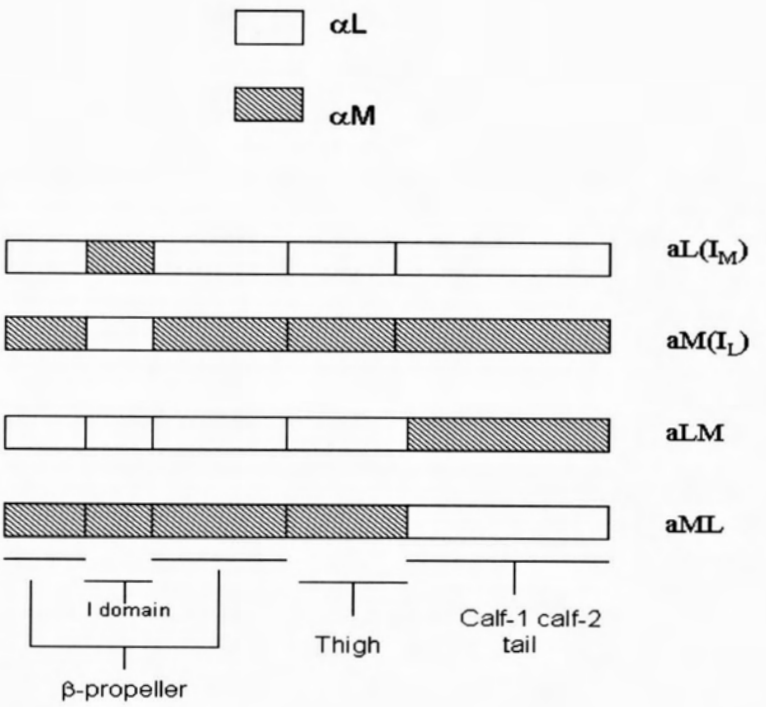

Fig. 4.2 Diagram of α subunit chimeras.

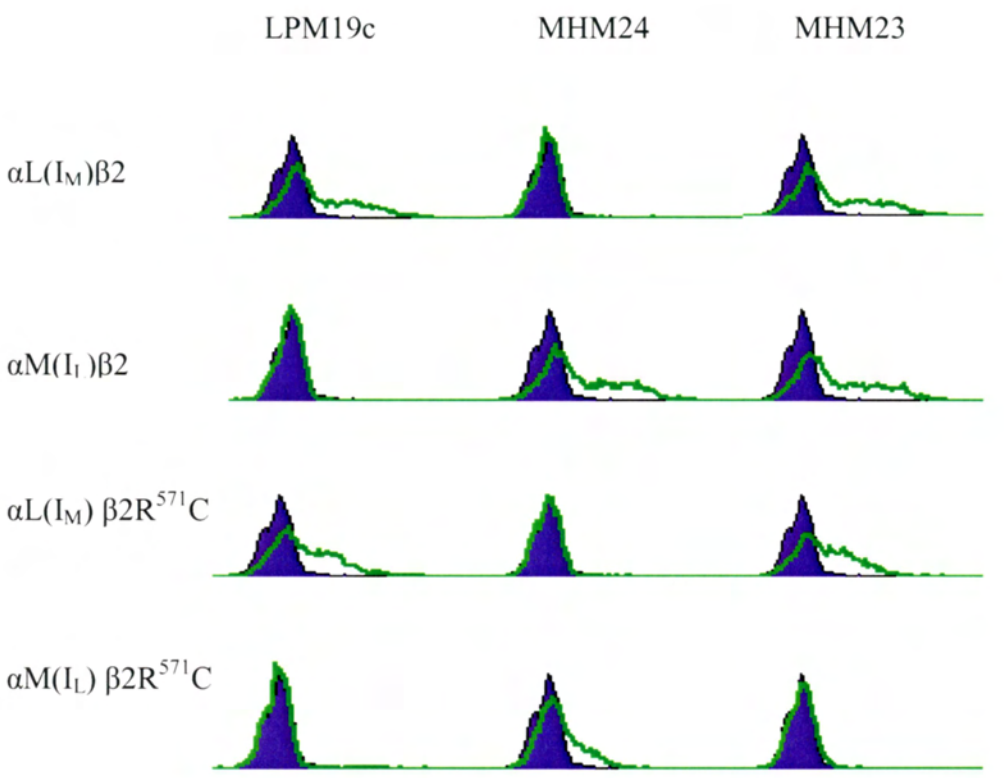

Fig. 4.3 αL(I$_M$) β2 can associate with β2R^{571}C to form variant heterodimer. FACS analysis of 293T cells transfected with different chimerical variants using heterodimer-specific mAb MHM23 or α subunit-specific mAb (LPM19c or MHM24) (green open histogram) and irrelevant mAb KB43 (blue shaded histogram).

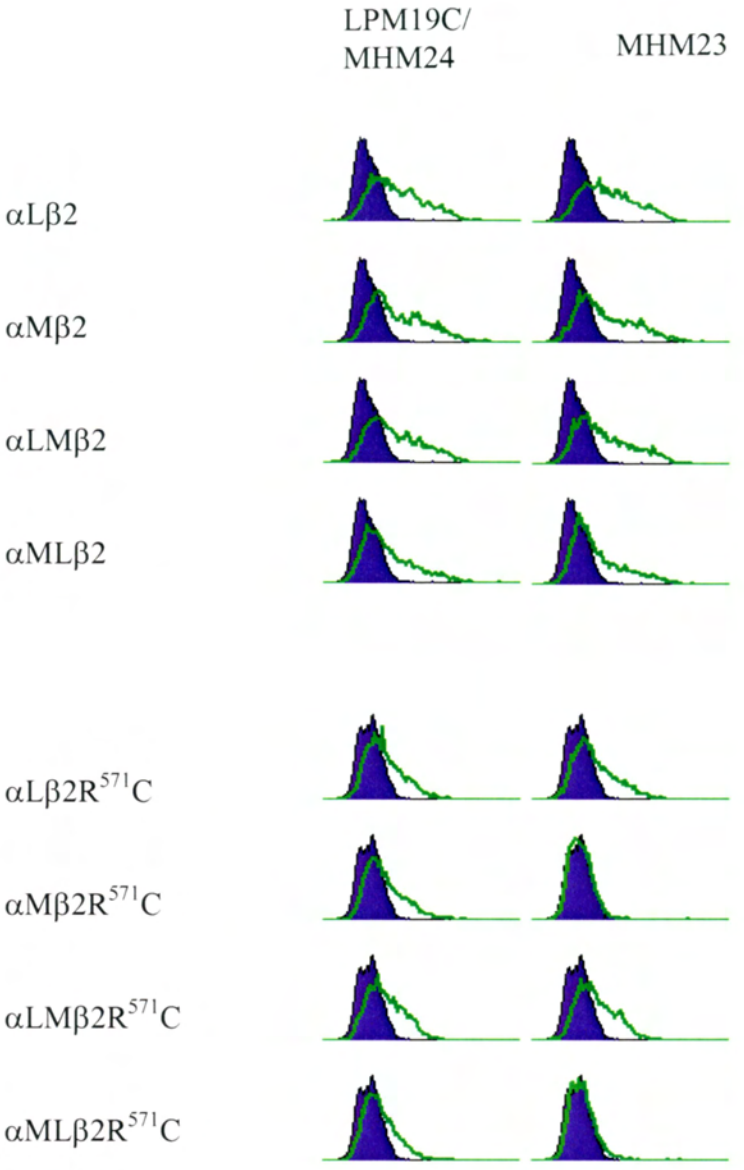

Fig. 4.4 αLMβ2 can associate with β2R^{571}C to form variant heterodimer. FACS analyse of 293T cells transfected with different chimerical variants using heterodimer-specific mAb MHM23 or α subunit-specific mAb (LPM19c or MHM24) (green open histogram). An irrelevant mAb KB43 (blue shaded histogram) was used as a background.

not affect heterodimer formation, the regions of interest therefore lies in the β-propeller and the thigh domain.

4.3 $R^{571}C$ mutation abolished KIM185 epitope expression

In this series of experiment, we would like to proceed to study the intracellular location of the β2 subunit variant when they cannot support αLβ2 and αMβ2 formation, the β2 subunit used were tagged with GFP in the C-terminal. Two-color flow cytometry were performed in which the secondary anti-mouse Ig antibody was conjugated with R-Phycoerythrin (sheep) (Sigma). Although αLβ2$R^{571}C$ can be expressed on the cell surface (Fig. 4.5 column 1 and 2), it cannot be stained by KIM185 by means of immunofluorescent flow cytometry, as indicated by the absence of cells in the upper right quadrant (Fig. 4.5). It should be noted that $R^{571}C$ is located at the N-terminal end of IEGF4 and is not include in the 23 amino acids in which the epitope of KIM185 was located (Lu et al., 2001a). Thus, the $R^{571}C$ mutation induces some conformational change in this IEGF4 domain.

4.4 Charge alteration in residue 571 of the β2 subunit

R^{571} is a positively charged amino acid. Three amino acid substitutions with alanine (non polar), glutamic acid (negatively charge) and lysine (positively charge) were constructed. These β2 variants were transfected into 293T with the three different α subunits. Anti-α antibody (MHM24, LPM19c or KB43), and anti-heterodimer mAb 1B4 were used to detect these variants surface expression. Since the β2 subunits have a GFP tag at the C-terminal, surface expression of the intgrin is shown by the cells in the upper right quadrant of the two-color flow cytometry plots. Heterodimer

formation can be detected by 1B4 in the variants including αLβ2R^{571}A, αLβ2R^{571}C, αLβ2R^{571}K and αLβ2R^{571}E. They can also be stained by anti-α subunit mAb MHM24. For Mac-1, only the αMβ2R^{571}K variant can be detected by anti-heterodimer mAb 1B4. As noted before that the monomeric αM subunit can express on the cell surface and it is shown here again by the positive staining of LPM19c on all transfectants. For p150,95, 1B4 and KB43 can only stain on αXβ2R^{571}K transfectant, but not on the αXβ2R^{571}A, αXβ2R^{571}E and αXβ2R^{571}C transfectants. Therefore, β2R^{571}K can associate with all three α subunits to form heterodimers. On the other hand, β2R^{571}A, β2R^{571}C and β2R^{571}E can only form dimer with αL subunit. Taken together, the amino acid in this location does not affect αLβ2 formation, and it plays a role in regulating the affinity state of the αLβ2 heterodimer since αLβ2R^{571}C can mediate ICAM-1 adhesion without activating agents. However, a positively charged amino acid is apparently required for the heterodimer formation with αM and αX.

Interestingly, the mutation of arginine to alanine, cysteine and glutamic acid abolishes the expression of the KIM185 epitope, suggesting its maintenance requires the presence of a positively charge residue at position 571.

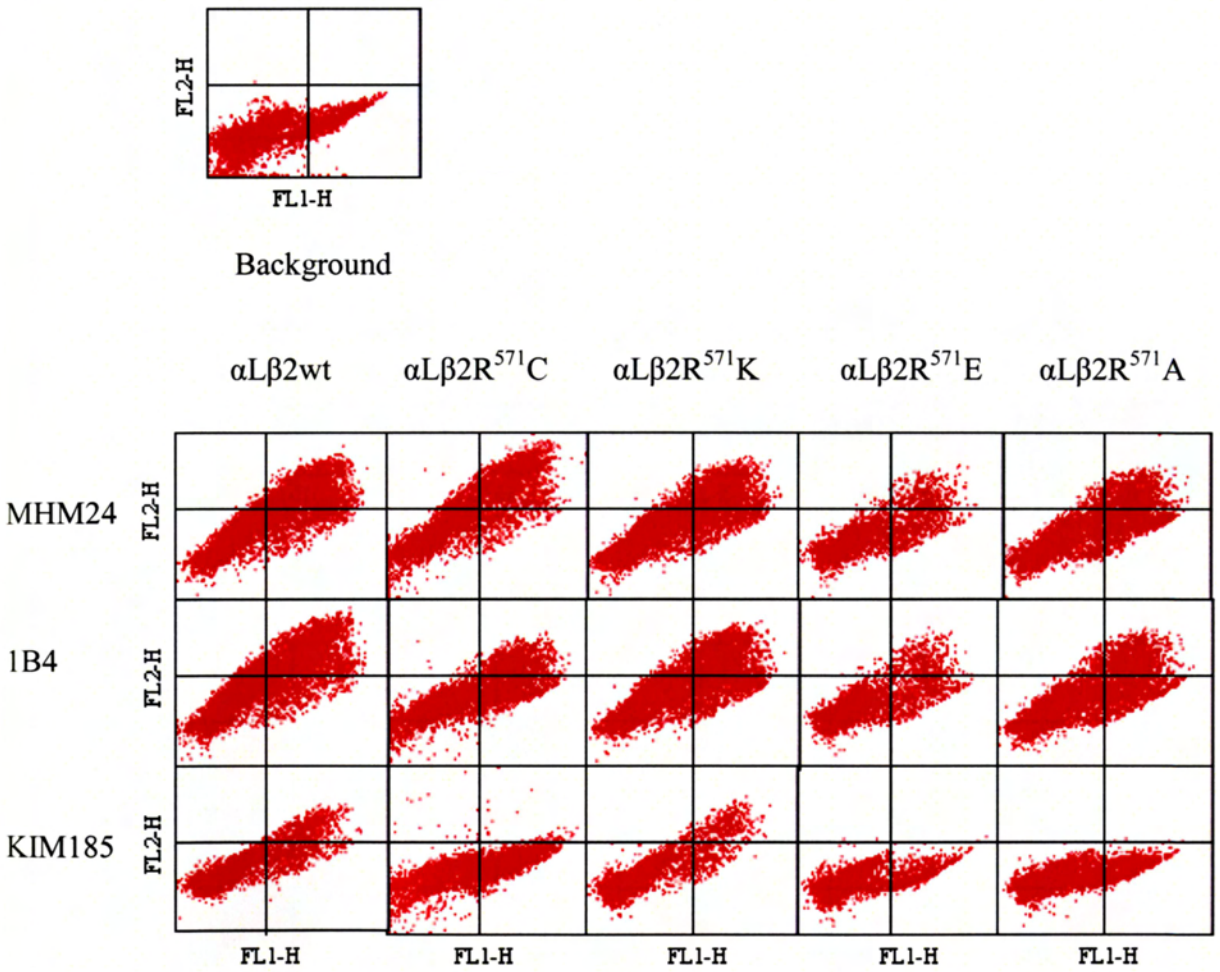

Fig. 4.5 $\beta 2R^{571}K$ can associate with aL subunit to form heterodimer and KIM185 epitope can be expressed. Surface expression of the variant are detected by heterodimer-specific mAb 1B4, α subunit specific mAb (MHM24 and LPM19c) and β2 specific mAb KIM185. β2 and β2 variants have a GFP tag, sheep anti-mouse Fab REP conjugated was used as the secondary antibody (FL2-H). Background is detected by irrelevant mAb BP6.

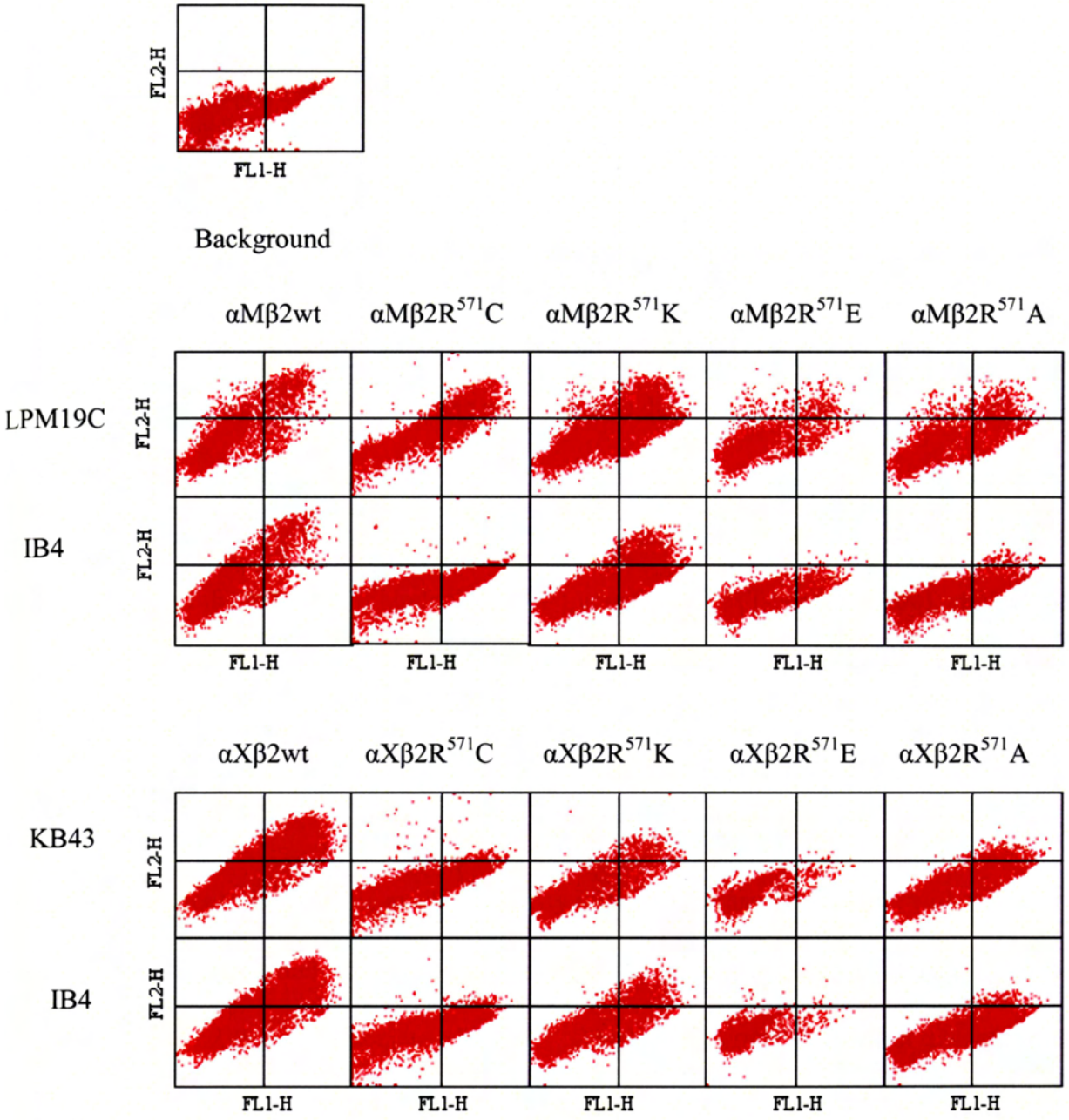

Fig. 4.6 β2R^{571}K can associate with αM or αX subunit to form heterodimer. Surface expression of the variant are detected by heterodimer-specific mAb 1B4, α subunit specific mAb (LPM19c and KB43). β2 and β2 mutants has a GFP tag, sheep anti-mouse Fab RPE conjugated was used as the secondary antibody (FL2-H). Background is detected by irrelevant mAb BP6.

4.5 Discussion

The cysteine residues in the I-EGF domain of the integrin β subunits are very conserved. Each of the I-EGF domains have eight cysteines arranging in a C1-C5, C2-C4, C3-C6, C7-C8 pattern. The $R^{571}C$ mutation introduces an extra cysteine in this region and may therefore perturb the disulfide bond arrangement. Indeed, the conformation of this region perturbed is emphasized by the abrogation of the KIM185 epitope, which according to the mapping data does not include Arg^{571}.

Although the expression indices for LFA-1 variants with this mutation is lower than that of the wildtype, it binds to ICAM-1 constitutively (Tng et al., 2004), and can be activated to bind to ICAM-3 with Mg/EGTA (see Chapter 5). However, the $\beta2R^{571}C$ can not support Mac-1 and p150,95 expression. In addition, it was shown that $\beta2R^{571}C$ could not combine with αM intracellularly.

In order to find out the mechanism why αM subunit can not associate with $\beta2R^{571}C$ to from heterodimer, four chimerical α subunits are constructed: $\alpha M(I_L)$, $\alpha L(I_M)$, αML, αLM. $\alpha L(I_M)$ can associate with $\beta2R^{571}C$ to form heterodimer, but not $\alpha M(I_L)$, which reveals that the I-domain of the α subunit is not critical for heterodimer formation. The fact that αLM, but not αML, can combine with $\beta2R^{571}C$ to form heterodimers shows that substituting the head-thigh domains of the αM subunit with those of αL can rescue the expression of $\alpha M\beta2R^{571}C$. Since we have eliminated the involvement of the I-domain, this result suggests that the propeller and thigh domain of αM are incompatible with the $R^{571}C$ mutation in the β2 subunit. However, from the crystal

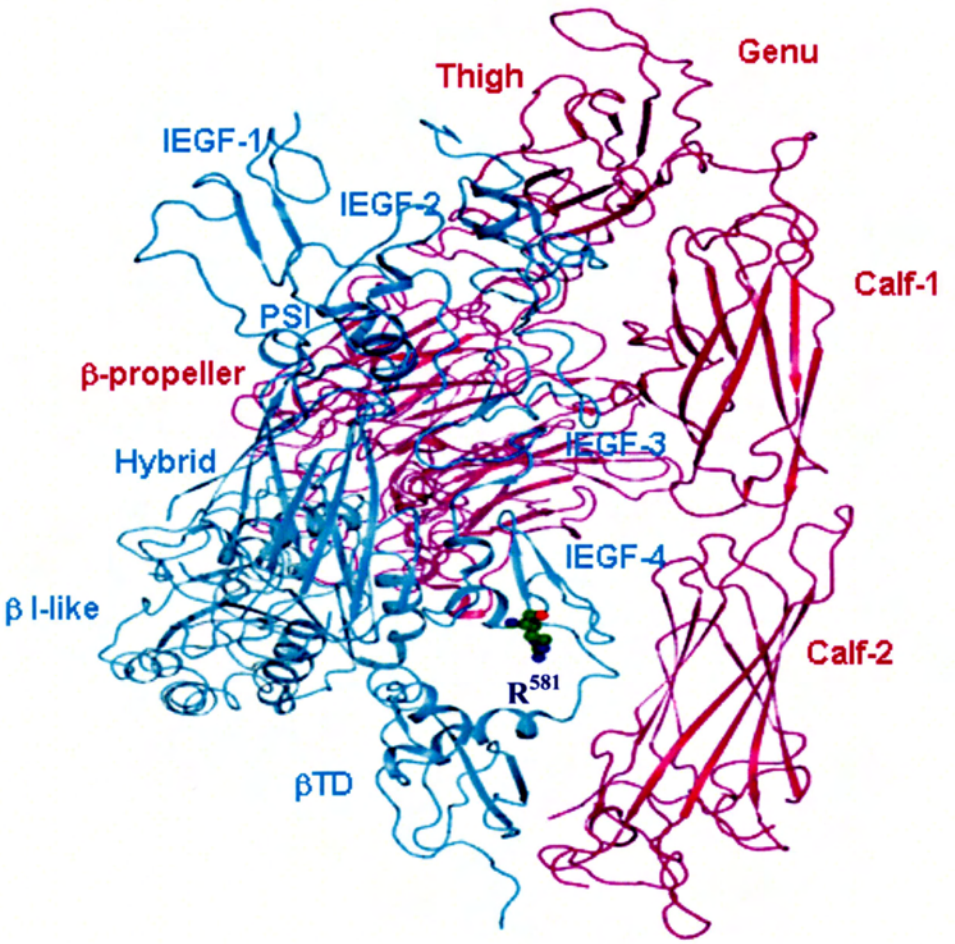

Fig. 4.7 Crystal structure of αVβ3. Ribbon drawing of crystallized αVβ3. Green color: β3 subunit; Red color: αV subunit.Adapted from (Xiong et al., 2001). Residue R^{581} in β3 which is corresponding to $R^{571}C$ in β2 is indicated.

structure of αVβ3 (Xiong et al., 2001) and EM data (Adair and Yeager, 2002; Takagi and Springer, 2002; Takagi et al., 2003), the equivalent R^{581} in β3 does not appear in close proximity of either the β-propeller or the thigh domain of the α subunit in the bent conformation (Fig. 4.7). Nevertheless, the model of αVβ3 may not be applicable to αMβ2. In any case, further experiments are required to pinpoint the residues that are responsible for the heterodimer formation for αMβ2 and αXβ2.

Through mutagenesis study, we find that β2R^{571}K can associate with αL, αM and αX to form individual heterodimers. β2R571A, β2R571E and β2R571C, however, can only combine with αL. While β2R^{571}A and β2R^{571}E behave like β2R^{571}C, β2R^{571}K behave like the wild type. Thus, we may conclude that the positively charged residue in this location is important for the heterodimer formation with αM and αX, whereas the nature of this residue is irrelevant in heterodimer formation with αL. In addition, positive charge is important in maintaining αLβ2 in a resting state. Through the studies with different amino acid substitutions, it also suggested that changes of the disulphide pattern are not relevant to the properties of β2R^{571}C.

Chapter 5: Conformational States of LFA-1 and Its Adhesion to ICAM-1 and -3

The binding of LFA-1 to ICAM-1, -2 and -3 has been extensively studied, and its affinity to the three ICAMs has been established to have the order of ICAM-1 > ICAM-2 > ICAM-3 based on experimental results from the adhesion of LFA-1 expressing cells to ligand coated surfaces (Shaw et al., 2001; Tang et al., 2005). This qualitative order is supported by plasmon resonance analysis of recombinant I-domain of LFA-1 with the three ligands (Shimaoka et al., 2001).

Previously we have mapped the crucial residue for the epitope of the monoclonal antibody (mAb) MEM148 to the Pro^{374} in the hybrid domain of the β2 subunit (Tng et al., 2004). Modeling the LFA-1 structure using the αVβ3 integrin as a template, the epitope is located on the face of β2 hybrid domain pointing towards the thigh of the αL subunit and may therefore be presumed buried in the resting (bent) LFA-1. We have demonstrated that the epitope is indeed not expressed on resting LFA-1 on MOLT-4, but can be exposed upon supplementation of the medium with 5 mM $MgCl_2$ and 1.5 mM EGTA (Mg/EGTA) (Tang et al., 2005), presumably by inducing the movement of the hybrid domain away from the αL leg. Mg/EGTA also reveals the epitope of KIM127, a reporter mAb for leg extension (Tang et al., 2005). Functionally, we have demonstrated that LFA-1 mediated adhesion of MOLT-4 to ICAM-1 can be promoted by Mg/EGTA, or by one of the activating mAbs. Adhesion to ICAM-3 would require one of the activating mAbs in addition to Mg/EGTA. Thus, three functional states of LFA-1 had been defined: a resting state LFA-1 not able to bind the two ligands, an intermediate state LFA-1 capable of binding ICAM-1 but not

ICAM-3, and an active state LFA-1 capable of binding both ligands. The resting state may associate with a bent LFA-1, but whether the intermediate and active states have a clear structural correlation with leg extension and/or hybrid displacement is not clear. In the work reported in this chapter, we use the four activating reagents, namely Mg/EGTA, and the three mAbs KIM127, MEM48 and KIM185 to study LFA-1 mediated adhesion to ICAM-1 and ICAM-3 coated surfaces, and correlate the functional states with leg extension and hybrid displacement, as reported by the expression of the KIM127 and MEM148 epitopes respectively.

5.1 Adhesion of MOLT-4 to ICAM-1 and ICAM-3 coated surfaces

Previously we have shown that LFA-1 mediated adhesion of MOLT-4 to ICAM-1 coated surface required either Mg/EGTA, or one of the two activation mAbs KIM185 and MEM48, but adhesion to ICAM-3 coated surface required Mg/EGTA and one of the mAbs (Tang et al., 2005). Similar results were obtained for K562 cells transfected with the cDNAs of both αL and β2 subunits (Hogg et al., 1999). Furthermore, COS-7 transfectants adhesion to ICAM-3 coated surfaces can also be demonstrated in the presence of both activating mAbs KIM185 and KIM127, although either mAb is sufficient for promoting their adhesion to ICAM-1 coated surfaces (Al-Shamkhani and Law, 1998).

To obtain a complete matrix of the conditions required for LFA-1 mediated adhesion to ICAM-3 coated surfaces, we used MOLT-4 as the standard cell for experiments. It was confirmed that none of the four reagents, namely Mg/EGTA, KIM127, KIM185 and MEM48, can promote LFA-1 mediated MOLT-4 adhesion to ICAM-3. However, Mg/EGTA with any one of the mAbs was sufficient to promote adhesion. Whereas we

confirmed that the combination of KIM127 and KIM185 can promote MOLT-4 adhesion to ICAM-3 coated surfaces, the other two combinations, MEM48 and KIM127, and MEM 48 and KIM185, can only do so at a limited level. Under all these conditions, MOLT-4 adhesion to ICAM-1 coated surfaces is not affected (Fig. 5.1).

5.2 Expression of MEM148 epitope on LFA-1

In order to observe the effects of the combinations of activating mAbs and Mg/EGTA, flow cytometry profiles of MEM148 epitope expression on MOLT-4 in the presence of the activating agents were obtained using FITC-labeled MEM148 (Fig. 5.2). Whereas the expression of the MEM148 in the presence of any of the three activating mAbs was minimal, higher expression level was detected with Mg/EGTA. The expression of the MEM148 epitope was significantly enhanced in the presence of any two of the four activating reagents. In our previous publication we had shown a higher level of expression of the MEM148 epitope with Mg/EGTA (Tang et al., 2005). This is likely due to the MEM148 used previously was from Professor V. Horejsi (Prague, Czech Republic) and the antibody used here was purchased commercially.

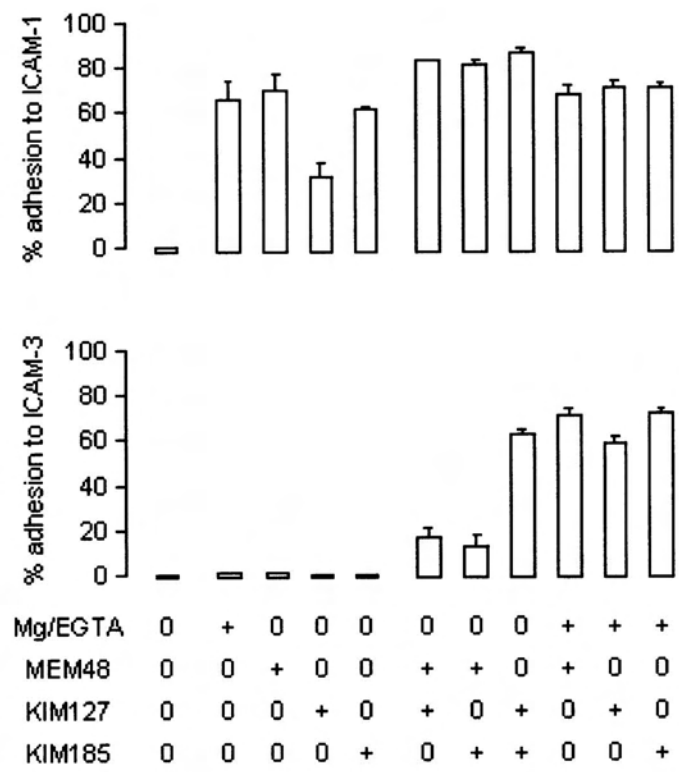

Fig. 5.1 Adhesion of Molt-4 cells to ICAM-1 and ICAM-3 in different combinations of activation reagents. Binding specificity was demonstrated using the αLβ2-specific function-blocking mAb MHM24, not shown in this particular experiment.

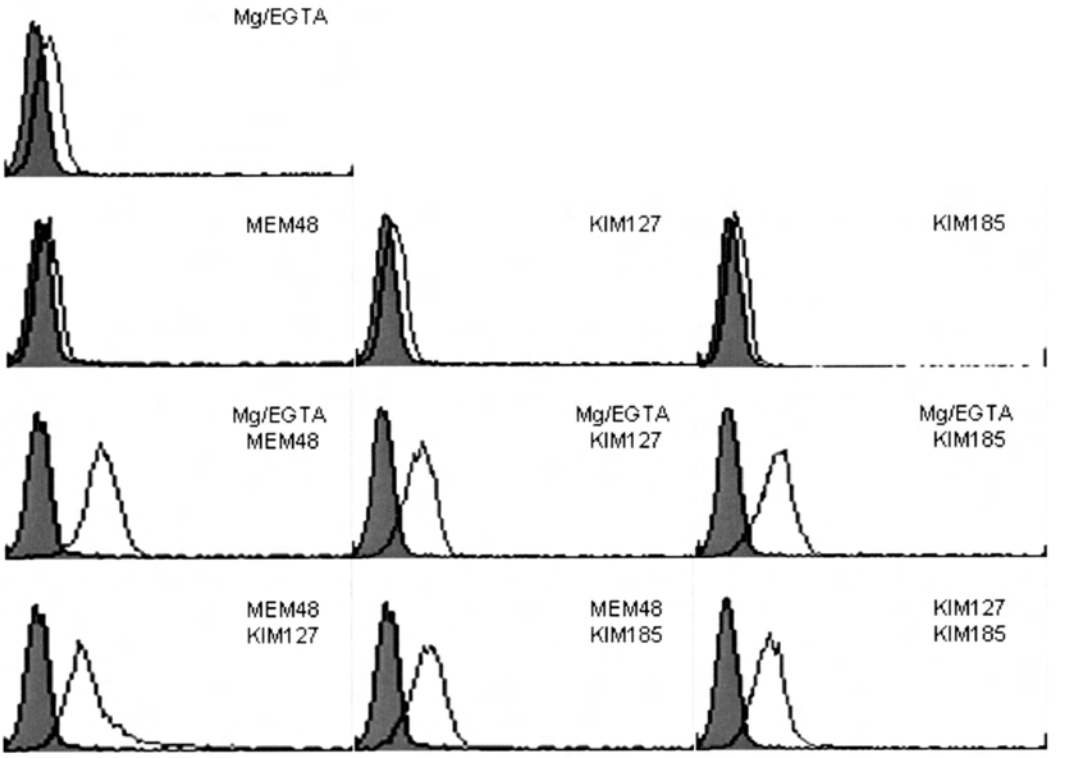

Fig. 5.2 Expression of MEM148 epitope on Molt-4 cells in the presence of different activation reagents. Molt-4 cells were stained with MEM148-FITC at 37°C under different conditions. MEM148-FITC without activation used as a control, shown as a gray shaded histogram. The flow cytometry histogram of MEM148-FITC with different activation reagents were shown as an open histogram.

5.3 Adhesion of COS-7 transfectants expressing LFA-1 variants to ICAM-1 and ICAM-3 coated surfaces

We have shown that several LFA-1 variants were constitutively active in mediating adhesion to ICAM-1 when transfected into 293T or COS-7 cells (Tng et al., 2004). They include αLβ2NV1, αLβ2C23*, αLβ2R^{571}C (see chapter 4), αLβ2N^{329}S (see chapter 3). β2C23*is a β2 truncation mutant in which the codon of Cys^{461} (the 23rd of the 56 conserved cysteines in the extracellular domain of the β2 subunit) was converted to a stop codon (Tan et al., 2000). β2NV1 is a human β2/β1 chimera in which the I-EGF and βTD domains of β2 were replaced with the corresponding region of β1 (Douglass et al., 1998). αLcc with an engineered disulfide bond by converting Lys^{287} and Lys^{294} into cysteines was also included in this study. αLccβ2, is also shown to be constitutively active in ICAM-1 adhesion (Lu et al., 2001b; Lu et al., 2001c) (chapter 3).

Transfectants expressing wild-type LFA-1 requires both Mg/EGTA and the activating mAb KIM185 for ICAM-3 adhesion (Fig. 5.3), as in the case of MOLT-4. However, the αLβ2N^{329}S variant does not require any activating agents for ICAM-3 adhesion. Mg/EGTA is required for promoting ICAM-3 adhesion of transfectants expressing the other four variants. KIM185 can also promote the adhesion of αLccβ2 transfectants to ICAM-3, but was not tested for the other three variants. The epitope of KIM185 was mapped to the I-EGF4/βTD domains (Lu et al., 2001a) and is therefore absent in β2NV1 and β2C23*, and we have found that the epitope of KIM185 was abolished in β2R^{571}C (see Chapter 4).

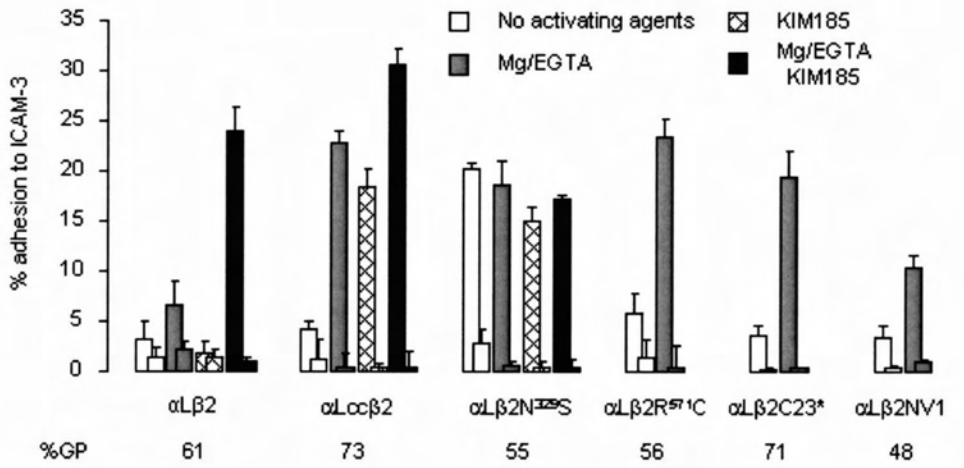

Fig. 5.3 Adhesion of LFA-1 variants on COS-7 cells to ICAM-3. Each corresponding forward bar represents adhesion in the presence of the αLβ2-specific function-blocking mAb MHM24.

5.4 Expression of the MEM148 and KIM127 epitopes on LFA-1 Variants

Since single β2 integrin subunit can be expressed on COS-7 transfectants in the absence of the αL subunit, single β2 subunit, in addition to the αLβ2 heterodimers, can be found on the cell surface of the αLβ2 transfectants (Tan et al., 2001a). It is therefore not possible to use flow cytometry to determine if the epitopes of MEM148 and KIM127 are expressed on the αLβ2 heterodimer variants since a positive signal is always seen because the epitopes are expressed on the single β2 subunit.

A different strategy was employed. We treated the surface biotinylated cells with the mAbs in the presence or absence of Mg/EGTA before lysing them. Immunoprecipitation was performed and analyzed for biotinylated LFA-1 bands as previously described (Cheng et al., 2007). MHM23, a heterodimer specific mAb (Hildreth et al., 1983) was used as a positive control. The presence of the αL bands will indicate the expression of the MEM148 and KIM127 epitopes on the β2 subunit of the heterodimer (Fig. 5.4).

In the absence of Mg/EGTA, the MEM148 epitope is not expressed on wild-type LFA-1, and the αLβ2R^{571}C and αLccβ2 variants. Significant expression of the MEM148 epitope is found on the αLβ2N^{329}S, αLβ2C23* and αLβ2NV1 variants. The expression of the epitope is enhanced to various degrees with Mg/EGTA. Note that the β2NV1 band is particularly heavy in the MEM148 precipitate when compared with the MHM23 precipitate, indicating the abundant presence of the single β2NV1 subunit on the cell surface.

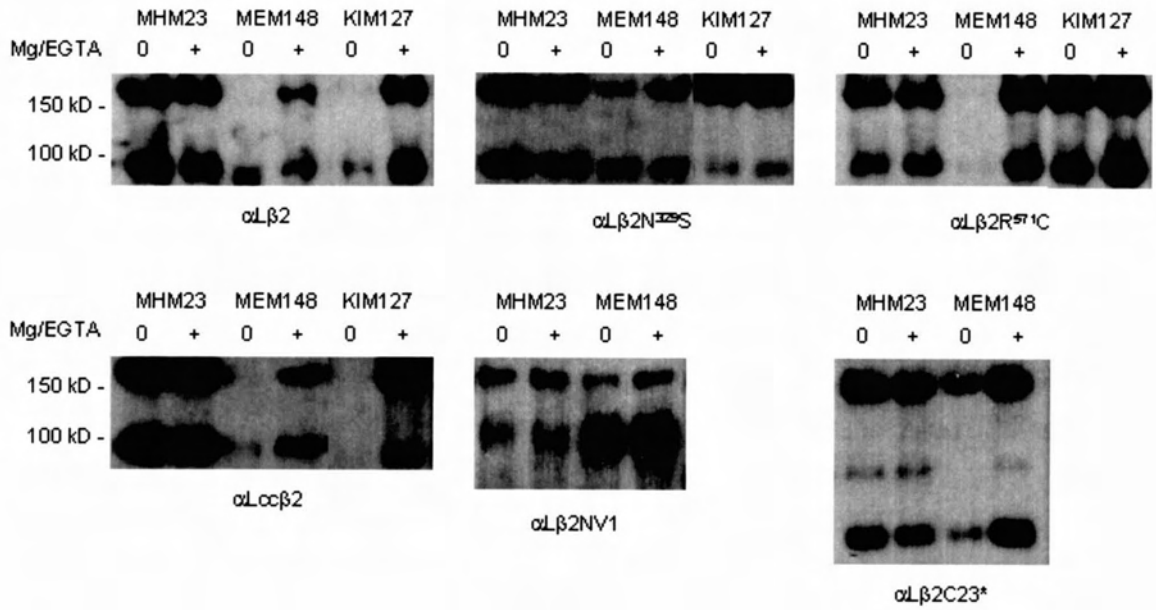

Fig. 5.4 Immunoprecipitation of different LFA-1 variants with MEM148 and KIM127. Cell surface labeled LFA-1 variants were incubated with mAbs MEM148 or KIM127 at 37°C with or without Mg/EGTA followed by precipitation using protein A-Sepharose beads (Experimental Procedures). Immunoprecipitated integrins were resolved on a 7.5% SDS-PAGE gel under reducing conditions, and detected by ECL. MHM23 were included as controls.

The expression of the KIM127 eptiope was also analyzed for the αLβ2N^{329}S, αLβ2R^{571}C, and αLccβ2 variants. It requires Mg/EGTA for expression on αLccβ2 but it is constitutively expressed on the other two variants. Its expression was not analyzed for the αLβ2NV1 and αLβ2C23* variants because they do not contain the β2 I-EGF domains to which the KIM127 epitope was mapped (Lu et al., 2001a).

5.5 The αLβ2cc variant

A β2 integrin fragment comprising the PSI, hybrid, and I-EGF1 and I-EGF2 domains was expressed and it structure was determined at a resolution of 1.75 Å using X-ray crystallography (Shi et al., 2007). It shows a severe bend at the junction between the I-EGF1 and I-EGF2 domains bringing the I-EGF2 domain to close proximity with the PSI domain. Two glycine residues, Gly^{33} in the PSI domain and Gly^{486} in the I-EGF2 domain, were changed to cysteines in a full length β2 construct denoted β2cc. When the modified β2 subunit was co-transfected into 293T cell with a wild-type αL subunit, the αLβ2cc variant was expressed. It was shown that a disulfide bond was formed and the αLβ2cc variant was locked into a bent configuration. Consistent with this interpretation is that the KIM127 epitope was not expressed on this variant even in the presence of Mg/EGTA (Fig. 5.5 A). It should be noted, however, the expression of the MEM148 epitope can be induced by Mg/EGTA (Fig. 5.5 A).

Transfectants expressing the αLβ2cc variant were shown to adhere to ICAM-1 coated surfaces (Shi et al., 2007). The level of adhesion is not affected by KIM127 but can be further enhanced by Mg/EGTA and KIM185 (Fig. 5B). Adhesion to ICAM-3 can be

promoted by Mg/EGTA, and to a lesser extent, by KIM185. Again, KIM127 has no effect on ICAM-3 adhesion.

The αLccβ2 variant does not express the KIM127 and MEM148 epitope in the absence of Mg/EGTA but it can mediate adhesion to ICAM-1 coated surfaces (Tng et al., 2004). We have shown in Fig.5.3 that KIM185 or Mg/EGTA can promote its adhesion to ICAM-3. In the presence of KIM127, transfectants expressing αLccβ2 can be promoted to adhere to ICAM-3 coated surfaces (Fig. 5.6).

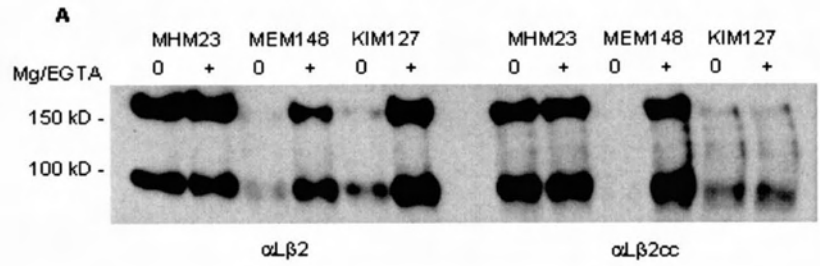

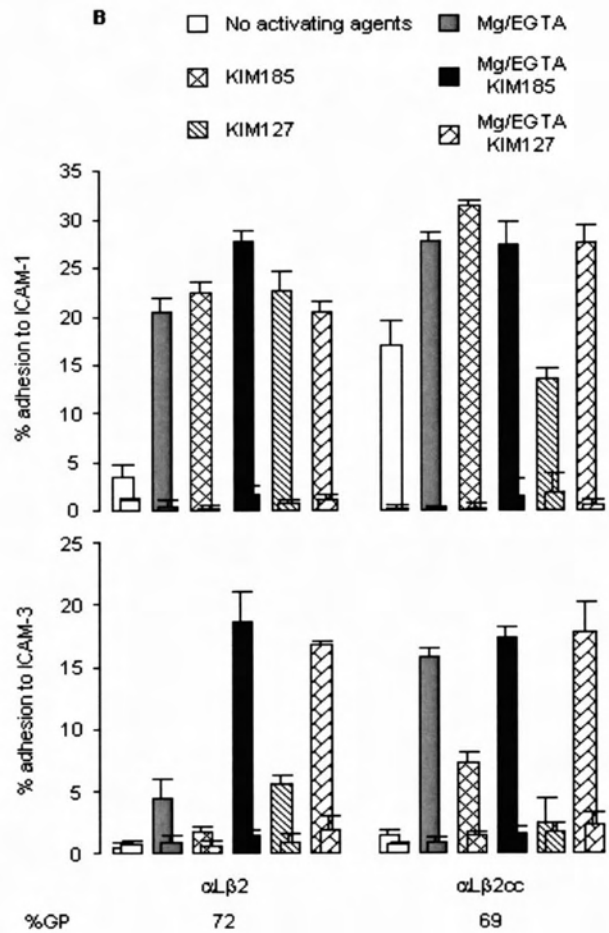

Fig. 5.5 A: Immunoprecipitation of LFA-1 variant αLβ2cc with MEM148 or KIM127. Surface labeled αLβ2c-c transfetant cells were subjected to MEM148 or KIM127 binding at 37°C with or without Mg/EGTA followed by precipitation. Immunoprecipitated integrins were resolved on a 7.5% SDS-PAGE gel under reducing conditions, and detected by ECL. MHM23 were included as controls. **B: Adhesion of LFA-1 variant αLβ2cc to ICAM-1 or ICAM-3.** Each corresponding forward bar represents adhesion in the presence of the αLβ2-specific function-blocking mAb MHM24.

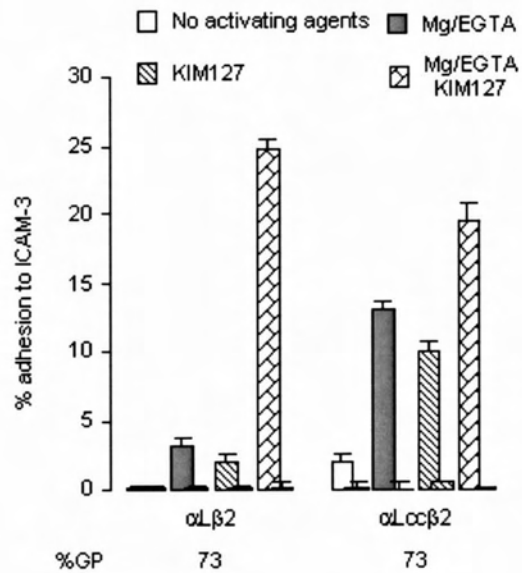

Fig. 5.6: Adhesion of LFA-1 variant αLccβ2 to ICAM-3. Each corresponding forward bar demonstrated blocking with the αLβ2-specific function-blocking mAb MHM24.

5.6 Discussion

We have previously reported three activity states for LFA-1 based on its adhesion properties to ICAM-1 and ICAM-3. The three states are: state 1, a resting state that cannot mediate adhesion to both ligands; state 2, an intermediate state that can promote adhesion to ICAM-1 but not ICAM-3; and state 3, a high affinity state that can promote adhesion to both ICAM-1 and ICAM-3 (Tang et al., 2005).

We report here the study of the conformation of the αLβ2 integrin and using the two mAb reporters, KIM127 for leg extension and MEM148 for hybrid displacement on MOLT-4. Whereas leg extension may correlate with the capacity to bind ICAM-1, it is not clear how hybrid displacement is related to the higher adhesion states. Mg/EGTA and any one of the three activating mAbs promote the full expression of the MEM148 epitope and ICAM-3 adhesion. However, the higher functional states do not have a clear-cut correlation with respect to hybrid displacement. In particular, the mAb combinations of MEM48 and KIM185 and of MEM48 and KIM127 can induce full expression of the MEM148 epitope (Fig. 5.2) but the adhesion to ICAM-3 is limited. We may argue that in both cases, the integrin is extended. In the first case, although KIM127 expression is not directly demonstrated, it has been shown previously that KIM185 can induce KIM127 epitope expression (Andrew et al., 1993). In the second case, KIM127 must bind the integrin since its presence leads to MEM148 expression, which is not induced with MEM48 alone. Thus, we may split the intermediate state into 2a and 2b, in which state 2a is KIM127 positive but MEM148 low/negative, and can mediate adherent to ICAM-1 but not ICAM-3, and state 2b is positive with both KIM127 and MEM148, can mediate ICAM-1 but only limited ICAM-3 adhesion.

COS-7 transfectants expressing wild-type LFA-1 behave like MOLT-4. Analyses of four LFA-1 variants, αLβ2N^{329}S, αLβ2R^{571}C, αLβ2C23*, and αLβ2NV1, provided the spectrum of LFA-1 mediated adhesion observed with MOLT-4 under various activating conditions (Tng et al., 2004). Thus αLβ2R^{571}C is in state 2a, αLβ2C23* and αLβ2NV1 in state 2b, and αLβ2N^{329}S in state 3 (Table 5.1). Expression of the KIM127 epitope is not taken into account for the αLβ2C23* and αLβ2NV1 variants since the I-EGF domains to which the epitope is located is either removed, as in the case of αLβ2C23*, or replaced, as in the case of αLβ2NV1. The classification receives support since αLβ2R^{571}C, αLβ2C23*, and αLβ2NV1 can all be promoted to state 3 in the presence of Mg/EGTA, and KIM185 when applicable.

Electron microscopic study of αLβ2 had revealed conformations that can be roughly grouped into three categories with a compact bent structure at the one end, and an extended and open structure at the other. The intermediate state is one that is extended but the legs remain together in the hinge close position (Nishida et al., 2006). In this article, we have provided functional data in support of the hierarchy of the three conformations but not necessarily on a one-to-one correspondence. Thus, the compact bent structure would correlate with the resting state 1; the intermediate state with state 2a; and the extended and open structure would contain αLβ2 both in state 2b and 3.

Table 5.1 Activation states of LFA-1 on MOLT-4 and COS-7 transfectants

	KIM127 expression	MEM148 expression	ICAM-1 adhesion	ICAM-3 adhesion	Activation State
MOLT-4					
none	0	0	0	0	1
Mg/EGTA	+	+/–	+	0	2a
MEM48	(+)a	0	+	0	2a
KIM127	na	0	+	0	2a
KIM185	+	0	+	0	2a
MEM48/KIM127	+	+	+	+/–	2b
MEM48/KIM185	+	+	+	+/–	2b
KIM127/KIM185	+	+	+	+	3
Mg/E MEM48	+	+	+	+	3
Mg/E KIM127	+	+	+	+	3
Mg/E KIM185	+	+	+	+	3
COS-7 transfectants					
Wild-type	0	0	0	0	1
$\alpha L\beta 2R^{571}C$	+	0	+	+/–	2a
αLβ2C23*	na	+	+	+/–	2b
αLβ2NV1	na	+	+	+/–	2b
$\alpha L\beta 2N^{329}S$	+	+	+	+	3

This line of reasoning pre-supposes that conformational changes leading to functional activation. The first piece of evidence that shed doubt on this was the observation that resting αLβ2 does not express the KIM127 epitope, yet the mAb can promote αLβ2 mediated adhesion to ICAM-1, both for MOLT-4 and COS-7 transfectants. This apparently contradicting observation had been reported previously (Lu et al., 2001a) and it was explained that the presence of the ligand must also contribute to the leg extension whereupon KIM127 can then lock it in the extended state. Thus, the two activities, ligand binding and conformational change, do not take place in a cause and effect fashion necessarily. Further supports are provided in the experiments involving the αLccβ2 and αLβ2cc variants. αLccβ2 does not express the KIM127 nor the MEM148 epitope, suggesting that it assumes a compact and bent conformation, yet it can mediate ICAM-1 adhesion of the transfectants. The experiment with ICAM-1 does not provide any information to distinguish if the bent integrin can adhere to ICAM-1 or the ligand can induce extension to stabilize the adhesion. However, KIM127 can promote αLccβ2 to adhere to ICAM-3. Using the same argument as for KIM127 activating wild-type αLβ2 adhesion to ICAM-1, the ligand ICAM-3 can contribute to leg extension to allow KIM127 to stabilize the integrin in the extended state.

αLβ2cc is locked into a bent state by an engineered disulfide bond between the PSI and I-EGF2 domain. The KIM127 epitope is not expressed and cannot be induced to be expressed in the presence of Mg/EGTA. αLβ2cc, however, can mediate adhesion to ICAM-1. The disulfide bond, though locking αLβ2cc into a bent conformation, must also poses restriction to the structure which may be deviant from the resting state

such that it can mediate adhesion to ICAM-1. In addition, Mg/EGTA can promote αLβ2cc to an ICAM-3 binding state and the epitope of MEM148 was concomitantly expressed. Thus, leg extension is not absolutely required for ligand binding or for hybrid displacement.

Taken together, the results presented here suggest that ligand binding, leg extension, and hybrid displacement may be observed in various combinations, but they are not necessarily coupled in a cause and effect fashion. Bent integrin binding ligands has also been observed in other systems, for example, EM image analyses of αVβ3 ectodomain in complex with fibronectin fragments showed minimal deviation from the bent X-ray structure (Adair et al., 2005). Furthermore, it has been demonstrated in α4β1 integrin and VCAM-1 adhesion system that ligand binding affinity and leg extension are independently regulated, and it was suggested that leg extension may contribute to the kinetics of cell adhesion (Chigaev et al., 2007). The movement of the hybrid domain away from the αL subunit may be viewed as the seed for lower leg separation, which eventually leads to separation of the cytoplasmic segments of the two subunits and outside-in signaling (Zhu et al., 2007b).

Chapter 6: Conclusion

The aim of our laboratory is to understand the structural feature that regulate integrin functions. In this thesis, the main integrin under study was LFA-1, the αLβ2 integrin. Experimental data were also obtained for the αMβ2, αXβ2 and αIIbβ3 integrin, but they are mainly for the purpose of supporting or contracting the findings for the αLβ2 integrin.

Until we approached the work described in chapter 5, it was reasonable to associate the bent compact form of integrins with their resting state and the extended form with or without hybrid domain displacement with their active state. Using LFA-1, the conformational states are refined to include an intermediate state being extended, and a fully active integrin being extended with the hybrid domain displacement. However, a fully extended LFA-1 with hybrid domain displacement may not be fully active, since LFA-1 stimulated by MEM48 and KIM127 or MEM48 and KIM185 have limited adhesion capacity to ICAM-3. Work on the αLccβ2 and αLβ2cc variants suggest that ligand binding and the conformational change are not causally related. In particular, αLβ2cc is locked into a bent conformation and cannot be induced to extend but it can mediate ICAM-1 adhesion. Furthermore, it can be induced to express the MEM148 epitope (hybrid domain displacement) and mediate adhesion to ICAM-3 (high affinity state).

Two mutants of β2 integrin from LAD-1 patients were studied. $\beta2N^{329}S$ can combine with αL to give a fully active LFA-1 because it can constitutively adhere to both ICAM-1 and ICAM-3, and it adopts an extended conformer with the hybrid domain displacement (both KIM127 and MEM148 positive).

αLβ2N^{329}A, αLβ2N^{329}T, αLβ2N^{329}Q, αLβ2N^{329}D exhibit the similar adhesion property with αLβ2N^{329}S. From structure modeling, Asn^{329}δ^{1}O may hydrogen-bond with a Ser^{324} side chain in the β2 I-like domain. Asn^{329} substituted with Gln, Ala, Ser, Thr, or Asp showed potential disruptions in hydrogen-bond formation between these residues at position 329 with Ser^{324} and main chain Glu^{322}, which explain the high affinity LFA-1 for these mutants. When this mutation was introduced into β3, αIIbβ3N^{339}S also exists in a higher affinity state and the I-like domain also adopts similar structural modification. Thus, our results showed that this Asn is critical in shaping the I-like domain by stabilizing the conformation of the α7 helix and the β6-α7 loop. Preliminary results suggest that β2N^{329}S can also combine with αM and αX. The adhesion property of these integrin variants have not been studied. At present, we have expressed a αIIbβ3 ectodomain with the N^{329}S mutation. We are aiming to solve this structure by X-ray crystallography.

The other mutant is β2R^{571}C. It has been reported previously that it can only combine with αL, but not αM and αX to form integrin heterodimer (Shaw et al., 2001). It was also found that αLβ2R^{571}C, unlike αLβ2R^{329}S, is not fully active, but is in an intermediate state, which is extended (KIM127 positive) but the hybrid domain is not displaced (MEM148 negative). In addition, we confirmed the positive charge in the position 571 is important in integrin heterodimer formation. Unexpected results were obtained when we tried to determine the reason why the R^{571}C mutation prohibits β2 from combine with αM. Since αL with the αM (β-propeller and thigh) fails to combine with β2R571C, but αM with the αL(β-propeller and thigh) can combine with β2R^{571}C, it appears that it is the αM β-propeller or the thigh are incompatible with the R^{571}C mutation in the β2 subunit. The result is unexpected since we cannot

see any potential interaction between the IEGF-4 domain (in which $R^{571}C$ resides) and the thigh or β-propeller domain of the α subunits from the αVβ3 integrin model. These series of experiment is incomplete and future experiment will start with mapping the region in the α subunit that affect its interaction with the $\beta2R^{571}C$ to finer details, and extend the study to interaction between $\beta2R^{571}C$ and the αX subunit.

In this thesis, $N^{329}S$ and $R^{571}C$ mutations are the focus of studying. $N^{329}S$ was identified from one allele of a LAD patient with recurrent bacterial infections (Nelson et al., 1992). Neutrophils from this patient failed to spread on surfaces, leading to a severe defect in chemotaxis and a mild impairment in phagocytosis (Crowley et al., 1980). Leukocytes from this patient synthesized normal amounts of a normal-sized CD18 precursor. Only 10-20% of this precursor underwent carbohydrate processing and cell surface expression (Dana et al., 1987). Sequence analysis suggested that the other allele of this patient contained a 12-base pair insertion and a $R^{564}W$ mutation (Nelson et al., 1992). β2 with this insertion co-transfected with αM into COS cells shows no expression of αMβ2. Expression of αMβ2 with $R^{564}W$ mutation was 75% of normal, $\beta2N^{329}S$ support 20% of normal αMβ2 surface expression (Nelson et al., 1992). Thus, the researchers suggested that the moderate CD18 phenotype in this patient's leukocytes appears to be mostly due to CD18 chains derived from the $N^{329}S$ allele with perhaps a small additional contribution from normally spliced transcripts derived from the insertion allele.

$R^{571}C$ have been identified from different LAD patients (Arnaout et al., 1990; Shaw et al., 2001; Wright et al., 1995). One Patient was shown to be homozygous for the mutation $R^{571}C$ (Shaw et al., 2001), both LFA-1 (~10%) and Mac-1 (~5%) were

detected on his neutrophils. Killer, natural killer and cytotoxic T-cell activity, helper T-cell activity and phytohaemagglutinin-induced proliferation were demonstrated with his lymphocytes (Shaw et al., 2001).

Both mutations give LFA-1 that is in the higher affinity state. How they confer the clinical phenotype of LAD is not clear but it may be speculated that they cause aberrant leukocyte migration. Future test may be conducted by making transgenic mice experiments expressing these missense mutations. The migration and the adhesion properties of the leukocyte can be studied in vivo system.

Currently, there are two models "switchblade-like" and "deadbolt" models regarding integrin activation, which had been discussed in chapter 1 (1.8.1). In chapter 5, we described both the bent and the extended conformation including two intermediate conformations. Our study on $N^{329}S$ suggested that the αLβ2 with $N^{329}S$ adopts an extended conformation with the hybrid domain displaced from the leg domain of the αL subunit. However, how the different conformations relate to different activation states on the leukocytes and how they are regulated or converted during immunological responses is still not clear. In our study, a bent LFA-1 still can be induced to hybrid domain displacement and mediating adhesion to ICAM-3. Therefore, the hybrid domain displacement and leg extension can be independently regulated. Accordingly, our data support the switchblade-like model in a general sense but with subtle variation. The detailed allosteric regulation still need further study; we hope to obtain the crystal structures of extracellular domain of LFA-1 in different intermediate activation states.

Publications from this study:

Cheng M, Foo SY, Shi M L, Tang RH, Kong LS, Law SK, Tan, SM. (2007) Mutation of a conserved asparagine in the I-like domain promotes constitutively active integrins alphaLbeta2 and alphaIIbbeta3. ***J Biol Chem***, *282*, 18225-32.

Tng E, Tan, SM, Ranganathan S, **Cheng M**, and Law SK. (2004) The integrin alphaLbeta2 hybrid domain serves as a link for the propagation of activation signal from its stalk regions to the I-like domain. ***J Biol Chem***, *279*, 54334-39

Cheng M, Foo SY, Shi ML, Tan SM, Law SK. Conformational states of LFA-1 and its adhesion to the Intercellular Adhesion Molecules (ICAM)-1 and -3. (Submitted)

Publications from other study:

Walters SE, Tang RH, **Cheng M**, Tan SM, Law SK. (2005) Differential activation of LFA-1 and Mac-1 ligand binding domains. ***Biochem BiophysRes Commun***. 337, 142-8.

International conferences attended:

FIBRONECTIN, INTEGRINS & RELATED MOLECULES
April 22-27, 2007 Il Ciocco Lucca (Barga), Italy

References

Adair, B. D., Xiong, J. P., Maddock, C., Goodman, S. L., Arnaout, M. A., and Yeager, M. (2005). Three-dimensional EM structure of the ectodomain of integrin {alpha}V{beta}3 in a complex with fibronectin. J Cell Biol *168*, 1109-1118.

Adair, B. D., and Yeager, M. (2002). Three-dimensional model of the human platelet integrin alpha IIbbeta 3 based on electron cryomicroscopy and x-ray crystallography. Proc Natl Acad Sci U S A *99*, 14059-14064.

Al-Shamkhani, A., and Law, S. K. (1998). Expression of the H52 epitope on the beta2 subunit is dependent on its interaction with the alpha subunits of the leukocyte integrins LFA-1, Mac-1 and p150,95 and the presence of Ca2+. Eur J Immunol *28*, 3291-3300.

Anderson, D. C., Schmalsteig, F. C., Finegold, M. J., Hughes, B. J., Rothlein, R., Miller, L. J., Kohl, S., Tosi, M. F., Jacobs, R. L., Waldrop, T. C., and et al. (1985). The severe and moderate phenotypes of heritable Mac-1, LFA-1 deficiency: their quantitative definition and relation to leukocyte dysfunction and clinical features. J Infect Dis *152*, 668-689.

Anderson, D. C., and Springer, T. A. (1987). Leukocyte adhesion deficiency: an inherited defect in the Mac-1, LFA-1, and p150,95 glycoproteins. Annu Rev Med *38*, 175-194.

Andrew, D., Shock, A., Ball, E., Ortlepp, S., Bell, J., and Robinson, M. (1993). KIM185, a monoclonal antibody to CD18 which induces a change in the conformation of CD18 and promotes both LFA-1- and CR3-dependent adhesion. Eur J Immunol *23*, 2217-2222.

Armulik, A., Nilsson, I., von Heijne, G., and Johansson, S. (1999). Determination of the border between the transmembrane and cytoplasmic domains of human integrin subunits. J Biol Chem *274*, 37030-37034.

Arnaout, M. A., Dana, N., Gupta, S. K., Tenen, D. G., and Fathallah, D. M. (1990). Point mutations impairing cell surface expression of the common beta subunit (CD18) in a patient with leukocyte adhesion molecule (Leu-CAM) deficiency. J Clin Invest *85*, 977-981.

Arnaout, M. A., Mahalingam, B., and Xiong, J. P. (2005). Integrin structure, allostery, and bidirectional signaling. Annu Rev Cell Dev Biol *21*, 381-410.

Bajt, M. L., Goodman, T., and McGuire, S. L. (1995). Beta 2 (CD18) mutations abolish ligand recognition by I domain integrins LFA-1 (alpha L beta 2, CD11a/CD18) and MAC-1 (alpha M beta 2, CD11b/CD18). J Biol Chem *270*, 94-98.

Barclay, A. N., Brown, M. H., Law, S.K., Mcknight, A.J., Tomlinson, M.G., and van de Merwe, P.A. (1997). The leukocyte Antigen Facts Book. 2nd edition 1997. Acedemic Press: San Diego and London.

Beglova, N., Blacklow, S. C., Takagi, J., and Springer, T. A. (2002). Cysteine-rich module structure reveals a fulcrum for integrin rearrangement upon activation. Nat Struct Mol Biol *9*, 282-287.

Bennett, J. S. (2001). Novel platelet inhibitors. Annu Rev Med *52*, 161-184.

Bennett, J. S. (2005). Structure and function of the platelet integrin alphaIIbbeta3. J Clin Invest *115*, 3363-3369.

Bennett, J. S., Chan, C., Vilaire, G., Mousa, S. A., and DeGrado, W. F. (1997). Agonist-activated alphavbeta3 on platelets and lymphocytes binds to the matrix protein osteopontin. J Biol Chem *272*, 8137-8140.

Berman, P. W., Nakamura, G. R., Riddle, L., Chiu, H., Fisher, K., Champe, M., Gray, A. M., Ward, P., and Fong, S. (1993). Biosynthesis and function of membrane bound and secreted forms of recombinant CD11b/CD18 (Mac-1). J Cell Biochem *52*, 183-195.

Bokel, C., and Brown, N. H. (2002). Integrins in Development: Moving on, Responding to, and Sticking to the Extracellular Matrix. Developmental Cell *3*, 311-321.

Bork, P., Doerks, T., Springer, T. A., and Snel, B. (1999). Domains in plexins: links to integrins and transcription factors. Trends Biochem Sci *24*, 261-263.

Brower, D. L., Brower, S. M., Hayward, D. C., and Ball, E. E. (1997). Molecular evolution of integrins: genes encoding integrin beta subunits from a coral and a sponge. Proc Natl Acad Sci U S A *94*, 9182-9187.

Buckley, C. D., Ferguson, E. D., Littler, A. J., Bossy, D., and Simmons, D. L. (1997). Role of ligands in the activation of LFA-1. Eur J Immunol *27*, 957-962.

Buensuceso, C., de Virgilio, M., and Shattil, S. J. (2003). Detection of integrin alpha IIbbeta 3 clustering in living cells. J Biol Chem *278*, 15217-15224.

Butcher, E. C. (1991). Leukocyte-endothelial cell recognition: three (or more) steps to specificity and diversity. Cell *67*, 1033-1036.

Butta, N., Arias-Salgado, E. G., Gonzalez-Manchon, C., Ferrer, M., Larrucea, S., Ayuso, M. S., and Parrilla, R. (2003). Disruption of the beta3 663-687 disulfide bridge confers constitutive activity to beta3 integrins. Blood *102*, 2491-2497.

Chen, J., Salas, A., and Springer, T. A. (2003). Bistable regulation of integrin adhesiveness by a bipolar metal ion cluster. Nat Struct Biol *10*, 995-1001.

Chen, J., Takagi, J., Xie, C., Xiao, T., Luo, B. H., and Springer, T. A. (2004). The relative influence of metal ion binding sites in the I-like domain and the interface with the hybrid domain on rolling and firm adhesion by integrin alpha4beta7. J Biol Chem *279*, 55556-55561.

Cheng, M., Foo, S. Y., Shi, M. L., Tang, R. H., Kong, L. S., Law, S. K., and Tan, S. M. (2007). Mutation of a conserved asparagine in the I-like domain promotes constitutively active integrins alphaLbeta2 and alphaIIbbeta3. J Biol Chem *282*, 18225-18232.

Chigaev, A., Waller, A., Zwartz, G. J., Buranda, T., and Sklar, L. A. (2007). Regulation of cell adhesion by affinity and conformational unbending of alpha4beta1 integrin. J Immunol *178*, 6828-6839.

Crowley, C. A., Curnutte, J. T., Rosin, R. E., Andre-Schwartz, J., Gallin, J. I., Klempner, M., Snyderman, R., Southwick, F. S., Stossel, T. P., and Babior, B. M. (1980). An inherited abnormality of neutrophil adhesion. Its genetic transmission and its association with a missing protein. N Engl J Med *302*, 1163-1168.

Dana, N., Clayton, L. K., Tennen, D. G., Pierce, M. W., Lachmann, P. J., Law, S. A., and Arnaout, M. A. (1987). Leukocytes from four patients with complete or partial Leu-CAM deficiency contain the common beta-subunit precursor and beta-subunit messenger RNA. J Clin Invest *79*, 1010-1015.

de Fougerolles, A. R., and Springer, T. A. (1992). Intercellular adhesion molecule 3, a third adhesion counter-receptor for lymphocyte function-associated molecule 1 on resting lymphocytes. J Exp Med *175*, 185-190.

Douglass, W. A., Hyland, R. H., Buckley, C. D., Al-Shamkhani, A., Shaw, J. M., Scarth, S. L., Simmons, D. L., and Law, S. K. (1998). The role of the cysteine-rich region of the beta2 integrin subunit in the leukocyte function-associated antigen-1 (LFA-1, alphaLbeta2, CD11a/CD18) heterodimer formation and ligand binding. FEBS Lett *440*, 414-418.

Du, X., Gu, M., Weisel, J. W., Nagaswami, C., Bennett, J. S., Bowditch, R., and Ginsberg, M. H. (1993). Long range propagation of conformational changes in integrin alpha IIb beta 3. J Biol Chem *268*, 23087-23092.

Dustin, M. L., Rothlein, R., Bhan, A. K., Dinarello, C. A., and Springer, T. A. (1986). Induction by IL 1 and interferon-gamma: tissue distribution, biochemistry, and function of a natural adherence molecule (ICAM-1). J Immunol *137*, 245-254.

Dustin, M. L., and Springer, T. A. (1989). T-cell receptor cross-linking transiently stimulates adhesiveness through LFA-1. Nature *341*, 619-624.

Ehlers, M. R. (2000). CR3: a general purpose adhesion-recognition receptor essential for innate immunity. Microbes Infect *2*, 289-294.

Emsley, J., King, S. L., Bergelson, J. M., and Liddington, R. C. (1997). Crystal structure of the I domain from integrin alpha2beta1. J Biol Chem *272*, 28512-28517.

Emsley, J., Knight, C. G., Farndale, R. W., Barnes, M. J., and Liddington, R. C. (2000). Structural basis of collagen recognition by integrin alpha2beta1. Cell *101*, 47-56.

Fawcett, J., Holness, C. L., Needham, L. A., Turley, H., Gatter, K. C., Mason, D. Y., and Simmons, D. L. (1992). Molecular cloning of ICAM-3, a third ligand for LFA-1, constitutively expressed on resting leukocytes. Nature *360*, 481-484.

Fernandez-Calotti, P. X., Salamone, G., Gamberale, R., Trevani, A., Vermeulen, M., Geffner, J., and Giordano, M. (2003). Downregulation of mac-1 expression in monocytes by surface-bound IgG. Scand J Immunol *57*, 35-44.

George, J. N., Caen, J. P., and Nurden, A. T. (1990). Glanzmann's thrombasthenia: the spectrum of clinical disease. Blood *75*, 1383-1395.

Ginsberg, M. H., Lightsey, A., Kunicki, T. J., Kaufmann, A., Marguerie, G., and Plow, E. F. (1986). Divalent cation regulation of the surface orientation of platelet membrane glycoprotein IIb. Correlation with fibrinogen binding function and definition of a novel variant of Glanzmann's thrombasthenia. J Clin Invest *78*, 1103-1111.

Goodman, T. G., DeGraaf, M. E., Fischer, H. D., and Bajt, M. L. (1998). Expression of a structural domain of the beta 2 subunit essential for alpha M beta 2 ligand recognition. J Leukoc Biol *64*, 767-773.

Gupta, V., Gylling, A., Alonso, J. L., Sugimori, T., Ianakiev, P., Xiong, J. P., and Arnaout, M. A. (2007). The beta-tail domain (betaTD) regulates physiologic ligand binding to integrin CD11b/CD18. Blood *109*, 3513-3520.

Hajishengallis, G., and Harokopakis, E. (2007). Porphyromonas gingivalis interactions with complement receptor 3 (CR3): innate immunity or immune evasion? Front Biosci *12*, 4547-4557.

Henderson, R. B., Lim, L. H., Tessier, P. A., Gavins, F. N., Mathies, M., Perretti, M., and Hogg, N. (2001). The use of lymphocyte function-associated antigen (LFA)-1-deficient mice to determine the role of LFA-1, Mac-1, and alpha4 integrin in the inflammatory response of neutrophils. J Exp Med *194*, 219-226.

Hildreth, J. E., Gotch, F. M., Hildreth, P. D., and McMichael, A. J. (1983). A human lymphocyte-associated antigen involved in cell-mediated lympholysis. Eur J Immunol *13*, 202-208.

Hogg, N., and Bates, P. A. (2000). Genetic analysis of integrin function in man: LAD-1 and other syndromes. Matrix Biol *19*, 211-222.

Hogg, N., Stewart, M. P., Scarth, S. L., Newton, R., Shaw, J. M., Law, S. K., and Klein, N. (1999). A novel leukocyte adhesion deficiency caused by expressed but nonfunctional beta2 integrins Mac-1 and LFA-1. J Clin Invest *103*, 97-106.

Horwitz, A., Duggan, K., Buck, C., Beckerle, M. C., and Burridge, K. (1986). Interaction of plasma membrane fibronectin receptor with talin--a transmembrane linkage. Nature *320*, 531-533.

Hubbard, A. K., and Rothlein, R. (2000). Intercellular adhesion molecule-1 (ICAM-1) expression and cell signaling cascades. Free Radic Biol Med *28*, 1379-1386.

Hughes, P. E., Diaz-Gonzalez, F., Leong, L., Wu, C., McDonald, J. A., Shattil, S. J., and Ginsberg, M. H. (1996). Breaking the integrin hinge. A defined structural constraint regulates integrin signaling. J Biol Chem *271*, 6571-6574.

Hughes, P. E., O'Toole, T. E., Ylanne, J., Shattil, S. J., and Ginsberg, M. H. (1995). The conserved membrane-proximal region of an integrin cytoplasmic domain specifies ligand binding affinity. J Biol Chem *270*, 12411-12417.

Humphries, M. J. (2000). Integrin structure. Biochem Soc Trans *28*, 311-339.

Huth, J. R., Olejniczak, E. T., Mendoza, R., Liang, H., Harris, E. A., Lupher, M. L., Jr., Wilson, A. E., Fesik, S. W., and Staunton, D. E. (2000). NMR and mutagenesis evidence for an I domain allosteric site that regulates lymphocyte function-associated antigen 1 ligand binding. Proc Natl Acad Sci U S A *97*, 5231-5236.

Hynes, R. O. (2002). Integrins: bidirectional, allosteric signaling machines. Cell *110*, 673-687.

Hynes, R. O., and Lander, A. D. (1992). Contact and adhesive specificities in the associations, migrations, and targeting of cells and axons. Cell *68*, 303-322.

Janeway CA., Travers P., Walport M., and M., S. (2001). Immunobiology Book. 5 edition.

Kamata, T., Tieu, K. K., Tarui, T., Puzon-McLaughlin, W., Hogg, N., and Takada, Y. (2002). The role of the CPNKEKEC sequence in the beta(2) subunit I domain in regulation of integrin alpha(L)beta(2) (LFA-1). J Immunol *168*, 2296-2301.

Katayama, Y., Hidalgo, A., Peired, A., and Frenette, P. S. (2004). Integrin {alpha}4{beta}7 and its counterreceptor MAdCAM-1 contribute to hematopoietic progenitor recruitment into bone marrow following transplantation. Blood *104*, 2020-2026.

Keely, P. J., Rusyn, E. V., Cox, A. D., and Parise, L. V. (1999). R-Ras signals through specific integrin alpha cytoplasmic domains to promote migration and invasion of breast epithelial cells. J Cell Biol *145*, 1077-1088.

Kieffer, J. D., Plopper, G., Ingber, D. E., Hartwig, J. H., and Kupper, T. S. (1995). Direct binding of F actin to the cytoplasmic domain of the alpha 2 integrin chain in vitro. Biochem Biophys Res Commun *217*, 466-474.

Kim, M., Carman, C. V., and Springer, T. A. (2003). Bidirectional transmembrane signaling by cytoplasmic domain separation in integrins. Science *301*, 1720-1725.

Klinghoffer, R. A., Sachsenmaier, C., Cooper, J. A., and Soriano, P. (1999). Src family kinases are required for integrin but not PDGFR signal transduction. Embo J *18*, 2459-2471.

Kodandapani, R., Veerapandian, B., Kunicki, T. J., and Ely, K. R. (1995). Crystal structure of the OPG2 Fab. An antireceptor antibody that mimics an RGD cell adhesion site. J Biol Chem *270*, 2268-2273.

Larson, R. S., and Springer, T. A. (1990). Structure and function of leukocyte integrins. Immunol Rev *114*, 181-217.

Lauffenburger, D. A., and Horwitz, A. F. (1996). Cell migration: a physically integrated molecular process. Cell *84*, 359-369.

Laurens, N., Koolwijk, P., and de Maat, M. P. (2006). Fibrin structure and wound healing. J Thromb Haemost *4*, 932-939.

Lee, J.-O., Bankston, L. A., and Robert C Liddington, M. A. A. a. (1995a). Two conformations of the integrin A-domain (I-domain): a pathway for activation? Structure *3*, 1333-1340.

Lee, J. O., Rieu, P., Arnaout, M. A., and Liddington, R. (1995b). Crystal structure of the A domain from the alpha subunit of integrin CR3 (CD11b/CD18). Cell *80*, 631-638.

Legge, G. B., Kriwacki, R. W., Chung, J., Hommel, U., Ramage, P., Case, D. A., Dyson, H. J., and Wright, P. E. (2000). NMR solution structure of the inserted domain of human leukocyte function associated antigen-1. J Mol Biol *295*, 1251-1264.

Leitinger, B., and Hogg, N. (2000). Effects of I domain deletion on the function of the beta2 integrin lymphocyte function-associated antigen-1. Mol Biol Cell *11*, 677-690.

Li, X., Regezi, J., Ross, F. P., Blystone, S., Ilic, D., Leong, S. P., and Ramos, D. M. (2001). Integrin alphavbeta3 mediates K1735 murine melanoma cell motility in vivo and in vitro. J Cell Sci *114*, 2665-2672.

Liu, S., Calderwood, D. A., and Ginsberg, M. H. (2000). Integrin cytoplasmic domain-binding proteins. J Cell Sci *113*, 3563-3571.

Liu, S., Thomas, S. M., Woodside, D. G., Rose, D. M., Kiosses, W. B., Pfaff, M., and Ginsberg, M. H. (1999). Binding of paxillin to alpha4 integrins modifies integrin-dependent biological responses. Nature *402*, 676-681.

Lu, C., Ferzly, M., Takagi, J., and Springer, T. A. (2001a). Epitope mapping of antibodies to the C-terminal region of the integrin beta 2 subunit reveals regions that become exposed upon receptor activation. J Immunol *166*, 5629-5637.

Lu, C., Shimaoka, M., Ferzly, M., Oxvig, C., Takagi, J., and Springer, T. A. (2001b). An isolated, surface-expressed I domain of the integrin alphaLbeta2 is sufficient for strong adhesive function when locked in the open conformation with a disulfide bond. Proc Natl Acad Sci U S A *98*, 2387-2392.

Lu, C., Shimaoka, M., Zang, Q., Takagi, J., and Springer, T. A. (2001c). Locking in alternate conformations of the integrin alphaLbeta2 I domain with disulfide bonds

reveals functional relationships among integrin domains. Proc Natl Acad Sci U S A *98*, 2393-2398.

Lu, C., Takagi, J., and Springer, T. A. (2001d). Association of the Membrane Proximal Regions of the alpha and beta Subunit Cytoplasmic Domains Constrains an Integrin in the Inactive State. J Biol Chem *276*, 14642-14648.

Lu, C. F., and Springer, T. A. (1997). The alpha subunit cytoplasmic domain regulates the assembly and adhesiveness of integrin lymphocyte function-associated antigen-1. J Immunol *159*, 268-278.

Luhn, K., Wild, M. K., Eckhardt, M., Gerardy-Schahn, R., and Vestweber, D. (2001). The gene defective in leukocyte adhesion deficiency II encodes a putative GDP-fucose transporter. Nat Genet *28*, 69-72.

Luo, B. H., Carman, C. V., and Springer, T. A. (2007). Structural basis of integrin regulation and signaling. Annu Rev Immunol *25*, 619-647.

Luo, B. H., and Springer, T. A. (2006). Integrin structures and conformational signaling. Curr Opin Cell Biol *18*, 579-586.

Luo, B. H., Springer, T. A., and Takagi, J. (2003). Stabilizing the open conformation of the integrin headpiece with a glycan wedge increases affinity for ligand. Proc Natl Acad Sci U S A *100*, 2403-2408.

Luo, B. H., Takagi, J., and Springer, T. A. (2004). Locking the beta3 integrin I-like domain into high and low affinity conformations with disulfides. J Biol Chem *279*, 10215-10221.

Madri, J. A., Graesser, D., and Haas, T. (1996). The roles of adhesion molecules and proteinases in lymphocyte transendothelial migration. Biochem Cell Biol *74*, 749-757.

Manara, G. C., Pasquinelli, G., Badiali-De Giorgi, L., Ferrari, C., Garatti, S. A., Fasano, D., and Berti, E. (1996). Human epidermal Langerhans cells express the ICAM-3 molecule. Immunohistochemical and immunoelectron microscopical demonstration. Br J Dermatol *134*, 22-27.

Mathew, E. C., Shaw, J. M., Bonilla, F. A., Law, S. K., and Wright, D. A. (2000). A novel point mutation in CD18 causing the expression of dysfunctional CD11/CD18 leucocyte integrins in a patient with leucocyte adhesion deficiency (LAD). Clin Exp Immunol *121*, 133-138.

Mayadas, T. N., and Cullere, X. (2005). Neutrophil beta2 integrins: moderators of life or death decisions. Trends Immunol *26*, 388-395.

Mizejewski, G. J. (1999). Role of integrins in cancer: survey of expression patterns. Proc Soc Exp Biol Med *222*, 124-138.

Mosesson, M. W. (2005). Fibrinogen and fibrin structure and functions. J Thromb Haemost *3*, 1894-1904.

Mould, A. P., Barton, S. J., Askari, J. A., Craig, S. E., and Humphries, M. J. (2003a). Role of ADMIDAS cation-binding site in ligand recognition by integrin alpha 5 beta 1. J Biol Chem *278*, 51622-51629.

Mould, A. P., Barton, S. J., Askari, J. A., McEwan, P. A., Buckley, P. A., Craig, S. E., and Humphries, M. J. (2003b). Conformational Changes in the Integrin beta A Domain Provide a Mechanism for Signal Transduction via Hybrid Domain Movement. J Biol Chem *278*, 17028-17035.

Mould, A. P., Symonds, E. J. H., Buckley, P. A., Grossmann, J. G., McEwan, P. A., Barton, S. J., Askari, J. A., Craig, S. E., Bella, J., and Humphries, M. J. (2003c). Structure of an Integrin-Ligand Complex Deduced from Solution X-ray Scattering and Site-directed Mutagenesis. J Biol Chem *278*, 39993-39999.

Nelson, C., Rabb, H., and Arnaout, M. A. (1992). Genetic cause of leukocyte adhesion molecule deficiency. Abnormal splicing and a missense mutation in a conserved region of CD18 impair cell surface expression of beta 2 integrins. J Biol Chem *267*, 3351-3357.

Nermut, M. V., Green, N. M., Eason, P., Yamada, S. S., and Yamada, K. M. (1988). Electron microscopy and structural model of human fibronectin receptor. Embo J *7*, 4093-4099.

Nishida, N., Xie, C., Shimaoka, M., Cheng, Y., Walz, T., and Springer, T. A. (2006). Activation of leukocyte beta2 integrins by conversion from bent to extended conformations. Immunity *25*, 583-594.

Noti, J. D. (2002). Expression of the myeloid-specific leukocyte integrin gene CD11d during macrophage foam cell differentiation and exposure to lipoproteins. Int J Mol Med *10*, 721-727.

O'Toole, T. E., Mandelman, D., Forsyth, J., Shattil, S. J., Plow, E. F., and Ginsberg, M. H. (1991). Modulation of the affinity of integrin alpha IIb beta 3 (GPIIb-IIIa) by the cytoplasmic domain of alpha IIb. Science *254*, 845-847.

Paul, B. Z., Vilaire, G., Kunapuli, S. P., and Bennett, J. S. (2003). Concurrent signaling from Galphaq- and Galphai-coupled pathways is essential for agonist-induced alphavbeta3 activation on human platelets. J Thromb Haemost *1*, 814-820.

Peterson, J. A., Visentin, G. P., Newman, P. J., and Aster, R. H. (1998). A recombinant soluble form of the integrin alpha IIb beta 3 (GPIIb-IIIa) assumes an active, ligand-binding conformation and is recognized by GPIIb-IIIa-specific monoclonal, allo-, auto-, and drug-dependent platelet antibodies. Blood *92*, 2053-2063.

Pober, J. S., Bevilacqua, M. P., Mendrick, D. L., Lapierre, L. A., Fiers, W., and Gimbrone, M. A., Jr. (1986a). Two distinct monokines, interleukin 1 and tumor necrosis factor, each independently induce biosynthesis and transient expression of the same antigen on the surface of cultured human vascular endothelial cells. J Immunol *136*, 1680-1687.

Pober, J. S., Gimbrone, M. A., Jr., Lapierre, L. A., Mendrick, D. L., Fiers, W., Rothlein, R., and Springer, T. A. (1986b). Overlapping patterns of activation of human endothelial cells by interleukin 1, tumor necrosis factor, and immune interferon. J Immunol *137*, 1893-1896.

Ponting, C. P., Schultz, J., Copley, R. R., Andrade, M. A., and Bork, P. (2000). Evolution of domain families. Adv Protein Chem *54*, 185-244.

Rojiani, M. V., Finlay, B. B., Gray, V., and Dedhar, S. (1991). In vitro interaction of a polypeptide homologous to human Ro/SS-A antigen (calreticulin) with a highly conserved amino acid sequence in the cytoplasmic domain of integrin alpha subunits. Biochemistry *30*, 9859-9866.

Rothlein, R., Dustin, M. L., Marlin, S. D., and Springer, T. A. (1986). A human intercellular adhesion molecule (ICAM-1) distinct from LFA-1. J Immunol *137*, 1270-1274.

Salas, A., Shimaoka, M., Kogan, A. N., Harwood, C., von Andrian, U. H., and Springer, T. A. (2004). Rolling adhesion through an extended conformation of integrin alphaLbeta2 and relation to alpha I and beta I-like domain interaction. Immunity *20*, 393-406.

Schwarzbauer, J. E., and Sechler, J. L. (1999). Fibronectin fibrillogenesis: a paradigm for extracellular matrix assembly. Curr Opin Cell Biol *11*, 622-627.

Seligsohn, U. (2002). Glanzmann thrombasthenia: a model disease which paved the way to powerful therapeutic agents. Pathophysiol Haemost Thromb *32*, 216-217.

Shattil, S. J. (2005). Integrins and Src: dynamic duo of adhesion signaling. Trends Cell Biol *15*, 399-403.

Shattil, S. J., and Newman, P. J. (2004). Integrins: dynamic scaffolds for adhesion and signaling in platelets. Blood *104*, 1606-1615.

Shaw, J. M., Al-Shamkhani, A., Boxer, L. A., Buckley, C. D., Dodds, A. W., Klein, N., Nolan, S. M., Roberts, I., Roos, D., Scarth, S. L., *et al.* (2001). Characterization of four CD18 mutants in leucocyte adhesion deficient (LAD) patients with differential capacities to support expression and function of the CD11/CD18 integrins LFA-1, Mac-1 and p150,95. Clinical & Experimental Immunology *126*, 311-318.

Shi, M., Foo, S. Y., Tan, S. M., Mitchell, E. P., Law, S. K., and Lescar, J. (2007). A Structural Hypothesis for the Transition between Bent and Extended Conformations of the Leukocyte beta2 Integrins. J Biol Chem *282*, 30198-30206.

Shi, M., Sundramurthy, K., Liu, B., Tan, S.-M., Law, S. K. A., and Lescar, J. (2005). The Crystal Structure of the Plexin-Semaphorin-Integrin Domain/Hybrid Domain/I-EGF1 Segment from the Human Integrin {beta}2 Subunit at 1.8-A Resolution. J Biol Chem *280*, 30586-30593.

Shimaoka, M., Lu, C., Palframan, R. T., von Andrian, U. H., McCormack, A., Takagi, J., and Springer, T. A. (2001). Reversibly locking a protein fold in an active conformation with a disulfide bond: integrin alphaL I domains with high affinity and antagonist activity in vivo. Proc Natl Acad Sci U S A *98*, 6009-6014.

Shimaoka, M., Lu, C., Salas, A., Xiao, T., Takagi, J., and Springer, T. A. (2002a). Stabilizing the integrin alpha M inserted domain in alternative conformations with a range of engineered disulfide bonds. Proc Natl Acad Sci U S A *99*, 16737-16741.

Shimaoka, M., and Springer, T. A. (2003). Therapeutic antagonists and conformational regulation of integrin function. Nat Rev Drug Discov *2*, 703-716.

Shimaoka, M., Takagi, J., and Springer, T. A. (2002b). Conformational regulation of integrin structure and function. Annu Rev Biophys Biomol Struct *31*, 485-516.

Shimaoka, M., Xiao, T., Liu, J. H., Yang, Y., Dong, Y., Jun, C. D., McCormack, A., Zhang, R., Joachimiak, A., Takagi, J., *et al.* (2003). Structures of the alpha L I domain and its complex with ICAM-1 reveal a shape-shifting pathway for integrin regulation. Cell *112*, 99-111.

Simon, D. I., Ezratty, A. M., Francis, S. A., Rennke, H., and Loscalzo, J. (1993). Fibrin(ogen) is internalized and degraded by activated human monocytoid cells via Mac-1 (CD11b/CD18): a nonplasmin fibrinolytic pathway. Blood *82*, 2414-2422.

Solomon, E., Palmer, R. W., Hing, S., and Law, S. K. (1988). Regional localization of CD18, the beta-subunit of the cell surface adhesion molecule LFA-1, on human chromosome 21 by in situ hybridization. Ann Hum Genet *52*, 123-128.

Springer, T. A. (1994). Traffic signals for lymphocyte recirculation and leukocyte emigration: the multistep paradigm. Cell *76*, 301-314.

Springer, T. A. (1997). Folding of the N-terminal, ligand-binding region of integrin alpha-subunits into a beta-propeller domain. Proc Natl Acad Sci U S A *94*, 65-72.

Springer, T. A., Jing, H., and Takagi, J. (2000). A novel Ca2+ binding beta hairpin loop better resembles integrin sequence motifs than the EF hand. Cell *102*, 275-277.

Stacker, S. A., and Springer, T. A. (1991). Leukocyte integrin P150,95 (CD11c/CD18) functions as an adhesion molecule binding to a counter-receptor on stimulated endothelium. J Immunol *146*, 648-655.

Staunton, D. E., Dustin, M. L., Erickson, H. P., and Springer, T. A. (1990). The arrangement of the immunoglobulin-like domains of ICAM-1 and the binding sites for LFA-1 and rhinovirus. Cell *61*, 243-254.

Sugino, H. (2005). ICAM-3, a ligand for DC-SIGN, was duplicated from ICAM-1 in mammalian evolution, but was lost in the rodent genome. FEBS Lett *579*, 2901-2906.

Switala-Jelen, K., Dabrowska, K., Opolski, A., Lipinska, L., Nowaczyk, M., and Gorski, A. (2004). The biological functions of beta3 integrins. Folia Biol (Praha) *50*, 143-152.

Takagi, J., Beglova, N., Yalamanchili, P., Blacklow, S. C., and Springer, T. A. (2001a). Definition of EGF-like, closely interacting modules that bear activation epitopes in integrin beta subunits. PNAS *98*, 11175-11180.

Takagi, J., DeBottis, D. P., Erickson, H. P., and Springer, T. A. (2002a). The role of the specificity-determining loop of the integrin beta subunit I-like domain in autonomous expression, association with the alpha subunit, and ligand binding. Biochemistry *41*, 4339-4347.

Takagi, J., Erickson, H. P., and Springer, T. A. (2001b). C-terminal opening mimics 'inside-out' activation of integrin alpha5beta1. Nat Struct Biol *8*, 412-416.

Takagi, J., Petre, B. M., Walz, T., and Springer, T. A. (2002b). Global Conformational Rearrangements in Integrin Extracellular Domains in Outside-In and Inside-Out Signaling. Cell *110*, 599-611.

Takagi, J., and Springer, T. A. (2002). Integrin activation and structural rearrangement. Immunol Rev *186*, 141-163.

Takagi, J., Strokovich, K., Springer, T. A., and Walz, T. (2003). Structure of integrin alpha5beta1 in complex with fibronectin. Embo J *22*, 4607-4615.

Tan, S. M., Hyland, R. H., Al-Shamkhani, A., Douglass, W. A., Shaw, J. M., and Law, S. K. (2000). Effect of integrin beta 2 subunit truncations on LFA-1 (CD11a/CD18) and Mac-1 (CD11b/CD18) assembly, surface expression, and function. J Immunol *165*, 2574-2581.

Tan, S. M., Robinson, M. K., Drbal, K., van Kooyk, Y., Shaw, J. M., and Law, S. K. (2001a). The N-terminal region and the mid-region complex of the integrin beta 2 subunit. J Biol Chem *276*, 36370-36376.

Tan, S. M., Walters, S. E., Mathew, E. C., Robinson, M. K., Drbal, K., Shaw, J. M., and Law, S. K. (2001b). Defining the repeating elements in the cysteine-rich region (CRR) of the CD18 integrin beta 2 subunit. FEBS Lett *505*, 27-30.

Tang, M. L., Kong, L. S., Law, S. K., and Tan, S. M. (2006). Down-regulation of integrin alpha M beta 2 ligand-binding function by the urokinase-type plasminogen activator receptor. Biochem Biophys Res Commun *348*, 1184-1193.

Tang, R. H., Tng, E., Law, S. K., and Tan, S. M. (2005). Epitope mapping of monoclonal antibody to integrin alphaL beta2 hybrid domain suggests different requirements of affinity states for intercellular adhesion molecules (ICAM)-1 and ICAM-3 binding. J Biol Chem *280*, 29208-29216.

Tng, E., Tan, S. M., Ranganathan, S., Cheng, M., and Law, S. K. (2004). The integrin alpha L beta 2 hybrid domain serves as a link for the propagation of activation signal from its stalk regions to the I-like domain. J Biol Chem *279*, 54334-54339.

Van de Walle, G. R., Vanhoorelbeke, K., Majer, Z., Illyes, E., Baert, J., Pareyn, I., and Deckmyn, H. (2005). Two functional active conformations of the integrin {alpha}2{beta}1, depending on activation condition and cell type. J Biol Chem *280*, 36873-36882.

Van der Vieren, M., Crowe, D. T., Hoekstra, D., Vazeux, R., Hoffman, P. A., Grayson, M. H., Bochner, B. S., Gallatin, W. M., and Staunton, D. E. (1999). The leukocyte integrin alpha D beta 2 binds VCAM-1: evidence for a binding interface between I domain and VCAM-1. J Immunol *163*, 1984-1990.

Van der Vieren, M., Le Trong, H., Wood, C. L., Moore, P. F., St John, T., Staunton, D. E., and Gallatin, W. M. (1995). A novel leukointegrin, alpha d beta 2, binds preferentially to ICAM-3. Immunity *3*, 683-690.

van Kooyk, Y., van de Wiel-van Kemenade, P., Weder, P., Kuijpers, T. W., and Figdor, C. G. (1989). Enhancement of LFA-1-mediated cell adhesion by triggering through CD2 or CD3 on T lymphocytes. Nature *342*, 811-813.

van Kooyk, Y., van Vliet, S. J., and Figdor, C. G. (1999). The actin cytoskeleton regulates LFA-1 ligand binding through avidity rather than affinity changes. J Biol Chem *274*, 26869-26877.

Vinogradova, O., Velyvis, A., Velyviene, A., Hu, B., Haas, T., Plow, E., and Qin, J. (2002). A structural mechanism of integrin alpha(IIb)beta(3) "inside-out" activation as regulated by its cytoplasmic face. Cell *110*, 587-597.

Violette, S. M., Rusche, J. R., Purdy, S. R., Boyd, J. G., Cos, J., and Silver, S. (1995). Differences in the binding of blocking anti-CD11b monoclonal antibodies to the A-domain of CD11b. J Immunol *155*, 3092-3101.

Vonderheide, R. H., Tedder, T. F., Springer, T. A., and Staunton, D. E. (1994). Residues within a conserved amino acid motif of domains 1 and 4 of VCAM-1 are required for binding to VLA-4. J Cell Biol *125*, 215-222.

Vorup-Jensen, T., Carman, C. V., Shimaoka, M., Schuck, P., Svitel, J., and Springer, T. A. (2005). Exposure of acidic residues as a danger signal for recognition of fibrinogen and other macromolecules by integrin alphaXbeta2. Proc Natl Acad Sci U S A *102*, 1614-1619.

Weisel, J. W. (2005). Fibrinogen and fibrin. Adv Protein Chem *70*, 247-299.

Weisel, J. W., Nagaswami, C., Vilaire, G., and Bennett, J. S. (1992). Examination of the platelet membrane glycoprotein IIb-IIIa complex and its interaction with fibrinogen and other ligands by electron microscopy. J Biol Chem *267*, 16637-16643.

Wiseman, P. W., Brown, C. M., Webb, D. J., Hebert, B., Johnson, N. L., Squier, J. A., Ellisman, M. H., and Horwitz, A. F. (2004). Spatial mapping of integrin interactions and dynamics during cell migration by image correlation microscopy. J Cell Sci *117*, 5521-5534.

Wong, D. A., Davis, E. M., LeBeau, M., and Springer, T. A. (1996). Cloning and chromosomal localization of a novel gene-encoding a human beta 2-integrin alpha subunit. Gene *171*, 291-294.

Wright, A. H., Douglass, W. A., Taylor, G. M., Lau, Y. L., Higgins, D., Davies, K. A., and Law, S. K. (1995). Molecular characterization of leukocyte adhesion deficiency in six patients. Eur J Immunol *25*, 717-722.

Xiao, T., Takagi, J., Coller, B. S., Wang, J. H., and Springer, T. A. (2004). Structural basis for allostery in integrins and binding to fibrinogen-mimetic therapeutics. Nature *432*, 59-67.

Xie, C., Shimaoka, M., Xiao, T., Schwab, P., Klickstein, L. B., and Springer, T. A. (2004). The integrin alpha-subunit leg extends at a Ca2+-dependent epitope in the thigh/genu interface upon activation. Proc Natl Acad Sci U S A *101*, 15422-15427.

Xiong, J.-P., Stehle, T., Goodman, S. L., and Arnaout, M. A. (2004). A Novel Adaptation of the Integrin PSI Domain Revealed from Its Crystal Structure. J Biol Chem *279*, 40252-40254.

Xiong, J. P., Stehle, T., Diefenbach, B., Zhang, R., Dunker, R., Scott, D. L., Joachimiak, A., Goodman, S. L., and Arnaout, M. A. (2001). Crystal structure of the extracellular segment of integrin alpha Vbeta3. Science *294*, 339-345.

Xiong, J. P., Stehle, T., Zhang, R., Joachimiak, A., Frech, M., Goodman, S. L., and Arnaout, M. A. (2002). Crystal structure of the extracellular segment of integrin alpha Vbeta3 in complex with an Arg-Gly-Asp ligand. Science *296*, 151-155.

Yalamanchili, P., Lu, C., Oxvig, C., and Springer, T. A. (2000). Folding and Function of I Domain-deleted Mac-1 and Lymphocyte Function-associated Antigen-1. J Biol Chem *275*, 21877-21882.

Yang, W., Shimaoka, M., Chen, J., and Springer, T. A. (2004a). Activation of integrin beta-subunit I-like domains by one-turn C-terminal alpha-helix deletions. Proc Natl Acad Sci U S A *101*, 2333-2338.

Yang, W., Shimaoka, M., Salas, A., Takagi, J., and Springer, T. A. (2004b). Intersubunit signal transmission in integrins by a receptor-like interaction with a pull spring. Proc Natl Acad Sci U S A *101*, 2906-2911.

Zhang, H., Colman, R. W., and Sheng, N. (2003). Regulation of CD11b/CD18 (Mac-1) adhesion to fibrinogen by urokinase receptor (uPAR). Inflamm Res *52*, 86-93.

Zhu, J., Boylan, B., Luo, B.-H., Newman, P. J., and Springer, T. A. (2007a). Tests of the Extension and Deadbolt Models of Integrin Activation. J Biol Chem *282*, 11914-11920.

Zhu, J., Carman, C. V., Kim, M., Shimaoka, M., Springer, T. A., and Luo, B. H. (2007b). Requirement of {alpha} and {beta} subunit transmembrane helix separation for integrin outside-in signaling. Blood.}*110*, 2475-83.